

INVESTIGATING APTAMERS FOR CAPILLARY ELECTROPHORESIS
AFFINITY ASSAYS

By

DANIELLE DENISE BUCHANAN

A DISSERTATION PRESENTED TO THE GRADUATE SCHOOL
OF THE UNIVERSITY OF FLORIDA IN PARTIAL FULFILLMENT
OF THE REQUIREMENTS FOR THE DEGREE OF
DOCTOR OF PHILOSOPHY

UNIVERSITY OF FLORIDA

2001

To my parents for all their love and support.

ACKNOWLEDGMENTS

I would like to thank Professor Robert T. Kennedy for his guidance and support during my graduate career. I would also like to thank Dr. Steven A. Benner and several past members of his research group including Dr. Thomas Battersby, Dr. Petra Burgstallar, and Dr. Darwin Ang for the opportunity to collaborate with them on a very interesting scientific endeavor. I am indebted to a wonderful group of women, Ms. Lisa Kauri, Ms. Cameron Church, Ms. Jacinth McKenzie, Ms. Gretchen Potts, and Mrs. Charina Paras de Silva, for their friendship, encouragement, and guidance over the past years. I would also like to thank the members of the Kennedy research group for their assistance over the years. I would like to thank Mr. Jon Thompson for his wonderful insight and friendship and Professor Michael T. Bowser for all the advice and suggestions to help me along the way. Most notably I would like to thank my parents, Charles and Lorraine Buchanan, for their love, support, and encouragement during some very rough times. I would like to thank my sisters, Julie and Meghan, for always reminding me of the important things in life. Above all I would like to thank the Lord for the patience, courage, and stamina to reach the end.

TABLE OF CONTENTS

| | <u>page</u> |
|----------------------------------------------------------------------------------------------------------------------------------------------|-------------|
| ACKNOWLEDGMENTS | iii |
| ABBREVIATIONS | vi |
| ABSTRACT | ix |
| CHAPTERS | |
| 1 INTRODUCTION | |
| Affinity Assays | 1 |
| Immunoassays | 1 |
| Capillary Electrophoresis | 3 |
| Instrumentation | 7 |
| Detection | 8 |
| Capillary Electrophoresis Immunoassays | 9 |
| Aptamers | 16 |
| 2 DEVELOPING A NONCOMPETITIVE APTAMER AFFINITY ASSAY EMPLOYING CAPILLARY ELECTROPHORESIS WITH LASER INDUCED FLUORESCENCE DETECTION | |
| Introduction | 28 |
| Materials and Methods | 33 |
| Results and Discussion | 35 |
| Conclusions..... | 41 |
| 3 INVESTIGATING THE EFFECTS OF ELECTRIC FIELD, COLUMN TIME, pH, AND BUFFER COMPOSITION ON APTAMER COMPLEX STABILITY | |
| Introduction | 51 |
| Materials and Methods | 53 |
| Results and Discussion | 55 |
| Conclusions | 63 |

| | | |
|---|-----------------------------------------------------------------------------------------|-----|
| 4 | INVESTIGATIONS OF ADENOSINE BINDING APTAMERS WITH AFFINITY CAPILLARY ELECTROPHORESIS | |
| | Introduction | 76 |
| | Materials and Methods | 80 |
| | Results and Discussion | 82 |
| | Conclusions | 88 |
| 5 | PREPARATION AND EVALUATION OF POLYMERIC CAPILLARY COATINGS FOR PROTEIN SEPARATIONS | |
| | Introduction | 103 |
| | Materials and Methods | 107 |
| | Results and Discussion | 112 |
| | Conclusions | 123 |
| 6 | SUMMARY AND FUTURE DIRECTIONS..... | 137 |
| | REFERENCES..... | 140 |
| | BIOGRAPHICAL SKETCH..... | 147 |

ABBREVIATIONS

| | |
|-------|---------------------------------------------------------|
| A* | free aptamer |
| Ab | antibody |
| Ab* | labeled antibody |
| ACE | affinity capillary electrophoresis |
| Ag | antigen |
| Ag* | labeled antigen |
| Ab-Ag | antibody-antigen complex |
| APCE | affinity probe capillary electrophoresis |
| BCECF | 2',7'-bis-(2-carboxyethyl)-5-(and-6)-carboxyfluorescein |
| C | complex |
| CE | capillary electrophoresis |
| CEC | capillary electrochromatography |
| CEIA | capillary electrophoretic immunoassay |
| cIEF | capillary isoelectric focusing |
| CEMSA | capillary electrophoresis mobility shift assay |
| CGE | capillary gel electrophoresis |
| CZE | capillary zone electrophoresis |
| EDTA | ethylenediaminetetraacetic acid disodium salt |
| ELISA | enzyme-linked immunosorbent assay |

| | |
|----------------|-----------------------------------------------------------|
| EMSA | electrophoresis mobility shift assay |
| EOF | electroosmotic flow |
| HPMC | hydroxypropylmethylcellulose |
| i.d. | inner diameter |
| IgE | immunoglobulin E |
| IS | internal standard |
| J | 5-(3''-aminopropynyl)-2'-deoxyuridine |
| K _d | dissociation constant |
| LC | liquid chromatography |
| LIF | laser induced fluorescence |
| μ | electrophoretic mobility |
| MEKC | micellar electrokinetic capillary chromatography |
| MOPS | 3-[N-morpholino]propanesulfonic acid |
| MW | molecular weight |
| o.d. | outer diameter |
| PCR | polymerase chain reaction |
| PEO | poly(ethylene oxide) |
| pI | isoelectric point |
| RIA | radioimmunoassay |
| SDS | sodium dodecyl sulfate |
| SELEX | systematic evolution of ligands by exponential enrichment |
| TBE/K | Tris, borate, EDTA, and potassium chloride buffer |
| TGK | Tris, glycine, and potassium phosphate buffer |

Tris tris(hydroxyaminomethane)

UV ultraviolet

Abstract of Dissertation Presented to the Graduate School
of the University of Florida in Partial Fulfillment of the
Requirements for the Degree of Doctor of Philosophy

INVESTIGATING APTAMERS FOR CAPILLARY
ELECTROPHORESIS AFFINITY ASSAYS

By

Danielle Denise Buchanan

August 2001

Chairman: Robert T. Kennedy

Major Department: Chemistry

Noncompetitive CE aptamer assays were developed for thrombin and IgE. Buffer and pH effects were investigated to determine the effect on complex formation and detection. In comparison to phosphate and MOPS buffers, larger complexes were detected using a tris(hydroxyamino)methane, glycine, and potassium phosphate (TGK) pH 8.4 buffer. Good resolution between the complex and free peaks was achieved in the TGK buffer for the IgE aptamer assay; however, bridging between the complex and free peaks was observed for the assay using the lower affinity thrombin aptamer. Detection limits for the thrombin and IgE aptamer complexes were determined in TGK as 70 nM and 5 nM respectively. Other separation parameters such as electric field strength and column time were investigated. The time on the column was shown to affect the amount of complex detected; however, electric fields in the range of 125-600 V/cm showed no adverse effects on the complex.

A DNA aptamer, initially selected for ATP, was characterized for use as an affinity stationary phase. Using affinity capillary electrophoresis (ACE), binding constants for this aptamer were determined for various adenosine containing molecules such as AMP, ADP, and ATP. Dissociation constants (K_d) of the DNA-ligand complex were found to be similar for adenosine and ADP but differed from AMP or ATP. Separation parameters such as pH, temperature, and salt concentration were optimized in order to maximize the precision and minimize the error in the electrophoretic mobility and binding constant measurements.

Using ACE the binding of another ATP selective DNA aptamer containing a non-naturally occurring positively charged nucleotide, 5-(3"-aminopropynyl)-2'-deoxyuridine (J), was investigated. The modified nucleotide "J" was incorporated into the aptamer in order to enrich the diversity of the initial aptamer selection pool as well as possibly enhance the binding affinity of the aptamer with the ATP ligand. The binding constant of the J-base aptamer (120 μ M) was determined and compared to that of the previously characterized standard nucleotide ATP aptamer (133 μ M). No enrichment in binding was measured with the modified base aptamer. With improvements in aptamer selections and further development of non-standard nucleotides, aptamer diversity and functionality will continue to be enriched increasing aptamer applicability for analytical diagnostic tools.

CHAPTER 1 INTRODUCTION

Affinity Assays

Affinity assays are selective, highly sensitive tools used to quantitate trace levels of analytes in complex mixtures. A tracer molecule or affinity probe is necessary to interact with the analyte and provide a means of detection. By incorporating fluorescent, chemiluminescent, enzyme or radioactive labels to the affinity probe, the sensitivity of the affinity assay is increased, and by utilizing specific interactions such as an antibody-antigen interaction, the selectivity of affinity assays is enhanced. Immunoassays are the most commonly employed affinity assays in which the interaction between an antigen and its specific antibody is utilized. Traditional immunoassay techniques such as the enzyme-linked immunosorbent assay (ELISA) are laborious and time consuming and typically only a single target molecule can be analyzed. Simultaneous, multi-analyte analysis is possible by coupling immunoassays with separation methods such as capillary electrophoresis (CE). Because of the speed and sensitivity associated with CE separations, rapid affinity assays with low detection limits have been developed. However, immunoassays can be difficult to develop so alternatives to the capillary electrophoretic immunoassay (CEIA) are necessary. With this work alternatives to CEIA's have been explored in hopes of developing new analytical diagnostic tools.

Immunoassays

Immunoassays are affinity assays that utilize the interaction between an antigen and its specific antibody. An antigen is any substance that elicits an immune response

from its host. An antibody is a protein known as an immunoglobulin produced by the immune system in response to an antigen. Antibodies are large proteins in which the antibody binding site is referred to as the paratope. The complimentary binding area on the antigen is the epitope. The specific binding of the epitope and paratope regions provides the selective interaction utilized in immunoassays.

Because of the selective antibody-antigen interaction as well as low limits of detection and applicability to a wide range of target analytes, immunoassays are commonly employed for clinical, biopharmaceutical, and environmental applications (Hage, 1993). In comparison to traditional chemical staining detection methods, coupling labeling techniques such as radioactivity, fluorescence, chemiluminescence, and enzyme amplification with immunoassays, the sensitivity of the method is increased enabling the quantitation of trace analytes in complex mixtures (Bao, 1997). Commonly employed immunoassays include the radioimmunoassay (RIA) in which a radioactive label is bound to the antigen and is used for quantitation, and the enzyme-linked immunosorbent assay (ELISA), in which the antibody or antigen is immobilized on a solid support such as a microtiter plate. For example, an ELISA experiment could employ an immobilized antibody. As a solution containing the antigen of interest is washed across the plate, the antigen binds with the immobilized antibody and is captured. Another antibody with an enzyme label is then added and binds with the captured antigen. By measuring the activity of the enzyme conjugated to the antibody the concentration of the antigen can be quantitated.

Though immunoassays offer low limits of detection and parallel analysis of multiple analytes, conventional immunoassay techniques are tedious and time consuming

due to long incubation and rinse times. Other disadvantages of immunoassays such as ELISA include slow reaction kinetics between immobilized antibodies and antigens, poor reproducibility in immobilization of the antibodies or antigens, as well as non-specific binding of reactants to the solid support (Bao, 1997). The radioactive labels used in RIA raise environmental concerns, as care must be taken in the use and disposal of all radioactive reagents. Also when coupling a gel electrophoresis separation with an immunoassay, the electric field necessary to drive the separation creates a current and subsequently heating the gel bed that can be detrimental to analytes. Typically low electric fields are applied to minimize the current and dissipate the heat produced in the gels; however, with lower electric fields, analysis times are increased ranging from hours to days.

Capillary Electrophoresis

Capillary electrophoresis is an analytical technique used to separate charged analytes such as proteins, peptides, and oligonucleotides with high efficiency and sensitivity. Typically separations are performed within fused silica capillaries with inner diameters of 5-100 μm and lengths from 10-100 cm. Because of the small cross-section of the capillary, smaller sample volumes are used for detection and larger electric fields may be employed. With conventional electrophoresis methods such as gel electrophoresis, the applied electric field generates large currents and heating of the capillary bed. However, the large electrical resistance of capillaries as well as their small cross-sections reduces the current and subsequent heating. Typically this heating phenomenon or Joule heating is minimal if the power generated at the capillary surface is below 0.01 W/cm. Compared to gel electrophoresis, the larger electrical fields employed

with capillary electrophoretic separations reduce the separation and total analysis time from hours to minutes. Also the flat flow profile of CE separations (generated from the electroosmotic flow induced in the capillary) does not contribute to broadening of the analyte zones therefore increasing peak efficiencies compared to other separation methods such as liquid chromatography.

Several modes of CE have been developed to expand the technique for varying types of analytes and applications. The simplest and most commonly used mode is capillary zone electrophoresis (CZE). Other CE modes include micellar electrokinetic capillary chromatography (MEKC), which is a valuable technique for separating neutral and ionic analytes (Mazzeo, 1997), capillary isoelectric focusing (cIEF) in which analytes such as proteins are separated according to their isoelectric points (Rodriguez-Diaz *et al.*, 1997), and capillary electrochromatography (CEC) which incorporates the resolving power of CE with solid stationary phases (Dermaux and Sandra, 1999). In this research CZE, affinity capillary electrophoresis (ACE), which separates analytes based on their binding with specific ligands, and capillary gel electrophoresis (CGE), which is valuable for analytes such as oligonucleotides which have similar charge to mass ratios, were employed.

Capillary Zone Electrophoresis

Capillary zone electrophoresis (CZE) is the simplest and most widely used mode of CE separation. Typically the capillary is filled with electrophoresis buffer and analytes are injected onto the column via hydrodynamic or electrokinetic means. Separation voltages range from 1-30 kV with electric fields in the range of 300 V/cm to 1200 V/cm. The electrophoretic separation is dependent on the inherent electrophoretic mobilities of the analytes and the electroosmotic flow within the capillary. The

electrophoretic mobility (μ) of a molecule is a function of its charge and Stokes radius as expressed by the following equation:

$$\mu = \frac{q}{6\pi\eta r} \quad (1.3)$$

where q is the charge of the molecule, η is the viscosity of the electrophoresis buffer, and r is the Stokes radius of the analyte. The molecular mass of the analyte (MW) can be related to the Stokes radius by the following relationship:

$$MW = \frac{4}{3}\pi r^3 V \quad (1.4)$$

in which V is the volume of the solute. The electrophoretic mobility of the analyte may than be approximated as:

$$\mu \propto \frac{q}{MW^{\frac{2}{3}}} \quad (1.5)$$

Electrophoretic mobility is specific for each molecule; however, electroosmotic flow (EOF) is a nonselective mode of fluid transport within the capillary. Typically at higher pHs, bare, fused silica capillary walls become negatively charged as silanol groups on the surface are deprotonated. The negatively charged walls induce the formation of a double layer at the interface adjacent to the stagnant double layer. Under the influence of the applied electric field, mobile cations from the electrophoresis buffer migrate towards the cathode, pulling solvent molecules in the same direction. The flat flow profile for CE is generated from the electroosmotic flow induced in the capillary, as the flow is prevalent around the capillary walls and reduces band broadening. The EOF within the capillary is often 10-100 times stronger than the electrophoretic mobility of an analyte and is advantageous in separating negatively charged analytes. For most CE separations

analytes are injected at the anode and migrate toward the cathode or more negative electrode. However, anions with their inherent negative electrophoretic mobilities migrate towards the anode and would remain undetected if not for the EOF in the capillary which pushes them towards the detector.

Affinity Capillary Electrophoresis

Affinity capillary electrophoresis (ACE) utilizes the change in electrophoretic mobility of an analyte upon binding with a ligand as the separation criteria. ACE measurements incorporate the ligand into the electrophoresis buffer, and the analyte binds with the ligand during the electrophoretic separation. By monitoring the change in electrophoretic mobility of the analyte with the changing ligand concentration, binding affinities and stoichiometries for a receptor-ligand system may be determined (Heegaard and Kennedy, 1999). ACE has been used to characterize interactions such as peptide-peptide binding (Gomez *et al.*, 1994), metal-protein interactions (Heegaard and Robey, 1993), and sugar-protein binding (Honda *et al.*, 1992). For this work, ACE was employed to determine binding constants for oligonucleotide-nucleotide complexes.

Capillary Gel Electrophoresis

Capillary gel electrophoresis (CGE) is a valuable technique for separating molecules such as large oligonucleotides and proteins, which have similar charge to mass ratios but differ in molecular size. Some of the first examples of CGE employed polyacrylamide crosslinked polymer gels similar to those used for gel electrophoresis methods (Zagursky and McCormick, 1990; Luckey *et al.*, 1990; Swerdlow *et al.*, 1991). Crosslinked polyacrylamide gels have been used to separate small DNA fragments for sequencing applications (Swerdlow and Gesteland, 1990; Cohen *et al.*, 1990); however, these gels are cumbersome and have limited stability in which bubble formation and

clogged gel pores commonly occur during electrophoretic separations (Sunada and Blanch, 1997). CE separations employing replaceable polymer solutions have been developed as alternatives to crosslinked gels. Polymers such as polyacrylamide (Chiari *et al.*, 1992), poly(ethyleneoxide) (PEO) (Fung and Yeung, 1995), cellulose derivatives (Barron *et al.*, 1993), agarose (Klepárník *et al.*, 1993), and dextran (Ganzler *et al.*, 1992) have been used for separating DNA fragments as well as SDS (sodium dodecyl sulfate)-protein complexes. By varying the polymer used, as well as the concentration and the molecular weight of the polymer, CGE separations can be employed for separating various analytes such as double stranded DNA, restriction fragments, oligonucleotides, and denatured proteins (Gelfi *et al.*, 1996; Barry *et al.*, 1996; Butler *et al.*, 1994; Benedek and Guttman, 1994).

Instrumentation

Figure 1-1 shows typical CE instrumentation in which fused silica capillaries with inner diameters of 5-100 μm are employed for electrophoretic separations. The ends of the capillary are placed within two buffer reservoirs (an inlet and outlet) which contain two electrodes that provide a connection between the capillary and the high voltage power supply (0-30 kV). After the capillary is filled with the separation buffer, samples are introduced onto the capillary via a pressure (hydrodynamic) or electrokinetic injection. To perform the separation, high voltage is applied across the capillary, and analytes migrate towards the opposite electrode. Analyte migration is a function of the mode of CE being employed; for example in traditional CZE positively charged analytes (cations) will be detected first, followed by unresolved neutrals, and then anionic (negatively charged) analytes. For detection, a small region of the polyimide coating

used to fortify the capillary must be removed to provide an optical path. Common online CE detection methods include ultraviolet (UV) absorbance and laser induced fluorescence (LIF).

Detection

Absorbance

Absorbance detection is the most common mode of detection employed for CE separations. Typically most compounds absorb in some region of the UV spectrum; therefore, derivatization is not necessary for detection. However, the small optical pathlengths of capillaries result in small absorbances. Lengthening the absorbance pathlength can increase the sensitivity of the method. Rectangular capillaries (Tsuda *et al.*, 1990), Z-shaped flow cells (Chervet *et al.*, 1990), multi-reflection cells (Wang *et al.*, 1991), and bubble cell capillaries (Xue and Yeung, 1994) have been used to increase the capillary optical pathlength. However, all these methods can contribute to increases in detector variance and reduce the resolution and efficiency of the separation.

Laser Induced Fluorescence

Laser induced fluorescence (LIF) is one of the most sensitive detection modes for CE separations. Concentration detection limits of 10^{-13} M (Timperman *et al.*, 1995) have been reported with mass limits of detection of yoctomoles (Chen *et al.*, 1994) as well as single molecule detection (Lee *et al.*, 1994). Commonly a microscope objective with a high numerical aperture objective is employed for collection of the fluorescence emission. Other optical collection schemes include the use of a parabolic reflector in which a collection efficiency approaching 50% has been reported (Pentoney *et al.*, 1992).

This work employed a commercial CE apparatus developed by Beckman-Coulter (Fullerton, CA) which uses a similar collection scheme (Figure 1-2) as that developed by

Pentoney, *et al.* (1992). Excitation light from the laser (488 nm line of a Argon ion laser) is focused onto the capillary window via a fiber optic. Once fluorescent analytes within the capillary are excited, the fluorescence emission is scattered, collected, and reflected by the ellipsoidal reflector towards a mirror and onto a bandpass filter. For this instrument a 520 nm bandpass filter (optimized for the emission of fluorescein dyes) is used to remove any excess excitation light but pass the fluorescence emission onto the PMT for detection.

Most analytes are not natively fluorescent; therefore derivatization with fluorophores is a necessity for LIF detection. Common derivatization reagents for oligonucleotides include fluorescein derivatives such as fluorescein isothiocyanate (FITC), tetramethylrhodamine (TMR) and its carboxylic acid (TAMRA), carboxy-X-rhodamine (ROX), and water-soluble cyanine dyes such as Cy3 and Cy5. Facile labeling of oligonucleotides with an array of chemical fluorophores is possible due to commercially available automated synthesis techniques.

Capillary Electrophoresis Immunoassays

Capillary electrophoresis immunoassays (CEIA) have emerged as alternatives to conventional affinity assays such as ELISA. Advantages of CEIA versus conventional immunoassays include the following: rapid analysis times, less sample and reagent consumption, automation, and simultaneous determination of multiple analytes (Bao, 1997). By coupling LIF detection with CEIA, low mass detection limits are possible; however, the concentration detection limits of CEIA are similar to conventional assays. High throughput assays are essential for analyzing large batches of analytes simultaneously, but CE is a serial method limiting the throughput of the technique.

Multiplexing capillaries and microfluidic devices are two methods that can increase the throughput of CE immunoassays (Zhang *et al.*, 1999; Cheng *et al.*, 2001).

Two types of immunoassays may be performed, competitive and noncompetitive assays. Figure 1-3 depicts the competitive CEIA in which the antigen (Ag) of interest is mixed with a known concentration of its labeled form (Ag^*) and they compete to bind with a limited concentration of corresponding antibody (Ab). Two zones are separated and detected, the free labeled Ag^* and the fluorescently labeled Ab- Ag^* complex. Upon addition of Ag, the ratios of the bound and free will change as the unlabeled antigen competes with the labeled antigen. At low concentrations of Ag, the labeled complex is large and a small Ag^* peak will be detected, and at high concentrations of Ag, Ab- Ag^* will be small whereas the Ag^* peak will be large. The increase in the signal of Ag^* , the decrease in the signal of Ab- Ag^* , or the bound to free ratio (Ab- Ag^*/Ag^*) can be used to indirectly quantitate the Ag in a sample.

In contrast the noncompetitive assay (Figure 1-4) incorporates a labeled antibody (Ab^*) to react with Ag. In this case the antigen may be quantitated directly by measuring the Ab^* -Ag complex which is separated from the free Ab^* . Noncompetitive assays offer several advantages to competitive assays including larger linear dynamic ranges, lower detection limits, and direct quantitation of the complex. In some instances antibodies form complexes with other analytes besides the antigen especially when the antibody specificity is weak; however, noncompetitive assays have the ability to distinguish between cross-reactive species. Since Ab^* is employed for the assay, all complexes will be labeled and may be detected after separation. However, developing noncompetitive immunoassays can be problematic since antibodies are difficult to fluorescently label and

separating the free Ab^* and Ab^*-Ag complex may be difficult due to the small differences in electrophoretic mobilities. The two types of affinity assays are compared in the following tables.

Table 1-1 Advantages of noncompetitive and competitive affinity assays.

| Noncompetitive | Competitive |
|--------------------------------|---------------------------------------------|
| Increased linear dynamic range | Simpler separation of Ag^* from $Ab-Ag^*$ |
| Detect cross-reactivity | Facile labeling of Ag |
| Lower limits of detection | |

Table 1-2 Disadvantages of noncompetitive and competitive affinity assays.

| Noncompetitive | Competitive |
|----------------------------------------------|-----------------------------|
| Difficult to label Ab | Non-linear calibration |
| Separating Ab^* and Ab^*-Ag is difficult | Slower binding kinetics |
| | Undetected cross-reactivity |

Competitive CE Immunoassays

Because of the ease of implementation, most CE immunoassays that have been developed employ the competitive format. Competitive CEIA is advantageous for small analytes such as peptides and low molecular weight organic molecules in which the electrophoretic mobility difference between the antibody-antigen complex and the free antibody is small (Schmalzing and Nashabeh, 1997). The first reported competitive CEIA was developed for insulin in which an antibody fragment for insulin was employed (Schultz and Kennedy, 1993). Insulin was labeled with fluorescein; however, insulin has

two labeling sites and HPLC purification was necessary to separate the labeled species before incorporation into CEIA. Separations were accomplished in less than 3 min when employing an electric field of 500 V/cm. A limit of detection for insulin was reported as 3 nM or 420 zmol injected. This immunoassay was then incorporated to measure the insulin content of single islets of Langerhans as well as insulin secretion from single islets (Schultz *et al.*, 1995).

Continuous on-line monitoring of insulin secretion from single islets was developed with further optimization of the competitive insulin CEIA and employing flow injection analysis (Tao and Kennedy, 1996). The capillary (5 μ m i.d.) effective length was 8 mm and a high electric field (4000 V/cm) was used for the separation. The complex and free (Ab-Ag* and Ag*) were separated in 1s and 1600 consecutive electropherograms could be collected before rinsing the capillary suggesting this system could be automated for high throughput analysis. The detection limit for the assay was reported as 270 pM with a mass detection limit of 430 zmol.

Competitive CE immunoassays have also been developed for determining analytes in complex matrices such as serum and urine. Schmalzing, *et al.* (1995) developed a CE-LIF immunoassay for cortisol, a steroid hormone, employing a Fab fragment of the antibody and fluorescently labeling cortisol with fluorescein. When quantitated in human serum, cortisol levels can provide diagnostic information about adrenal malfunction. No sample cleanup was necessary to determine the cortisol levels in the serum and detection was possible within the clinically relevant range (30-1700 nM) for diagnostic purposes (Schmalzing *et al.*, 1995). Also demonstrating the utility of CEIA for complex matrices, Chen and Evangelista (1994) developed an assay to

simultaneously determine two drugs in urine, morphine and PCP. For this assay, the antigens morphine and PCP were labeled with the water-soluble cyanine dyes Cy 5 and Cy 5.5 respectively. The two complexes were found to co-elute; however, it was possible to use the change in the free antigen (Ag^*) concentration to quantitate the levels of the drug found in urine samples. Separation times were under 5 minutes with reported limits of detection of 4 nM for PCP and 40 nM for morphine. Furthering the utility of the competitive CEIA for diagnostics, assays have been developed for antigens such as scrapie protein (PrP^{Sc}), cyclosporin A, and staphylococcal enterotoxin A (SEA) (Schmerr and Jenny, 1998; Ye *et al.*, 1998; Lam *et al.*, 1999)

Noncompetitive CE Immunoassays

Noncompetitive CEIA or affinity probe capillary electrophoresis (APCE) is a direct method for quantitating an antigen or antibody of interest (Shimura and Karger, 1994). For quantitating an antigen, the antibody is labeled with a fluorophore (Ab^*) and is added in excess to the antigen (Ag). After formation of the antibody-antigen complex (Ab^*-Ag) and injection onto the separation capillary, two zones are separated the labeled Ab^*-Ag complex and the free Ab^* . The noncompetitive CE assay directly quantitates Ag by measuring the amount of complex formed or the decrease in the free Ab^* . Antibodies may also be detected via a noncompetitive CEIA by incorporating a labeled Ag^* as the affinity probe.

Considerable work has been published demonstrating the use of noncompetitive CE assays for detecting antibodies. To demonstrate the concept of employing CZE-LIF for noncompetitive immunoassays, FITC-insulin (Ag^*) was used to determine anti-insulin (Ab) with a 3 min separation in which a concentration detection limit of 2 nM and a mass detection limit of 280 zmol was reported (Schultz and Kennedy, 1993). By

doubling the electric field strength from 500 V/cm to 1000 V/cm the separation time was reduced to 1 min. This reduction in separation time is especially advantageous for investigating antibodies with weak affinities for an antigen. With long separation times, a weaker antibody-antigen complex may dissociate affecting detection and quantitation of the assay. In other applications, noncompetitive CEIA was used to screen antibodies for a specific antigen (morphine) (Envagelista and Chen, 1994). Four commercially available antibodies were screened for affinity with a morphine-Cy 5 conjugate. Three were found to have low or no affinity with the antigen. The antibody with the highest affinity was then screened for cross-reactivity with opiate derivatives in which morphine based opiates showed varying affinity for the antibody. This assay demonstrates the ability of noncompetitive CEIA to evaluate antibodies for incorporation into analytical applications.

To demonstrate the use of labeled antibodies (Ab^*) for determining analytes, a noncompetitive CE assay was developed for human growth hormone (hGH) (Shimura and Karger, 1994). In this report, tetramethylrhodamine-iodoacetamide was employed to label an antibody fragment of anti-hGH. With this fluorophore a thiol group in a hinge region of the antibody was labeled ensuring the binding site of the antibody was not hindered. Capillary isoelectric focusing (cIEF) was employed to separate the Ab^* -Ag complex from the free Ab^* . In comparison to CZE, a 100-fold enhancement of the detection limit was predicted by employing cIEF as the sample zones were concentrated and separated simultaneously. The assay was linear over three orders of magnitude for the antigen and a detection limit of 0.1 ng/mL (5 pM) was reported. An advantage of noncompetitive assays is the ability to distinguish between cross-reactive species, as each

antigen should form an individual complex with the labeled antibody. With this assay, Ab* was incubated with three variants of hGH, and three well resolved complexes were observed upon separation demonstrating the detection of cross-reactive species.

Upon binding with small antigens, separating the free Ab* and Ab*-Ag complex may be difficult due to small changes in the electrophoretic mobility of Ab*. To improve the use of antibodies for noncompetitive assays, adding "shift ligands" to the separation buffer have been investigated (Tim *et al.*, 2000). A shift ligand is a charged competitive ligand that binds Ab* with weak affinity increasing the electrophoretic mobility of Ab*. Tim *et al.* (2000) developed a noncompetitive CE-LIF assay for human carbonic anhydrase II (HCAII). The HCAII was labeled with 5-iodoacetamidofluorescein (5IAF) and binds selectively with the drug dorzolamide (Dz) ($K_d = 0.6$ nM). When the labeled HCAII was mixed with Dz, the HCAII-Dz complex was formed but co-migrated with the free HCAII. The sulfonamide para-carboxybenzenesulfonamide (p-CBS) was added to the separation buffer to bind with the free HCAII (K_d in the low micromolar range). Upon binding with the negatively charged p-CBS, the free HCAII peak was shifted and migrated faster than before. When Dz and HCAII were incubated together, the HCAII-Dz complex was formed and the weaker shift ligand (p-CBS) was effectively blocked from binding with the complexed antibody. However, the excess HCAII reacted with the p-CBS in the separation buffer increasing the resolution of the free HCAII and the HCAII-Dz complex. This APCE method was employed to determine Dz concentrations in aqueous, urine, and plasma samples. Limits of detection were reported as 16 pM in aqueous solutions and 62 pM for the urine and plasma samples.

Another limitation of noncompetitive assays is the electrophoretically heterogeneous products encountered when antibodies or antibody fragments are fluorescently labeled. Hafner *et al.* (2000) used a thiol specific labeling reagent 5-iodoacetamidofluorescein (5-IAF) to produce a homogenous, labeled affinity probe. The 5-IAF was used to selectively derivatize a single-chain antibody fragment (scFv), the smallest construct of an antibody that contains the binding site, specific for digoxin. Site directed mutagenesis was used to introduce a cysteine residue into the scFv fragment providing a single labeling site for the 5-IAF. After incubating the labeled fragment (scFv*) with digoxin, electrophoretic separation produced two distinct zones, the excess scFv* and the scFv*-digoxin complex. The limit of detection were reported as 10 pM for digoxin. To increase the sensitivity of the assay, solid-phase extraction was employed for preconcentration of digoxin before analysis. Digoxin limits of detection of 200 fM and 400 fM were reported for aqueous and serum samples respectively when coupling solid-phase extraction with the APCE separation.

In addition to these methods, alternatives to antibodies have been pursued to further improve noncompetitive assays for use as analytical diagnostic tools. Oligonucleotides or aptamers are affinity probe alternatives for use in affinity assays. Aptamers, which are highly negatively charged, low molecular weight oligonucleotides that are easily labeled with fluorescent dyes, should be ideal affinity probes for CE separations.

Aptamers

Aptamers, derived from the Latin word "aptus" meaning "to fit," are short RNA or DNA sequences designed to bind to a target molecule with high affinity and specificity (Ellington and Szostak, 1990). Aptamers are developed with an *in vitro* selection method

coined SELEX (systematic evolution of ligands by exponential enrichment) (Tuerk and Gold, 1990). In comparison to antibodies, aptamers do not require animal hosts during production or *in vivo* conditions; thus they may be developed for almost any target of interest. Aptamers are developed via chemical synthesis techniques, providing reproducible products that can be purified with techniques such as HPLC and gel electrophoresis. Aptamers can be derivatized with organic dyes such as fluorescein or conjugated with molecules such as biotin for incorporation into analytical diagnostic tools, and aptamers undergo reversible denaturation making them stable for extended storage (Jayasena, 1999).

SELEX

SELEX is an iterative *in vitro* process in which a large random pool of oligonucleotides (DNA or RNA) is screened for affinity to target analytes. The SELEX process is illustrated in Figure 1-5. In developing the oligonucleotide library, all sequences are composed of two fixed primer regions to allow for amplification and transcription. One primer is present at the beginning of the sequence and the other at the end of the sequence. The diversity of the oligonucleotide library is dependent on the number of randomized nucleotides positions (N) found between the two primer regions. Since four basic building blocks (nucleotides) are used for any oligonucleotide, the theoretical sequence space of the library can be composed of 4^N molecules. Because of experimental limitations with analyzing such a large pool of sequences, typical SELEX libraries consist of 10^{14} - 10^{15} molecules (James, 2000). After composing the library, the oligonucleotides are incubated with a limited amount of the analyte in order to screen for high affinity sequences. In many examples, analytes have been immobilized on solid supports and as the library is washed over the target, sequences with higher affinity are

captured and retained whereas non-binding sequences are rinsed away. However, by immobilizing the target, the interaction between the target and the aptamer sequences is impeded. With target analytes such as proteins, other aptamer screening techniques have been employed. Nitrocellulose filters are one screening alternative as they can retain the aptamer-protein complexes without requiring binding to a support and the lower affinity sequences are passed through the filter. Once the non-binding sequences are removed, subsequent rinses can be used to remove the higher affinity oligonucleotides from the target. These binding sequences are collected and amplified by the polymerase chain reaction (PCR). With subsequent rounds of binding, collection, and amplification, a few higher affinity oligonucleotides are isolated which are then sequenced and characterized.

Aptamers can be characterized by measuring the binding affinity for their specific analytes. The binding relationship is depicted in the following equilibrium in which the aptamer (A) and the analyte (T) bind forming the aptamer-analyte complex (A-T).



One common term used to express complex affinities is the dissociation constant (K_d). The dissociation constant is an expression relating the concentration of the complex present in relation to the concentrations of the aptamer and analyte.

$$K_d = \frac{[A - T]}{[A][T]} \quad (1.2)$$

Dissociation constants will be used in the remainder of this test as a measure of affinity between an aptamer and its analyte.

Aptamer Characteristics

The molecular weights of aptamers range from 7.5 – 32 kDa generally consisting of 15-100 nucleotide sequences. The length of an aptamer sequence is determined by the sequence space (number of randomized nucleotides) of the original library used during selection. Also contributing to the length of the sequence is the two primer regions that are necessary for amplification and transcription processes. Generally a small aptamer is desired for use in therapeutic and diagnostic applications. Most aptamers generated from a selection are quite long (40-100 nucleotides); therefore, further analysis is required to truncate the sequence length but still maintain the functionality of the aptamer. For example a 23 nucleotides (nt) long RNA aptamer was developed for the protein vascular endothelial growth factor (VEGF), a 41nt DNA aptamer was developed for the sugar cellobiose, and a DNA aptamer for the protein thrombin was 15 nt long (Jellinek *et al.*, 1994; Yang *et al.*, 1998; Bock *et al.*, 1992). These few aptamers demonstrate the variation in sequence lengths generated from SELEX selections.

Aptamers have been generated for a wide array of targets including small ions, nucleotides, peptides, organic dyes, sugars, proteins, and even whole cells (Ciesiolka and Yarus, 1996; Nieuwlandt *et al.*, 1995; Williams *et al.*, 1997; Ellington and Szostak, 1992; Sassanfar and Szostak, 1993; Bock *et al.*, 1992; Morris *et al.*, 1998). Aptamer dissociation constants (K_d) range from the low nanomolar (nM) to high micromolar range (μ M). For example, RNA aptamer dissociation constants (K_d) of 0.3 μ M to 65 μ M were reported for the small molecules citrulline and arginine (Famulok, 1994; Geiger *et al.*, 1996). A K_d of 700 nM was determined for a DNA aptamer selective for cellobiose, the sugar monomer of cellulose (Yang *et al.*, 1998). Bock *et al.* (1992) reported a K_d of 280

nM for a DNA aptamer specific for thrombin, a serine protease (MW 34 kDa); however, an RNA aptamer with a higher affinity ($K_d = 25$ nM) was also developed (Kubik *et al.*, 1994). Typically RNA aptamers have displayed higher affinity for targets relative to DNA aptamers. For larger proteins such as human neutrophil elastase, HNE, (MW 200 kDa), Immunoglobulin E, IgE, (MW 200 kDa), and L-selectin (MW 100 kDa), DNA aptamers K_d 's of 17 nM, 10 nM, and 1.8 nM respectively were reported (Lin *et al.*, 1995; Wiegand *et al.*, 1996; Hicke *et al.*, 1996). This trend suggests aptamers form higher affinity complexes with larger targets such as proteins.

Aptamers have been developed to not only display high affinity but also be specific for their target molecules. For example, a RNA aptamer for theophylline was found to have a 10,000 fold greater affinity for its target than for caffeine, though caffeine and theophylline only differ by one methyl group (Jenison *et al.*, 1994). Other aptamers have been found to be selective for enantiomers. For example a RNA aptamer was reported to display a 12,000 fold greater affinity for L-arginine than D-arginine (Geiger *et al.*, 1996). However, there are limits of aptamer specificity. A DNA aptamer selective for cellobiose was also found to bind the polymer cellulose, in which cellobiose is the monomer or repeating unit (Yang *et al.*, 1998). However, the aptamer was able to discriminate against similar disaccharides such as lactose and maltose.

Diagnostic and Therapeutic Applications

Many cases have been reported detailing how aptamers may affect cellular processes. For example, DNA and RNA aptamers isolated with *in vitro* selection were found to be antagonists for the IgE antibody (Wiegand *et al.*, 1996). IgE antibodies play a key role in allergic responses by releasing biogenic amines upon binding its receptor. Each aptamer was found to competitively bind to IgE inhibiting the immunoglobulin

from interacting with its receptor molecule blocking the release of biogenic amines such as serotonin. By inhibiting the release of serotonin, the IgE aptamers may possibly be used as new therapies for allergies.

In another example, a DNA aptamer was found to block the enzyme activity of thrombin, a serine protease that plays a key role in blood coagulation (Bock *et al.*, 1992). Developing an inhibitor for thrombin to promote anticoagulation is highly desired for therapeutic treatment of vascular diseases. Heparin is the most common anticoagulant employed; however, the long lifetime of heparin makes anticoagulation difficult to reverse and in some instances bleeding is induced (Wang *et al.*, 1993). *In vitro* investigations showed the DNA aptamer inhibited thrombin dependent blood clotting by 50% (Bock *et al.*, 1992). The thrombin aptamer has been incorporated into *in vivo* investigations and employed in pre-clinical studies to further explore the possibility of using aptamers for therapeutics (Li *et al.*, 1994; DeAuda *et al.*, 1994; Famulok and Mayer, 1999).

Analytical Applications

Aptamers are alternatives to antibodies for affinity based analytical applications, and have been incorporated into analytical applications such as flow cytometry, sensors, and ELISA type assays (Kleijnung *et al.*, 1998; Potyarailo *et al.*, 1998; Davis *et al.*, 1996; Drolet *et al.*, 1996). An affinity sensor for L-adenosine was developed employing a biotinylated RNA aptamer immobilized on a fiber derivatized with streptavidin (Kleijnung *et al.*, 1998). For detection L-adenosine was labeled with fluorescein, and the affinity between the bound aptamer and labeled L-adenosine was similar to that previously found in solution. The aptamer sensor was found to have a 1700-fold greater affinity for its target L-adenosine than with other similar analytes (Kleijnung *et al.*,

1998). Another sensor employed a DNA aptamer specific for thrombin in which the protein was detected by fluorescence anisotropy (Potyarailo *et al.*, 1998). The 5' end of the aptamer was modified with fluorescein whereas the 3' end was modified with an alkyl amine to promote attachment to a glass slide. Upon addition of thrombin, a change in polarization was measured for the aptamer, as its movement is restricted upon binding with the target. Specificity of the thrombin aptamer sensor was demonstrated as no change in fluorescence anisotropy was measured when another similar protein, elastase, was washed over the sensor. The sensor was used for repeated measurements by removing the bound thrombin with a denaturing agent thus regenerating the sensor surface (Potyarailo *et al.*, 1998)

Continued research is necessary to further explore and develop aptamers for analytical applications. This work has investigated using aptamers as alternatives to antibodies for use in noncompetitive capillary electrophoresis affinity assays in hopes of expanding the utility of aptamers as bioanalytical tools.

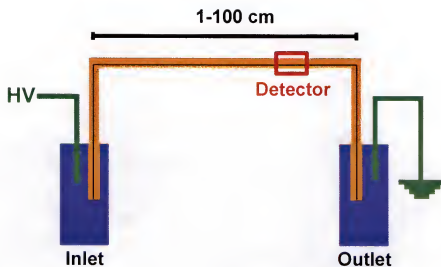


Figure 1-1 Schematic of capillary electrophoresis (CE). The ends of a fused, silica capillary (5-150 μm inner diameters, 1-100 cm lengths) are immersed into two buffer reservoirs that contain electrodes to connect the capillary to a power supply. Once an electric field is applied, analytes migrate through the capillary and are detected.

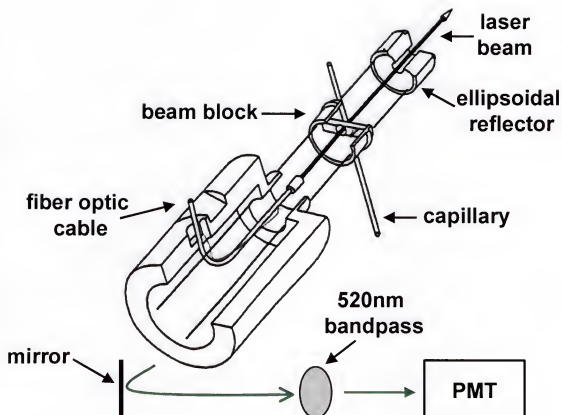


Figure 1-2 Laser induced fluorescence (LIF) optical detector in which excitation light from an Argon ion laser is focused onto the capillary. The fluorescence emission is collected by the elliptical reflector and reflected towards a mirror and the 520 nm bandpass filter. The filtered fluorescence emission is detected with a PMT. Copyright Beckman-Coulter, Inc. Fullerton, CA.

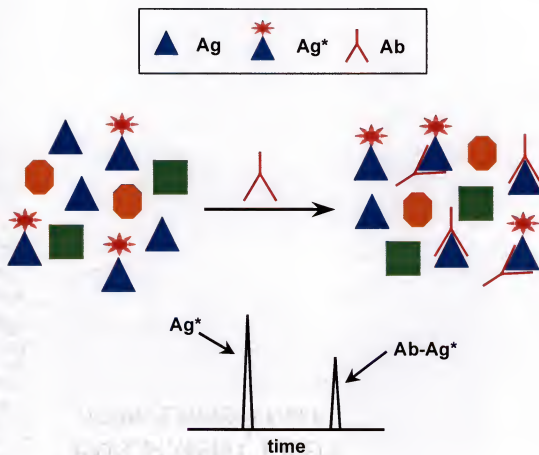


Figure 1-3 Competitive CE immunoassay in which a known concentration of labeled antigen (Ag^*) is added to a limited amount of its specific antibody (Ab). As unlabeled antigen (Ag) is added to the mixture, Ag and Ag^* compete to bind with the limited amount of Ab decreasing the $Ab-Ag^*$ peak. With electrophoretic separation two zones are detected, the labeled complex ($Ab-Ag^*$) and free Ag^* .

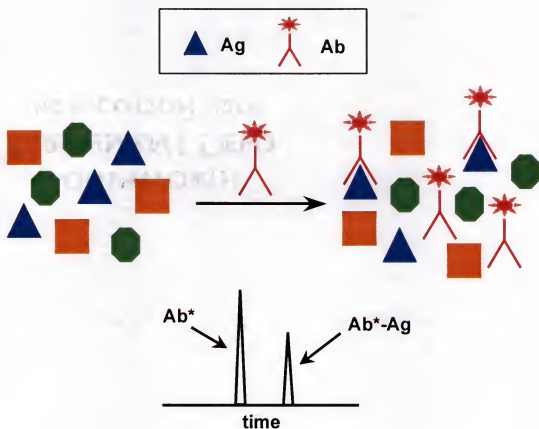


Figure 1-4 Noncompetitive CE immunoassay in which a limited amount of the labeled antibody (Ab^*) is added to a mixture containing its specific antigen (Ag). After injection onto the capillary and separation, two zones are detected, the labeled Ab^* -Ag complex and free Ab^* .

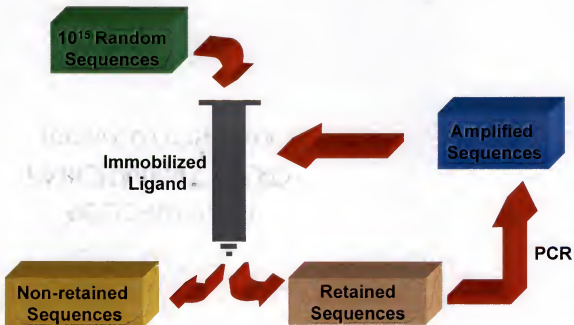


Figure 1-5 Schematic of systematic evolution of ligands by exponential enrichment (SELEX). A large pool of random oligonucleotides is screened for affinity for an immobilized target molecule. The column is rinsed removing low affinity oligonucleotides or non-retained sequences. Sequences with higher affinity can then be collected but need to be amplified with PCR (polymerase chain reaction). With 8-10 cycles of selection and amplification, several high affinity sequences can be isolated for characterization.

CHAPTER 2

A NONCOMPETITIVE APTAMER AFFINITY ASSAY EMPLOYING CAPILLARY ELECTROPHORESIS WITH LASER INDUCED FLUORESCENCE DETECTION

Introduction

Most capillary electrophoretic immunoassays (CEIA) have utilized a competitive format; however, noncompetitive assays offer several advantages to competitive assays including larger linear dynamic ranges (due to direct quantitation of the complex), the ability to distinguish between cross-reactive species, and detection limits which are less dependent on binding affinities (Shimura and Karger, 1994). A noncompetitive assay typically incorporates an excess of labeled affinity probe such as an antibody (Ab^*) to react with a specific antigen (Ag). The antigen is quantitated directly by measuring the Ab^* -Ag complex which is electrophoretically separated from the free Ab^* .

Development of noncompetitive immunoassays can be problematic since fluorescently labeling of antibodies typically produces heterogeneous products, and separating the free Ab^* and Ab^* -Ag complex may be complicated due to small changes in electrophoretic mobilities. One technique for producing homogenous, labeled affinity probes is to use thiol specific labeling reagents such as 5-iodoacetamidofluorescein which selectively derivatize cysteine residues present in the antibody (Shimura and Karger, 1994; Hafner *et al.*, 2000; Tim *et al.*, 2000). Also to aid in the separation of Ab^* and Ab^* -Ag, a “shift ligand,” which binds with weak affinity to the binding site of Ab^* , can be added to the separation buffer (Hafner *et al.*, 2000; Tim *et al.*, 2000). The charged shift ligand increases the electrophoretic mobility of Ab^* ; however, once Ab^* -Ag is

formed, the weaker affinity shift ligand is effectively blocked from binding with the complexed antibody. Any remaining free Ab* interacts with the charged ligand, increasing the electrophoretic mobility difference between the “shift ligand”-Ab* complex and Ab*-Ag subsequently enhancing the separation of Ab* from Ab*-Ag.

Though several techniques have been developed to improve noncompetitive CE immunoassays, alternatives to antibodies, such as aptamers, are being explored. Aptamers are short, single-stranded oligonucleotide sequences developed with the combinatorial chemistry technique SELEX (systematic evolution of ligands by exponential enrichment) to bind with a target molecule with high specificity and affinity (Ellington and Szostak, 1990; Tuerk and Gold, 1990). Aptamers possess several favorable characteristics making them suitable affinity probes for noncompetitive CE affinity assays. Automated chemical synthesis techniques are rapid and relatively inexpensive and enable facile labeling of aptamers with fluorescent dyes. Also aptamers are low molecular weight ligands with a high degree of charge, and upon binding with an analyte such as a protein, the negative charge of the aptamer is reduced and its overall mass is increased. The resolution of the complex from the free aptamer should be greatly enhanced due to the large difference in the electrophoretic mobilities (μ) of the free aptamer and the aptamer-protein complex.

One concern with aptamer complexes, especially those formed with proteins, is dissociation over the course of the separation. Proteins adhere quite rapidly to the walls of unmodified capillaries typically employed in CZE. If the aptamer-protein complex is adsorbed onto the capillary walls, dissociation may occur as the aptamer is pulled through the capillary (by the EOF or electric field) but the protein remains behind on the capillary

surface. Employing coated capillaries is one method to reduce protein absorption (Hjertén, 1985; Cobb *et al.*, 1990; Schmalzing *et al.*, 1993; Malik *et al.*, 1993). Coating of the capillary walls with substances such as polyacrylamide not only reduces the absorption sites on the walls but also reduces the EOF within the capillary. Under these separation conditions, the complex, which has the less negative electrophoretic mobility (μ), migrates slower than the free aptamer.

Because of the decrease in the EOF when employing coated capillaries, the aptamer complex spends more time on the column providing ample time for partial or complete complex dissociation to occur. Incorporating polymer gel networks into the electrophoresis buffer is another technique to reduce complex dissociation. The most widely used method for analyzing protein-oligonucleotide interactions is the electrophoresis mobility shift assay (EMSA) (Lane *et al.*, 1992). Gel electrophoresis, employing crosslinked polymers such as polyacrylamide or agarose, is used to separate the protein-oligonucleotide complex from the free protein and free oligonucleotide. Several studies have shown greater stability of protein complexes in a gel relative to free solution (Lane *et al.*, 1992). This increase in stability has been described as an excluded volume or “caging” effect (Fried and Bromberg, 1981; Fried and Crothers, 1997). Once the complex begins to dissociate, the protein and oligonucleotide begin to move away from each other; however, with a gel present, the diffusion of the free analytes is impeded. The oligonucleotide and protein from the dissociated complex is maintained within a small zone; therefore, reassociation is favored, hence a “caged” complex. EMSA is essentially a gel electrophoresis technique that is laborious and time consuming. The capillary electrophoresis mobility shift assay (CEMSA) offers several

advantages to the conventional EMSA including ease of automation, increased resolution, rapid analysis times, small sample volumes, and on-line detection giving rise to increased sensitivity (Foulds and Etzkorn, 1998).

CEMSA with LIF detection has been demonstrated for several protein-oligonucleotide complexes (Foulds and Etzkorn, 1998; Xian *et al.*, 1996; Stebbens *et al.*, 1996; Janini *et al.*, 1995). Typically the oligonucleotide is labeled with a suitable fluorophore to allow for detection. Foulds and Etzkorn (1998) developed a CEMSA method utilizing unmodified capillaries and a MOPS (3-(N-morpholino)-propane sulfonic acid) electrophoresis buffer. With this method, binding affinities for several DNA-protein complexes were determined (Foulds and Etzkorn, 1999). However, most CEMSA applications have employed dilute polymer buffers to optimize the resolution of the complex and free oligonucleotide. Xian *et al.* (1996) employed a tris(hydroxyaminomethane), borate, ethylenediamine tetraacetic acid, pH 8.3 buffer (TBE) with 0.2% polyacrylamide (MW 750,000-1,000,000) to analyze a transcription factor (SpP3A2) from nuclear extracts, egg lysates, and a single sea urchin egg lysed within the capillary. Stebbins *et al.* (1996) investigated optimizing separation conditions for trp repressor-DNA complexes in which methyl cellulose (MW 100,000) buffers of varying concentrations (0.25%, 0.5%, and 0.75%) were investigated. Greater resolution and improved efficiency of the complex peak was achieved with a 0.75% methyl cellulose, TBE pH 8 buffer, demonstrating the effect of polymer concentration on the resolution of the free oligonucleotide from the protein-DNA complex.

Most reported CEMSA applications have employed dilute polymer solutions to enhance the separation of the free oligonucleotide from its complex; however, entangled

networks are necessary to achieve sieving that is characteristic of crosslinked gels typically employed for EMSA. With dilute polymer solutions, the polymer chains are isolated from each other and do not interact. Once the polymer concentration approaches the entanglement threshold, the polymer chains start to overlap and become densely packed. The entanglement threshold (c^*) may be expressed as:

$$c^* \approx \frac{3M_w}{4\pi N_A R_g^3} \approx \frac{1.5}{[\eta]} \quad (2.1)$$

in which M_w is the average molecular weight of the polymer, N_A is Avogadro's number, R_g is the radius of gyration, and $[\eta]$ is the intrinsic viscosity of the solution. Semidilute polymer solutions are those with polymer concentrations above the entanglement threshold. Entangled polymer solutions have been employed with CE for applications such as DNA sequencing and separating SDS denatured protein mixtures (Ruiz-Martinez *et al.*, 1996; Benedek and Guttman, 1994). Ultradilute polymer solutions have also been shown to improve resolution and efficiency of DNA separations (Barron and Blanch, 1994; Hubert *et al.*, 1996). With ultradilute polymer buffers, DNA molecules drag polymer molecules with them as they migrate through the capillary, resulting in a reduction of the mobility of the DNA. The number of polymer molecules an oligonucleotide can interact with is proportional to the length of the sequence; thus the increased resolution of the separation.

The aim of this work was to develop a noncompetitive CE-LIF aptamer assay for a 15-nucleotide long DNA aptamer (labeled with fluorescein) specific for thrombin (MW 34 kDa). To determine the most suitable separation conditions for detecting the aptamer-thrombin complex, capillary zone electrophoresis with unmodified capillaries,

polyacrylamide coated capillaries, and capillary electrophoresis with dilute polymer solutions were investigated.

Materials and Methods

Chemicals

A concentrated Tris/glycine buffer (250 mM Tris/1.92 M glycine) was purchased from Bio-Rad Laboratories (Hercules, CA). Methyl cellulose (25 cp @ 2% w/v), hydroxypropylmethylcellulose (100 cp @ 2% w/v), potassium chloride, and thrombin from human plasma (0.26 mg/mL), were purchased from Sigma Chemical (St. Louis, MO). A 10% polyacrylamide (MW 700,000-1,000,000) solution in water was purchased from Polysciences, Inc (Warrington, PA). Poly(ethylene oxide) (MW 300,000 and 2,000,000) was purchased from Aldrich Chemical (Milwaukee, WI). Boric acid, Tris(hydroxymethyl)aminomethane (Tris), and ethylenediaminetetraacetic acid disodium salt (EDTA) were purchased from Fisher chemical (Pittsburgh, PA). Dr. Andrew Ellington, University of Texas, generously donated the first sample of thrombin aptamer. Subsequent samples of the thrombin aptamer were purchased from Integrated DNA Technologies (Coralville, IA). For the labeled aptamer, fluorescein or a fluorescein derivative was chemically attached to the 5' end of the aptamer (5'GGTTGGTGTGGTTGG-3') and then purified with HPLC. All solutions were prepared with deionized water purified with a Milli-Q Plus system (Millipore Corp., Marlborough, MA).

Aptamer preparation

Before experiments, a 4 μ M stock of aptamer in electrophoresis buffer was prepared and annealed. For the annealing process, the stock solution was heated at 72°C

for 2.5 min and cooled to room temperature. All samples were prepared from the annealed 4 μ M DNA stock.

CGE buffer preparation

A 89 mM Tris, 89 mM borate, 2 mM EDTA, 5 mM KH_2PO_4 pH 8.3 buffer (TBE/K) was employed for all CGE experiments. The buffer was heated in an oil bath at 70° C for 5-10 min with constant stirring. HPMC (hydroxypropylmethylcellulose) or methyl cellulose was added slowly to the buffer (since neither are very water-soluble) in order to avoid forming large clumps of undissolved polymer. The solution was stirred continuously until the entire polymer had dissolved, typically on the order of 30-90 min. Solutions were cooled at room temperature before using. Preparation of polyacrylamide and polyethylene oxide solutions was accomplished by adding the appropriate concentration of polymer to the buffer and stirring continuously until the entire polymer was dissolved. Polyethylene oxide (PEO) solutions were difficult to prepare since PEO was found to be very insoluble.

Apparatus

All separations were performed with a Beckman P/ACE 2200 capillary electrophoresis system (Beckman Coulter Fullerton, CA). Bare, fused silica capillaries (50 μ m i.d., 360 μ m o.d.) were from Polymicro Technologies (Phoenix, AZ). Laser induced fluorescence (LIF) detection employed the 488 nm excitation line of a 3 mW Argon Ion laser (Beckman-Coulter) and emission was collected at 520 nm. Data was recorded and analyzed with P/ACE software (Beckman-Coulter).

Results and Discussion

In our initial attempts to develop an aptamer affinity assay, a thrombin binding DNA aptamer was investigated with CZE. Figure 2-1A shows an electropherogram of 1 μ M aptamer in a 20 mM NaH_2PO_4 pH 7.0 buffer. As seen in the electropherogram, several impurities are present in the aptamer sample (labeled IMP). With addition of excess thrombin (2 μ M), a decrease in the DNA* peak was observed (Figure 2-1B), but no complex was detected. One possible reason for no complex detection is adsorption of the thrombin to the capillary walls, subsequently promoting dissociation of the complex. At the pH used for our work (pH 7), the silanol groups on the capillary surface are deprotonated leaving a negatively charged surface for adsorption of analytes especially proteins. In hopes of preventing adsorption of the thrombin to the capillary surface, CE separations employing a polyacrylamide coated capillary were investigated.

A polyacrylamide capillary was prepared with a method adapted from Hjerten, (1985) and Clark *et al.* (1994) and is described in more detail later in this text (Chapter 5). The electroosmotic flow (EOF) is greatly suppressed in a coated capillary, since the polymer effectively covers the silanol groups on the capillary surface. With EOF suppression, the electrophoretic mobility of the analyte will be the primary mechanism for migration through the capillary. Since aptamers are highly negative analytes, the electrodes were reversed so the separation will proceed towards the anode. Upon binding with the protein, the aptamer-complex mobility is less negative than the free aptamer; therefore, the complex is predicted to elute after the free. Figure 2-2A shows the electropherogram of 1 μ M aptamer (DNA*) on a polyacrylamide capillary. Only a single peak is detected, as resolution of the impurities (Figure 2-1A) has been lost. Upon

addition of 0.5 μM thrombin, a large decrease in the free is observed (Figure 2-2B); however, once again no complex is detected. With an even larger addition of thrombin (0.75 μM), the free DNA* continues to decrease (Figure 2-2C) indicating complex formation is occurring, but again no complex is detected. Other separation conditions were investigated in order to facilitate detection of the aptamer-thrombin complex.

Flow Assisted CE

Continuing work to develop an aptamer assay was accomplished elsewhere in our lab with an in house instrument described elsewhere (German *et al.*, 1998). For this work, a polyacrylamide coating was again employed for the electrophoretic separations to reduce any adsorption of the thrombin. Figure 2-3A shows an electropherogram collected for 2 μM aptamer (DNA*) in a phosphate pH 7.4 buffer. With addition of an excess of protein (3 μM) a large decrease in the free aptamer was observed and again no well-formed complex was detected (Figure 2-3B). However, the free aptamer peak was tailing which may be indicative of the complex dissociating during the electrophoretic run. To aid the movement of the complex and prevent dissociation, vacuum induced flow was utilized in conjunction with the separation voltage. Essentially the sample was injected onto the capillary and the electric field was applied to separate the free and bound zones. After the free aptamer peak was detected, vacuum was applied to the outlet of the capillary while the electric field was still being applied to pull the complex towards the detector. When utilizing the flow-assisted CE method and adding an excess of thrombin, a complex peak was detected (Figure 2-4B). The complex and free peaks were bridged indicative of the aptamer-thrombin complex still dissociating during the

separation; however, the assay was quantitative with a reported complex limit of detection of 40 nM.

The dissociation constant (K_d) of the thrombin-aptamer complex was previously published as 200 nM (Bock *et al.*, 1992), and was also determined with the flow-assisted CE method as ~ 450 nM (German *et al.*, 1998). Two reasons were suggested to explain the differences in the dissociation constants. Different buffers were employed for the measurements and buffer composition could greatly affect the amount of complex being formed. Also the dissociation of the complex occurring within the CE separation could have caused the K_d to appear falsely higher. With a K_d in the mid nanomolar range, a relatively weak complex is being formed which may increase the rate of dissociation during the separation and cause the bridging seen between the free and complex peaks. Though the aptamer investigated in the CE assay was derivatized with fluorescein, no adverse effects on binding were observed due to the fluorescent label.

A noncompetitive aptamer assay for the protein IgE was also developed utilizing the flow-assisted CE method. This assay was more sensitive with a 46 pM limit of detection (37 zmol mass detection limit) due to the higher affinity aptamer ($K_d = 10$ nM) for IgE (Wiegand *et al.*, 1996). The IgE aptamer assay was determined to be highly selective since no appreciable binding was measured for a structurally similar antibody IgG. Also complex samples (human serum was used for experiments) were found to have little effect on the separation, detection limit, or dynamic range of the IgE aptamer CE assay (German *et al.*, 1998).

Capillary Electrophoresis with Polymer Buffers

Though a flow-assisted method was successfully used to develop noncompetitive aptamer assays, a simpler method was desired to increase the applicability of aptamer CE

assays as analytical tools. Polymer networks were investigated to reduce dissociation of the aptamer-thrombin complex. Capillary electrophoretic mobility shift assays (CEMSA) have been demonstrated as valuable techniques for analyzing protein-oligonucleotide complexes (Foulds and Etzkorn, 1998; Xian *et al.*, 1996; Stebbens *et al.*, 1996).

Typically dilute polymer buffers are used to improve the resolution and efficiency of the free DNA and the DNA-protein complex.

Generally to prevent adsorption of protein analytes, polyacrylamide coated capillaries are employed in CEMSA. To investigate the effects of polymer gel networks on aptamer complex stability, a polyacrylamide coated capillary was prepared using a method adapted from Cobb *et al.* (1990) and Dolnik *et al.* (1998), which is further explained later in this text (Chapter 5). Several polymers were investigated as buffer additives including polyacrylamide, poly(ethyleneoxide), methyl cellulose, and hydroxypropylmethyl cellulose (HPMC). Most polymer solutions utilized for experiments were dilute; therefore, an entangled network was not achieved. However, improvements in complex resolution were achieved with a 89 mM Tris, 89 mM borate, 2 mM EDTA, 5 mM KH_2PO_4 pH 8.3 buffer (TBE/K) containing 0.6 % HPMC. With addition of excess thrombin (3 μM) to 2 μM aptamer (DNA*) and using the TBE/K 0.6 % HPMC buffer for the separation, the thrombin-aptamer complex was formed and detected (Figure 2-5B). To insure this new peak was the complex, an excess of unlabeled aptamer (4.5 μM DNA) was added to compete with the labeled aptamer (DNA*) for binding with the thrombin. Because the unlabeled aptamer is in excess, a decrease in the labeled complex is predicted. Figure 2-5C shows the decrease in the labeled complex

upon addition of the unlabeled aptamer verifying the labeled aptamer-thrombin complex was formed and detected in the TBE/K 0.6% HPMC buffer.

Only a dilute polymer was necessary to facilitate detection of the thrombin-aptamer complex. Figure 2-6 shows the difference in the aptamer assays when no polymer is used (2-6A) and when a TBE/K buffer with 0.6% HPMC was employed (2-6B). Unfortunately the separation with the dilute polymer buffer did not provide baseline resolution of the complex and free aptamer. This bridging of the complex and free may again be indicative of the weak complex dissociating. In hopes of improving the resolution of the aptamer complex from the free DNA*, other buffer concentrations were investigated. As mentioned earlier, only a dilute polymer buffer was necessary for the electrophoretic separation; however, entangled networks are necessary to promote sieving within a gel. A HPMC concentration of 1.8% or greater is necessary in order to form an entangled network. When buffers containing these concentrations were explored, no complex was detected; only decreases in the free aptamer were observed. Though the same preparation was used to prepare the polymer buffer, when a fresh 0.6% HPMC solution was prepared and employed for the separation, no complex was detected. Several other methods of HPMC buffer preparation were investigated to no avail. The irreproducibility of preparing the polymer buffer proved to be detrimental for using CEMSA for aptamer assays; therefore, other separation parameters were investigated to facilitate complex detection.

Optimizing the Electrophoresis Buffer

In our previous attempts to develop an aptamer affinity assay, buffer compositions have included phosphate and TBE/K. The buffer composition has been shown in conventional gel electrophoresis investigations to play a vital role in forming a DNA-

protein complex (Lane *et al.*, 1992). For example protein-DNA complexes were shown to form in a Tris-glycine buffer but not the standard TBE buffer generally employed for EMSA and CEMSA applications (Alazard *et al.*, 1992). With this in mind, a commercially available Tris/glycine buffer (25 mM Tris, 192 mM glycine) was investigated. The buffer was supplemented with K^+ ions (5 mM K_2HPO_4) as potassium cations have been suggested previously to enhance binding of thrombin and its aptamer (Wang *et al.*, 1993). An unmodified, fused silica capillary was employed for the initial investigations with the Tris, glycine, potassium phosphate pH 8.4 buffer (TGK). Figure 2-7 shows several electropherograms of the thrombin aptamer assay utilizing a TGK pH 8.4 separation buffer. With increasing concentration of thrombin, the complex peak (C) increased and the free peak (A^*) decreased as expected with the noncompetitive assay. The complex is not fully resolved from the free DNA*, and this bridging effect is again indicative of the weakly formed complex dissociating. To determine if less time on the column would reduce the complex dissociation, the separation distance was shortened to 7 cm (Figure 2-8). The peak height of the complex increased, but the two peaks are not baseline resolved. Since CZE is employed with the TGK buffer, the complex, which has a less negative electrophoretic mobility than the free aptamer, travels faster to the cathode (negative electrode) thus being detected before the free aptamer. Also with an unmodified capillary, EOF is present which aids in the migration of the negatively charged aptamer to the cathode for detection.

The TGK buffer appears to be a suitable separation buffer for detection of the thrombin-aptamer complex; however, a well resolved complex was not achieved on an unmodified capillary. A polyacrylamide coated capillary was investigated with the TGK

buffer to determine if any improvements in resolution could be achieved. As shown in Figure 2-9B, upon addition of the thrombin to the aptamer, no well formed complex was detected though the free peak was tailing. Because of the large decrease in the free upon addition of the thrombin (comparing Figures 2-9A and 2-9B), the complex is formed but is not migrating through the capillary for detection. The EOF present when employing an unmodified capillary appears to aid in the migration of the complex through the capillary and enables detection of the aptamer-thrombin complex.

Conclusions

By optimizing the separation buffer a noncompetitive aptamer assay for thrombin has been developed. A vacuum flow-assisted method has been previously shown, but employing a TKG separation buffer allows applicability of this assay to commercial instruments. Though polymer gels showed initial success, consistently preparing the polymer buffer proved to be problematic in developing a reproducible aptamer assay. Further investigations are necessary to measure the quantitative aspects of this assay to compare with the previously developed flow-assisted assay. Also other aptamers need to be investigated to see if the TKG separation conditions are suitable for other aptamer complexes.

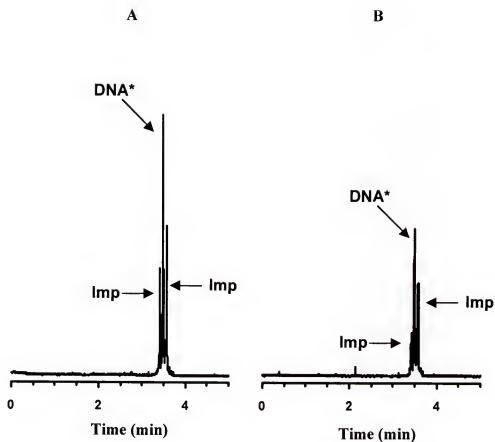


Figure 2-1 Thrombin aptamer assay on an unmodified capillary employing a 40 cm effective, 47 cm total separation capillary. The separation voltage was 25 kV and a 5s 10 kV injection was employed. (A) Electropherogram of 1 μ M aptamer (DNA*) in a 20 mM NaH_2PO_4 pH 7.0 buffer. The impurities are denoted as Imp. (B) Upon addition of 2 μ M thrombin, a decrease in DNA* is seen but no complex is detected.

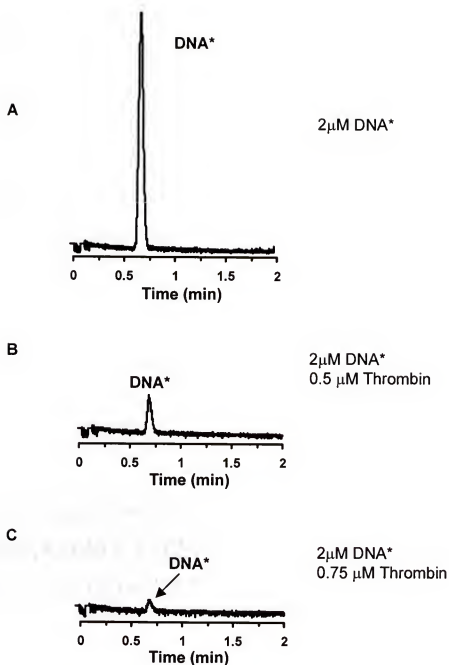


Figure 2-2 Thrombin aptamer assay on a polyacrylamide coated capillary employing a 7 cm effective, 47 cm total separation capillary. The separation voltage was 25 kV and a 5s 10 kV injection was employed. (A) 1 μ M aptamer (DNA*) in a 20 mM NaH_2PO_4 pH 7.0 buffer. Upon addition of 0.5 μ M thrombin (B) or 0.75 μ M thrombin (C), a decrease in DNA* is seen but no complex is detected.

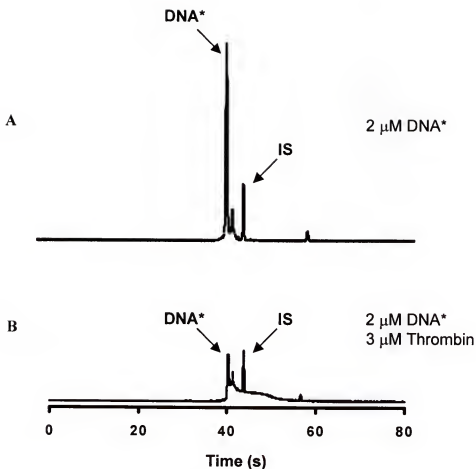


Figure 2-3 Thrombin aptamer assay employing a polyacrylamide coated capillary. (A) Electropherogram of 2 μM aptamer in a 5 mM Na_2HPO_4 , 5 mM KH_2PO_4 , MgCl_2 pH 7.4 buffer. The internal standard (IS) is fluorescein. (B) Upon addition of 3 μM thrombin, a decrease in the aptamer is observed, but no complex is detected. Considerable tailing of the free aptamer peak occurred, indicative of complex dissociation. From reference: German, I.; Buchanan, D.D.; Kennedy, R.T. *Anal. Chem.* **1998**, 70, 4540.

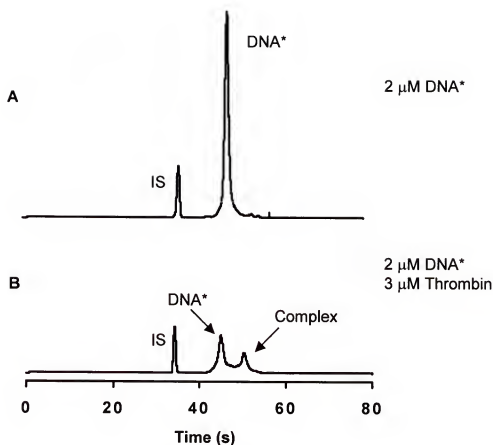


Figure 2-4 Thrombin aptamer assay employing a polyacrylamide coated capillary and vacuum assisted flow. (A) Electropherogram of 2 μ M aptamer in a 5 mM Na_2HPO_4 , 5 mM KH_2PO_4 , MgCl_2 pH 8.2 buffer. The internal standard (IS) is 4(5)-carboxyfluorescein. (B) Upon addition of 3 μ M thrombin, a decrease in the aptamer is observed and the aptamer complex is detected. From reference: German, I.; Buchanan, D.D.; Kennedy, R.T. *Anal. Chem.* **1998**, 70, 4540.

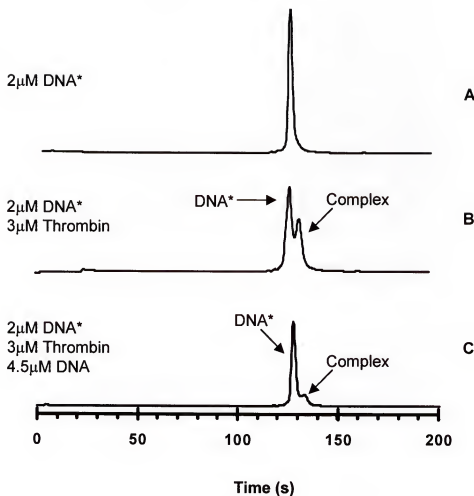


Figure 2-5 Thrombin aptamer assay employing a dilute polymer HPMC buffer. (A) Electropherogram of 2 μ M aptamer in a TBE/K 0.6% HPMC pH 8.3 buffer. (B) Upon addition of 3 μ M thrombin, a decrease in the aptamer is detected as well as the aptamer complex. (C) Competition experiment in which an excess of unlabeled aptamer (4.5 μ M) is added and a subsequent decrease in the labeled complex is detected.

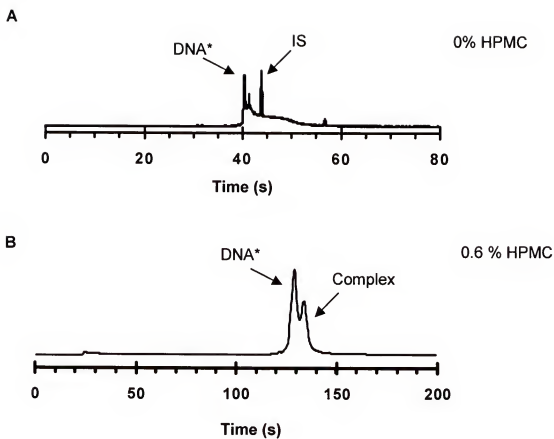


Figure 2-6 Effect of polymer gel on complex detection. (A) Assay in a 5 mM Na_2HPO_4 , 5 mM KH_2PO_4 , MgCl_2 pH 8.2 buffer without any additive. (B) Assay utilizing a TBE/K 0.6% HPMC pH 8.3 separation buffer.

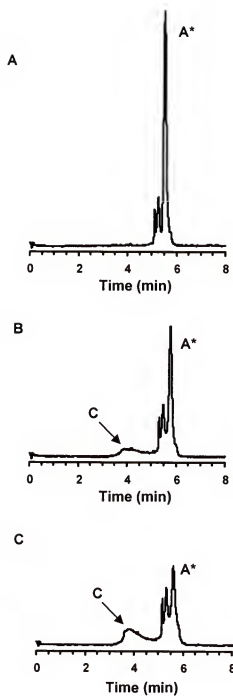


Figure 2-7 Thrombin aptamer assay on an unmodified capillary employing the TGK separation buffer. The capillary was 37 cm total with a 30 cm effective length. A 1 s pressure injection was used and the separation voltage was 16.5 kV. The aptamer concentration was 2 μM for all separations. (A) 0 μM thrombin (B) 1 μM thrombin (C) 2 μM thrombin.

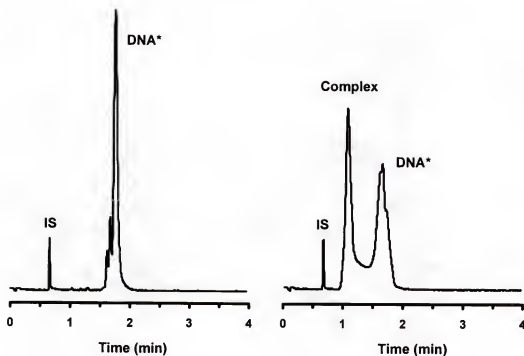


Figure 2-8 Thrombin aptamer assay on an unmodified capillary with a TGK pH 8.4 buffer. Separation conditions were: 3 s 2.5 kV injection, 13 kV separation, 7 cm effective distance with a total capillary length of 37 cm. (A) 2 μ M aptamer (B) 2 μ M aptamer and 2 μ M thrombin. Riboflavin (5 μ M) was employed as the internal standard.

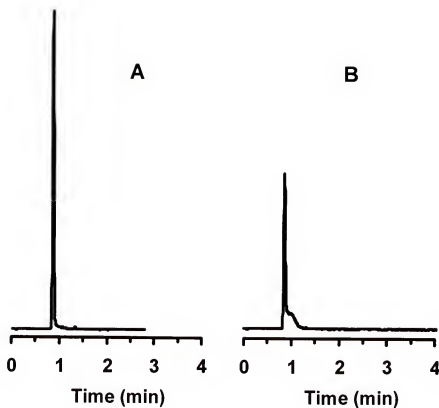


Figure 2-9 Thrombin aptamer assay on a polyacrylamide coated capillary. The separation buffer was TGG pH 8.4 and the effective separation distance was 7 cm with a total capillary length of 27 cm. Injections were 5 s at 2.5 kV and a 400 V/cm electric field was used for the separations. (A) 1 μ M aptamer (B) 1 μ M aptamer and 550 nM thrombin.

CHAPTER 3

INVESTIGATING THE EFFECTS OF ELECTRIC FIELD, COLUMN TIME, pH, AND BUFFER COMPOSITION ON APTAMER COMPLEX STABILITY

Introduction

Capillary electrophoresis with laser induced fluorescence detection (LIF) has emerged as a valuable technique for performing affinity assays (Schultz and Kennedy, 1993; Shimura and Karger, 1994; Evangelista and Chen, 1994; Tao and Kennedy, 1996; Schmalzing *et al.*, 1995). Both competitive and noncompetitive immunoassays may be performed. Most work utilizes the competitive format in which antigen (Ag) of interest is mixed with a labeled form (Ag*) and a limited concentration of antibody (Ab) setting up a competition for binding to Ab. CE separation yields two zones: free Ag* and Ab-Ag* complex, and Ag is quantitated indirectly by the relative size of the Ab-Ag* and Ag* peaks. In contrast, the noncompetitive assay incorporates a labeled antibody (Ab*) to react with Ag. In this case the antigen may be quantitated directly by measuring the Ab*-Ag complex which is separated from the free Ab*. Noncompetitive assays offer several advantages over competitive assays including larger linear dynamic range (since the complex is separated and detected directly), the ability to distinguish between cross-reactive species, and detection limits that are less dependent on binding affinities (Shimura and Karger, 1994). Despite these advantages, noncompetitive immunoassays have only rarely been implemented. Since antibodies are difficult to fluorescently label, noncompetitive assays are tedious to develop. Also separating the free Ab* and Ab*-Ag

complex may be difficult due to small changes in the electrophoretic mobility of Ab* upon binding with the small Ag.

To overcome these disadvantages, several techniques have been investigated to improve the use of antibodies for noncompetitive assays. Homogenous, labeled affinity probes have been reported when thiol specific labeling reagents such as 5-iodoacetamidofluorescein have been used to fluorescently tag antibodies or antibody fragments (Shimura and Karger, 1994; Hafner *et al.*, 2000; Tim *et al.*, 2000). To aid in the separation of Ab* and Ab*-Ag, a “shift ligand” can be added to the separation buffer (Hafner *et al.*, 2000; Tim *et al.*, 2000). This charged competitive ligand binds with weak affinity to the binding site of Ab* increasing the electrophoretic mobility of Ab*. Upon incubation with Ag and formation of Ab*-Ag, the weaker affinity shift ligand is effectively blocked from binding with the complexed antibody; however, the free Ab* can interact with the charged ligand. The electrophoretic mobility difference between the “shift ligand”-Ab* complex and Ab*-Ag is considerably larger enhancing the separation of Ab* from Ab*-Ag.

In addition to these methods, alternatives to antibodies have been pursued. In particular, we have previously reported using aptamers as affinity probes (German *et al.*, 1998). Aptamers are single-stranded oligonucleotide sequences developed with the combinatorial technique SELEX (systematic evolution of ligands by exponential enrichment) to bind with a target molecule with high specificity and affinity (Gold and Tuerk, 1990; Ellington and Szostak, 1990). Aptamers appear to be quite versatile as they have been developed for numerous targets including peptides, proteins, organic dyes, and small molecules (Tuerk *et al.*, 1992; Nieuwalandt *et al.*, 1995; Williams *et al.*, 1997;

Ellington and Szostak, 1992; Famulok, 1994; Sassanfar and Szostak, 1993; Huizenga and Szostak, 1995; Jenison *et al.*, 1994).

In comparison to antibodies, aptamers possess several advantages making them attractive for incorporation into noncompetitive CE affinity assays. Automated chemical synthesis techniques are rapid and relatively inexpensive and enable facile labeling of the aptamer with fluorescent dyes. Also aptamers are low molecular weight ligands (7.5 – 32 kDa) which aids in maximizing the resolution of the complex from the free aptamer during the electrophoretic separation. Previously in our lab, noncompetitive CE aptamer assays for the proteins IgE and thrombin were successfully developed (German *et al.*, 1998). Unfortunately, the aptamer-analyte complex was not detected unless hydrodynamic flow was used to force the complex through the column. Though the flow-assisted method allowed quantification of the complex, it was an inconvenient procedure that eliminated some of the advantages of CE. Improving the separation conditions to eliminate the use of vacuum assisted flow was sought in order to enhance the applicability of aptamers for analytical diagnostic tools. By investigating several electrophoresis buffers, separation conditions were found in which the aptamer complex integrity was maintained and detected over the time course of the separation without any additional flow enhancement. The developed affinity assays were further evaluated by investigating the effects of pH, electric field strength and column time on the complex.

Materials and Methods

Chemicals

A 10X Tris/glycine buffer was purchased from Bio-Rad Laboratories (Hercules, CA). Potassium diphosphate, sodium diphosphate, sodium fluorescein, MOPS (3-[N-morpholino]propanesulfonic acid), and thrombin from human plasma (0.26 mg/mL) were

purchased from Sigma Chemical (St. Louis, MO). Potassium phosphate monobasic and sodium phosphate dibasic were purchased from Fisher chemical (Pittsburgh, PA). BCECF (2',7'-bis-(2-carboxyethyl)-5-(and-6)-carboxyfluorescein) was purchased from Molecular Probes (Eugene, OR) and 5(6)-carboxyfluorescein was purchased from Aldrich Chemical (Milwaukee, WI). Human myeloma IgE (1.5 mg/mL) was from Athens Research and Technology (Athens, GA). Aptamers were synthesized, fluorescently labeled, and purified by Integrated DNA Technologies (Coralville, IA). The fluorescein label was chemically attached to the 5' end of the thrombin binding aptamer (5'GGTTGGTGTGGTTGG-3'). For the IgE binding aptamer the fluorescein label was attached via an ethylene glycol spacer to the 5' end (5'GGGGCACGTTTATCCGTCCCTCTAGTGGCGTGCCCC-3'). All solutions were prepared with deionized water purified with a Milli-Q Plus system (Millipore Corp., Marlborough, MA).

Aptamer preparation

Before beginning aptamer experiments, a 4 μM stock of the DNA aptamer in electrophoresis buffer (TGE, phosphate or MOPS) was prepared and annealed by heating at 72 $^{\circ}\text{C}$ for 2.5 min and cooling to ambient temperature. For the thrombin aptamer assay, experimental samples consisted of 1 μM thrombin aptamer from the annealed stock solution, 192 nM BCECF (internal standard), and 0-1.25 μM thrombin. IgE aptamer samples consisted of 1 μM IgE aptamer from the annealed stock solution, 46 nM fluorescein (internal standard), and 0-300 nM IgE.

Apparatus

All separations were performed with a Beckman P/ACE 2200 capillary electrophoresis system (Beckman Coulter Fullerton, CA). Bare, fused silica capillaries

(50 μm i.d., 360 μm o.d.) from Polymicro Technologies (Phoenix, AZ) were 37 cm in total length unless otherwise indicated. While the total length of the capillary remained 37 cm, the effective length of the capillary was changed from 30 cm to 7 cm by reversing the polarity of the electrodes. Capillaries were pretreated by rinsing with 1 M NaOH, deionized H_2O , and buffer for 10 min each. Between each electrophoretic separation the capillary was rinsed with base, water, and buffer again for 3 min each to remove any residual sample from the capillary walls. The separation buffer contained 25 mM Tris, 192 mM glycine, 5 mM K_2HPO_4 , pH 8.4 (TGK) unless otherwise stated. Samples were injected electrokinetically for 5s at 2.5 kV. Laser induced fluorescence (LIF) detection employed the 488 nm excitation line of a 3 mW Argon Ion laser (Beckman-Coulter) and emission was collected at 520 nm. Data was recorded and analyzed with P/ACE software (Beckman-Coulter).

Results and Discussion

Buffer Effects

In traditional slab gel electrophoresis, the buffer composition has been found to be highly important in forming DNA-protein complexes (Lane *et al.*, 1992); therefore, the effects of several buffers on formation and detection of a thrombin-aptamer complex were investigated. The electropherograms obtained for the thrombin aptamer assay in a TGK buffer (25 mM Tris, 192 mM glycine, 5 mM K_2HPO_4 , pH 8.4), phosphate buffer (5 mM Na_2HPO_4 and 5 mM KH_2PO_4 , pH 8.4) and MOPS buffer (10 mM MOPS, 5 mM K_2HPO_4 , Et_3N , pH 8.4) are shown in Figure 3-1. In the TGK buffer (Figures 3-1A and 3-1B), upon addition of 550 nM thrombin to 1 μM aptamer (3-1B), a decrease in the free aptamer peak (A^*) is apparent and the bridged complex peak (C) elutes before A^* .

Smaller decreases in A^* were observed and smaller complexes were detected when employing the phosphate (3-1C and 3-1D) or MOPS buffer (3-1E and 3-1F). (The electroosmotic flow was suppressed in the MOPS buffer so it was necessary to employ another internal standard (IS) than in the other buffers. For the TGK and phosphate buffer, 192 nM BCECF (Figure 3-2) was used. However, in the MOPS buffer the BCECF was undetectable so 146 nM 5(6)-carboxyfluorescein (Figure 3-2) was used, and with these separation conditions the IS migrated before the complex and the free aptamer.)

The percent decrease in A^* with addition of thrombin can be used as a measure of the complex being formed in solution. Peak height ratios (peak height A^* / peak height IS) were calculated for A^* with and without the thrombin present in all the investigated buffers in order to determine the percent decrease in A^* upon complex formation.

$$\% \text{ decrease } A^* = \left(1 - \frac{\text{Pk Ht } A^* (\text{with protein})}{\text{Pk Ht } A^* (\text{without protein})} \right) * 100 \quad (3.1)$$

Percent decreases for A^* were calculated as 68% in the TGK buffer (Figures 3-1A and 3-1B), 46% in the phosphate buffer (3-1C and 3-1D) and 26% in the MOPS buffer (3-1E and 3-1F). With a dissociation constant of 200 nM (Bock *et al.*, 1992), an aptamer concentration of 1 μM , and 550 nM thrombin, 410 nM of complex is theoretically expected corresponding to a 41% decrease in A^* . A larger decrease in A^* was measured in the TGK buffer suggesting more complex is being formed and the published K_d , which was determined in a 20 mM Tris-acetate, 140 mM NaCl, 5 mM KCl, 1 mM CaCl_2 , 1 mM MgCl_2 pH 7.4 buffer, may not accurately describe the affinity of the aptamer and

thrombin in TGK. The effects of buffer composition on the thrombin complex are summarized in Table 3-1.

Table 3-1 Summary of the effects of buffer composition on the thrombin aptamer complex.

| Buffer | Pk Ht A* (with protein) | Pk Ht A* (without protein) | % Decrease | Pk Ht Complex |
|-----------|----------------------------|-------------------------------|------------|------------------|
| TGK | 1.59 | 4.92 | 68 | 0.462 |
| Phosphate | 3.25 | 6.00 | 46 | 0.228 |
| MOPS | 2.16 | 2.91 | 26 | 0.163 |

A similar trend was observed with a higher affinity DNA oligonucleotide specific for IgE ($K_d = 10$ nM) (Wiegand *et al.*, 1996). In the TGK buffer, upon addition of IgE (175 nM) to 1 μ M IgE aptamer (A*), a well resolved complex (C) was detected (Figure 3-3B). No bridging of the complex and free aptamer is apparent as with the lower affinity thrombin aptamer. Again the largest aptamer complex was detected in the TGK buffer compared to the phosphate (Figure 3-3C and 3-3D) and MOPS (Figure 3-3E and 3-3F) buffers. Theoretically, with a dissociation constant of 10 nM, 1 μ M aptamer, and 175 nM thrombin, 170 nM of complex should be formed and a 17% decrease in A* would be predicted. A 52% decrease in A* was measured in TGK (Figures 3-3A and 3-3B) with decreases upon protein addition of 43% and 51% with the phosphate (3-3C and 3-3D) and MOPS buffer (3-3E and 3-3F) respectively. Though similar decreases in A* were observed in the three buffers, the largest complex was detected in the TGK buffer in which the peak height ratios of the complex (peak height of complex versus the peak height of the IS) were determined as 0.80 in TGK, 0.71 in phosphate, and 0.10 in MOPS. As with the thrombin binding aptamer, a larger decrease in the free aptamer occurred than would be predicted. Figures 3-3B, 3-3D, and 3-3F show the base of the aptamer is

wider upon addition of the protein suggesting other processes such as adsorption to the capillary walls may be contributing to the large decrease in the height of the A* peak.

The effects of buffer composition on the IgE aptamer are summarized in Table 3-2.

Table 3-2 Summary of the effects of buffer composition on the IgE aptamer complex.

| Buffer | Pk Ht A* (with protein) | Pk Ht A* (without protein) | % Decrease | Pk Ht Complex |
|-----------|----------------------------|-------------------------------|------------|------------------|
| TGK | 1.68 | 3.47 | 52 | 0.665 |
| Phosphate | 1.82 | 3.16 | 43 | 0.712 |
| MOPS | 1.18 | 2.41 | 26 | 0.102 |

pH Effects

To determine the effects of pH on the complex, the TGK buffer pH, typically pH 8.4, was altered by the addition of NaOH or HCl to achieve a pH of 9.4 or 7.6 respectively. Figure 3-4B depicts the thrombin aptamer complex (C) formed in the TGK buffer at a pH of 8.4 when 1 μ M aptamer and 550 nM thrombin are mixed together. If the same concentrations of aptamer and protein are mixed and the separation is performed at the lower pH of 7.6, a very small complex was observed (Figure 3-4A). Also at the lower pH smaller signals were produced for all the peaks, which may be a result of the suppressed electroosmotic flow and less sample being injected onto the capillary. The increased electroosmotic flow at a pH of 8.4 may be aiding in the migration of the complex and reducing any complex dissociation thus producing a larger complex. At the high alkaline pH of 9.4 (Figure 3-4C) no complex is detected. To further illustrate the smaller complexes being formed in the pH 7.6 and 9.4 buffers, the percent decrease in A* was measured. At a pH of 7.6 a 3 % decrease was calculated with 68 % and 16 % decreases measured at pH 8.4 and 9.4 respectively.

Effects of Electroosmotic Flow

The largest aptamer-thrombin complex was detected when employing the TGK pH 8.4 buffer, but the complex and free peaks (Figure 3-1B) are not baseline resolved and a bridging effect is apparent. This bridging effect is likely due to dissociation of the relatively weak complex ($K_d = 200$ nM) over the course of the separation (Bock *et al.*, 1992). Adsorption of proteins occurs quite readily when employing unmodified, fused silica capillaries. If the thrombin is adsorbing to the capillary surface, dissociation of the thrombin-aptamer may be induced. Coated capillaries are one possible alternative to reduce absorption of the thrombin to the capillary walls (Hjertén, 1985; Cobb *et al.*, 1990; Schmalzing *et al.*, 1993; Malik *et al.*, 1993); however, coating the capillary also reduces EOF possibly increasing the time the complex spends on the column. Under these separation conditions, the complex now migrates after the free aptamer as the separation is in the direction of the cathode and thus the more negative analyte (the aptamer) has the greatest mobility and is detected first.

Using the TGK pH 8.4 buffer, a polyacrylamide coated capillary was employed for the thrombin CE aptamer assay. Figure 3-5A depicts 1 μ M free aptamer (A*) under no flow conditions. Upon addition of 550 nM thrombin (Figure 3-5B), a decrease in the free aptamer is apparent (51 % measured decrease in A*) but a well-formed complex peak is not detected. The A* peak is tailing relative to the free aptamer in the absence of the protein. This tailing may be indicative of any formed complex still dissociating on column. In our previous experiments a coated capillary was employed and the applied vacuum was necessary to instill flow conditions into the capillary and move the complex through the column (German *et al.*, 1998). However, with the TGK buffer and flow

conditions (Figure 3-1B), the thrombin-aptamer complex is being formed and the EOF is aiding in the movement and subsequent detection of the complex. Reducing complex dissociation with coated capillaries is not advantageous, as it appears electroosmotic flow in the capillary aids in complex detection.

Capillary electrophoresis with replaceable polymer gel networks is another technique that may aid in the reduction of complex dissociation. These polymer gels “cage” the complex preventing the protein and the aptamer from migrating away from each other upon complex dissociation making association highly favorable (Fried and Bromberg, 1981; Fried and Crothers, 1997). Generally to employ these replaceable gels a coated capillary is necessary to prevent electroosmotic flow. Under these conditions, the complex was again undetected (Figure 3-6B) so no improvements were found when employing the use of a gel network.

Assay Quantification

Figure 3-7 shows the calibration curve for the thrombin-aptamer assay with a linear dynamic range from 0 to 1.25 μM . Quantitating the free aptamer above protein concentrations of 1.25 μM was difficult due to an impurity peak, which was a byproduct of the synthesis. A complex limit of detection of 70 nM was calculated as two times the calibration sensitivity. However, a detection limit of 4 nM was determined for the free aptamer, suggesting the complex limit of detection appears to be limited by the stability of the complex and not by the instrument sensitivity.

The linear dynamic range for the IgE aptamer assay was 0-250 nM with saturation occurring at IgE concentrations above 250 nM (Figure 3-8). A detection limit of 5 nM was determined for the IgE-aptamer complex and 6 nM for the free aptamer. The

sensitivity of the instrument is the limiting factor in the detection of the IgE complex and aptamer as their detection limits are comparable to that found for fluorescein (2 nM). The detection limits for both aptamer assays may be improved with a more sensitive detection scheme than that found with the commercial CE instrument used in our experiments.

Field and time effects

Buffer composition, pH, and electroosmotic flow have been shown to affect the formation and detection of the aptamer complex. Other factors that may affect the complex are the electric field strength and the time spent on the column. High electric fields can be advantageous due to the decreased separation times and higher peak efficiencies; however, high electric fields may shear the complex inducing dissociation. In contrast with weak electric fields the complex may be spending too much time on the column resulting in partial or complete dissociation.

To investigate the effects of electric field and time on the aptamer complex, a sample consisting of 1 μ M aptamer, 175 nM IgE, and 46 nM fluorescein (IS) was separated on three different capillary effective lengths (7, 20, and 30 cm) with electric fields ranging from 125 – 600 V/cm. For analysis of 7 cm and 30 cm effective lengths, a 37 cm capillary was employed so separation voltages ranged from 4.6 – 22.5 kV. The capillary was cut in order to obtain a 20 cm effective length thus changing the total capillary length to 27 cm. Separation voltages were altered to maintain the same field strength on the 20 cm separation as in the 7 and 30 cm separations. By changing the field and the length of the separation capillary, the time the complex spent on the column was

also altered. The peak height ratio of the complex versus the IS was used for quantification.

With increasing electric field strength, no adverse effects were observed for the aptamer complex. Only small changes in the peak height ratio were observed for each capillary effective length over the electric field range (Figure 3-9). However, a large difference in the complex peak height was measured for the three separate separation distances. For example, with a 460 V/cm electric field, complex peak heights were measured as 0.79, 0.55, and 0.34 for 7, 20, and 30 cm effective lengths respectively. By lengthening the separation distance, the total time the complex spends on the column was increased. At 460 V/cm, complex migration times were 37 s, 94 s, and 140 s for the 7, 20, and 30 cm separation distances. This suggested a relationship of complex stability with respect to total column time. With increasing column time, the peak height of the complex decreased rapidly until reaching a plateau after 200 s (Figure 3-10). However, no trend was observed for the free aptamer (Figure 3-11) further suggesting complex stability decreases with increased column time due to complex dissociation. Upon analyzing the free aptamer peak with respect to electric field, again no large changes in peak height were observed (Figure 3-12).

With this range of electric fields (150-600 V/cm), no detrimental effects were observed for the aptamer complex; however, column time does effect the detectable concentration of the complex. Shorter separation distances with mid range fields (~ 400 V/cm) appear optimal for maximum complex detection and quantitation.

Conclusions

In previous CE aptamer assays, a flow-assisted method was necessary in order to detect the aptamer complex. However, by employing a TKG pH 8.4 electrophoresis buffer, two noncompetitive aptamer assays, one for the lower affinity thrombin aptamer and the other for the higher affinity IgE aptamer, were developed. Both assays were quantitative with limits of detection for the thrombin-aptamer complex of 70 nM and 5 nM for the IgE-aptamer complex. Bridging between the thrombin-aptamer complex and the free aptamer occurred indicating the dissociation of the complex over the course of the separation. The detectable complex concentration was affected by the time spent on the separation column but not by the electric field used for the separation. At shorter separation times a large complex was detected; however, with increasing column time the complex peak height dissipated rapidly until plateauing. By characterizing these variables for their affects on the complex, conditions were found for detecting the thrombin and IgE aptamer complexes. These optimized separation conditions may be useful for other aptamer systems and analytical applications.

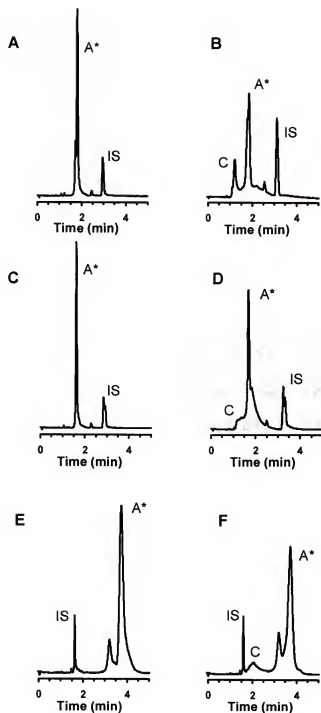


Figure 3-1 Thrombin-aptamer assay in TGK pH 8.4 buffer (A,B), phosphate buffer pH 8.4 (C,D), and MOPS pH 8.4 buffer (E,F). The aptamer (A*) concentration was 1 μ M for all separations, and 550 nM thrombin was used for complex formation (B,D,F). The internal standard (IS) was 192 nM BCECF for the TGK and phosphate buffers but 146 nM 5(6)-carboxyfluorescein for the MOPS buffer. The effective capillary length was 7 cm. Injections were 5 s at 2.5 kV and a 351 V/cm field was used for the separations.

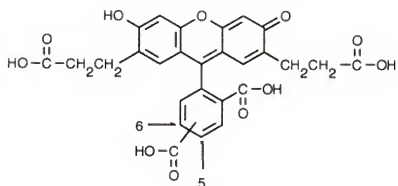
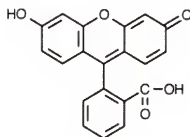
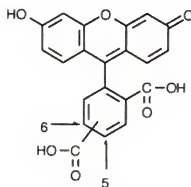
**BCECF****Fluorescein****5(6)-carboxyfluorescein**

Figure 3-2 Chemical structures of BCECF, fluorescein, and 5(6)-carboxyfluorescein.

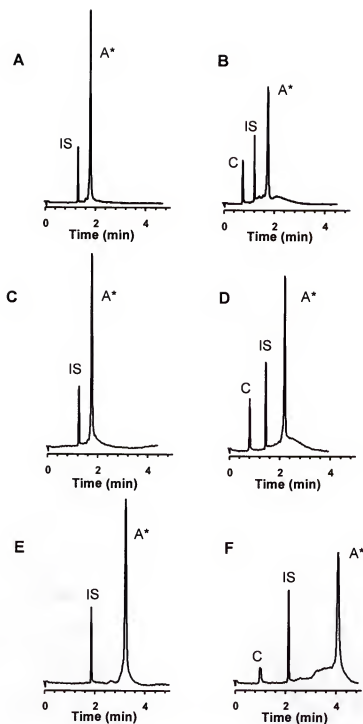


Figure 3-3 IgE-apptamer assay in TKG pH 8.4 buffer (A,B), phosphate buffer pH 8.4 (C,D), and MOPS pH 8.4 buffer (E,F). The aptamer (A*) concentration was 1 μ M for all separations, and 175 nM IgE was used for complex formation (B,D,F). The internal standard (IS) was 46 nM fluorescein. The effective capillary length was 7 cm. Injections were 5 s at 2.5 kV and a 350 V/cm field was used for the separations.

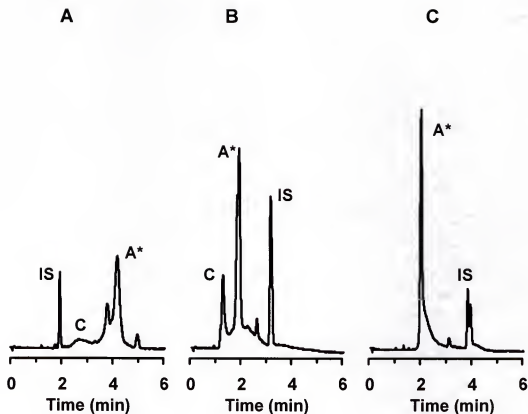


Figure 3-4 pH effects on the thrombin aptamer. A TKG buffer was used for all separations and the pH was adjusted accordingly. (A) pH 7.6 (B) pH 8.4 (C) pH 9.4 Each electropherogram is 1 μ M aptamer and 550 nM thrombin. BCECF was used as the internal standard for B and C, but 4(5)-carboxyfluorescein was used in A. The effective capillary length was 7 cm. Injections were 5 s at 2.5 kV and a 350 V/cm field was used for the separations.

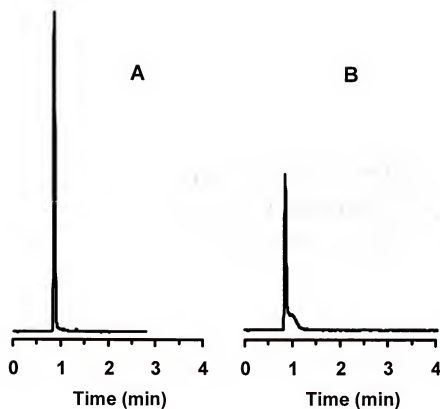


Figure 3-5 Thrombin aptamer assay on a polyacrylamide coated capillary. The separation buffer was TGG pH 8.4 and the effective separation distance was 7 cm with a total capillary length of 27 cm. Injections were 5 s at 2.5 kV and a 400 V/cm field was used for the separations. (A) 1 μ M aptamer (B) 1 μ M aptamer and 550 nM thrombin.

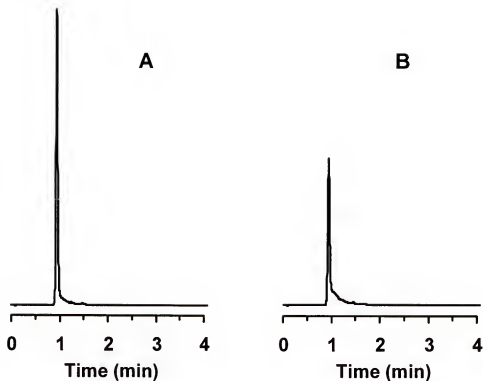


Figure 3-6 Thrombin aptamer assay on a polyacrylamide coated capillary with a dilute polymer solution. The separation buffer was TGG, 0.6 % HPMC pH 8.4 and the effective separation distance was 7 cm with a total capillary length of 27 cm. Injections were 5 s at 2.5 kV and a 400 V/cm field was used for the separations. (A) 1 μ M aptamer (B) 1 μ M aptamer and 550 nM thrombin.

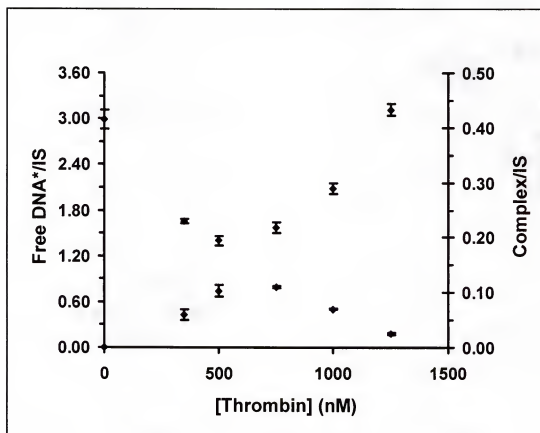


Figure 3-7 Calibration curve for the thrombin aptamer assay. The aptamer concentration was 1 μM and the thrombin concentration was varied from 0-1.25 μM . Injections were 5 s at 2.5 kV and a 365 V/cm electric field was employed for all separations. The injector to detector length was 30 cm (37 cm total). Peak heights were corrected for any variations in injection by dividing by the peak height of the internal standard. Each measurement is the average corrected peak height of three electropherograms ($n=3$).

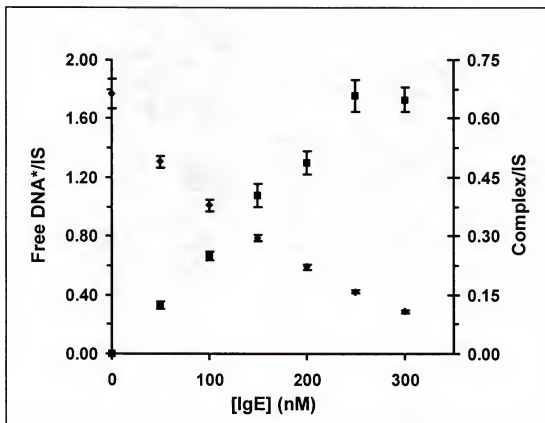


Figure 3-8 Calibration curve for the IgE aptamer assay. The aptamer concentration was 1 μ M and the IgE concentration was varied from 0-300 nM. Saturation occurred at concentrations above 250 nM IgE. Injections were 5 s at 2.5 kV and a 365 V/cm electric field was employed for all separations. The injector to detector length was 7 cm (37 cm total). Peak heights were corrected for any variations in injection by dividing by the peak height of the internal standard. Each measurement is the average corrected peak height of three electropherograms ($n=3$).

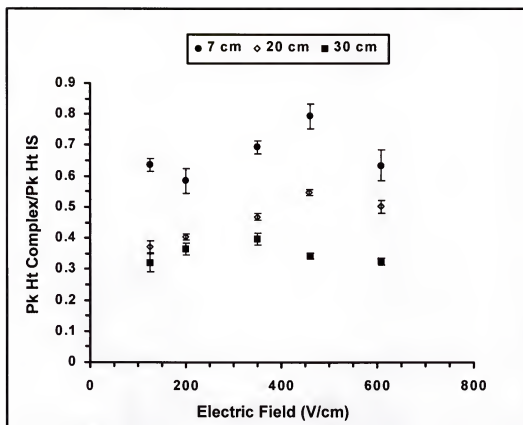


Figure 3-9 Effect of electric field on the IgE-aptamer complex. The electric field was varied from 125-600 V/cm. Samples contained 1 μ M aptamer, 175 nM IgE, and 46 nM fluorescein. The complex peak height is a ratio of the complex/IS heights to correct for changes in flow and injection.

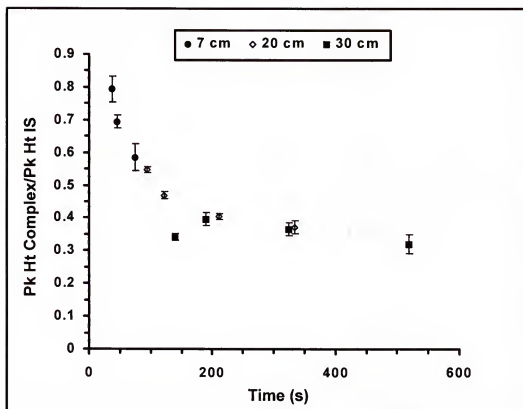


Figure 3-10 Effect of column time on the IgE-aptamer complex. The time the complex spent on the column, which ranged from 46- 519 s, was varied by changing the length of the separation capillary as well as the employed electric field, which varied from 125-600 V/cm. After 200 s or longer on the column, the complex peak height was observed to plateau. Samples contained 1 μ M aptamer, 175 nM IgE, and 46 nM fluorescein. The complex peak height is a ratio of the complex/IS heights to correct for changes in flow and injection.

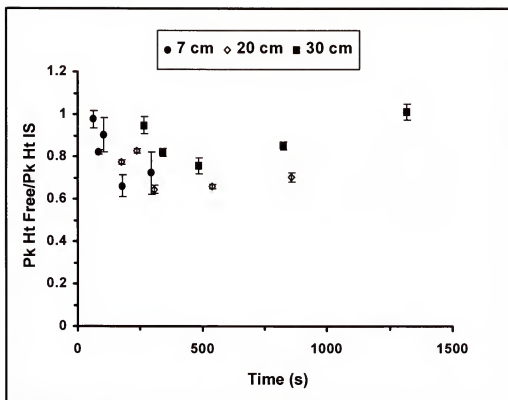


Figure 3-11 Effect of column time on the free IgE-aptamer. The free aptamer migration times ranged from 60- 1300 s. The migration time was varied by changing the length of the separation capillary as well as the separation voltage (the electric field ranged from 125-600 V/cm). Samples contained 1 μ M aptamer, 175 nM Ige, and 46 nM fluorescein. The complex peak height is a ratio of the complex/IS heights to correct for changes in flow and injection.

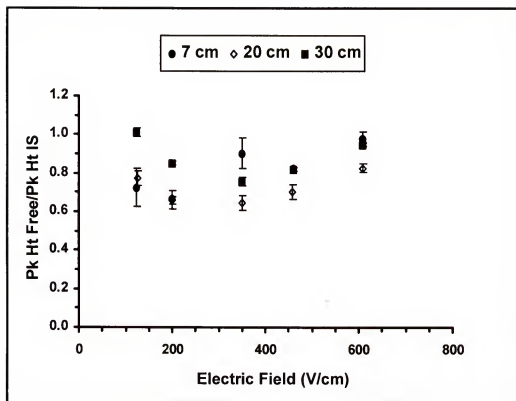


Figure 3-12 Effect of electric field on the free IgE-aptamer. The electric field was varied from 125-600 V/cm. Samples contained 1 μ M aptamer, 175 nM Ige, and 46 nM fluorescein. The complex peak height is a ratio of the complex/IS heights to correct for changes in flow and injection.

CHAPTER 4

INVESTIGATING ADENOSINE BINDING APTAMERS WITH AFFINITY CAPILLARY ELECTROPHORESIS

Introduction

Aptamers are short, typically single-stranded, oligonucleotides generated with *in vitro* selection or systematic evolution of ligands by exponential enrichment (SELEX) (Ellington and Szostak, 1990; Tuerk and Gold, 1990). SELEX is an iterative process in which a pool of randomized oligonucleotides is screened for a specific analyte ultimately producing a few (typically 10-15) higher affinity oligonucleotides selective for the analyte. Aptamers have been developed for an array of target molecules such as organic dyes, proteins, nucleotides, and sugars (Ellington and Szostak, 1992; Bock *et al.*, 1992; Nieuwlandt *et al.*, 1995; Sassanfar and Szostak, 1993; Ciesiolka and Yarus, 1996; Williams *et al.*, 1997; Morris *et al.*, 1998).

Oligonucleotides can be comprised of adenine (A), guanine (G), cytosine (C), thymine (T) (DNA oligonucleotides) or uracil (U) (RNA oligonucleotides). The diversity of an aptamer selection is limited by constructing the oligonucleotide library with these standard building blocks. One method to enrich the diversity of oligonucleotides is to employ functionalized, nonstandard bases. One functionalized nucleotide that has been developed is 5-(3"-aminopropynyl)-2'-deoxyuridine (dJ), an analog of uracil containing a positively charged side chain (Figure 4-1). Battersby *et al.* (1999) developed and incorporated the "dJ" nucleotide into a DNA aptamer selected against ATP, ADP, and AMP in which "J" was used in place of thymine. The employed selection method was

similar to that used previously by Huizenga and Szostak (1995) to develop a standard base DNA aptamer for ATP. The nucleotides (ATP, ADP, and AMP) are negatively charged ligands; therefore, when binding with a standard DNA aptamer, which is also negatively charged, a weak complex could be formed due to the repulsion of like charges. However, with the positively charged functionality of the J base, enhancement in binding may be possible between the aptamer and the negatively charged analytes. The aim of this work was to measure the binding affinity of the nonstandard J base aptamer and the standard base aptamer for ATP in order to determine if any enhancement in binding affinity was achieved by incorporating the positively charged J base into the aptamer.

Affinity capillary electrophoresis (ACE) is a powerful technique for determining binding affinities and stoichiometries of receptor-ligand systems. ACE is an equilibrium method for determining binding affinities in which the ligand is incorporated into the separation buffer (Figure 4-2). For example, once the aptamer (receptor) is injected onto the column, it can interact and bind with the ATP (ligand). The ATP is present throughout the capillary in large excess of the aptamer; therefore, the aptamer-ATP equilibrium is maintained over the length of the separation. The charge to mass ratio and subsequently the electrophoretic mobility (μ) of the aptamer changes upon binding with ATP. By monitoring the change in electrophoretic mobility ($\Delta\mu$) of the aptamer with increasing concentration of ATP, the binding affinity of the aptamer-ATP complex can be determined.

The changing migration time of the aptamer (upon binding with ATP) is used as an approximation of the changes in the electrophoretic mobility ($\Delta\mu$) (Chu *et al.*, 1995). In the absence of ATP (Figure 4-3A), the aptamer migrates freely through the capillary

(t_A), but the aptamer peak is shifted (Figure 4-3B) upon interacting with the ATP ($t_{A,L}$). The maximum shift in the aptamer ($t_{A,L}^{\max}$) occurs once the binding site is saturated with the ATP (Figure 4-3C). By measuring the difference in migration times of the complexed and free aptamer ($\Delta t_{A,L}$ and $\Delta t_{A,L}^{\max}$), the electrophoretic mobilities ($\Delta \mu_{A,L}$ and $\Delta \mu_{A,L}^{\max}$) are determined and can be used to determine the binding constant (Chu *et al.*, 1995). Generally binding affinities are expressed in terms of the complex dissociation constant (K_d), which will be used in the remainder of this text.

Several factors must be considered when developing an ACE experiment including the change in electroosmotic flow (EOF) as the concentration of ligand is increased. Correction for changes in the bulk flow is typically accomplished by using an EOF marker, which is subtracted from the migration time of the analyte to account for any changes occurring in the EOF. To account for physical changes in buffer viscosity as the ligand concentration is increased, a correction factor “ v ” can be used. Bowser and Chen (1998) describe a method for quantitating the binding affinity of an analyte-ligand system by relating the change in the electrophoretic mobility of the analyte to the changing ligand concentration. The total electrophoretic mobility of the analyte (μ_{ep}^A) can be characterized as the sum of the electrophoretic mobilities of the fraction of free and bound analyte as shown in Equation 4.1, in which v is the viscosity correction factor, f_A is the fraction of free, unbound analyte, $\mu_{ep,A}$ is the electrophoretic mobility of the free analyte (A), f_{AC} is the fraction of bound analyte (AC), and $\mu_{ep,AC}$ is the electrophoretic mobility of the complex (AC).

$$v\mu_{ep}^A = f_A\mu_{ep,A} + f_{AC}\mu_{ep,AC} \quad (4.1)$$

The fraction of A and AC present can be described using the following expressions:

$$f_A = \frac{\text{amount of unbound species A}}{\Sigma \text{ total A containing species}} \quad (4.2)$$

$$f_{AC} = \frac{\text{amount of species AC}}{\Sigma \text{ total A containing species}} \quad (4.3)$$

The fraction of A and AC present and the total electrophoretic mobility of all species containing the analyte (A) can be related to the binding affinity by utilizing the following equilibrium:



in which C is the ligand and K_{AC} is the binding constant for the formation of the complex.

By employing the complex equilibrium depicted in Eqn 4.4 and relating the ligand and analyte concentrations, the following equation (Eqn 4.5) is derived.

$$v\mu_{ep}^A = \frac{1}{1 + K_{AC}[C]} \mu_A + \frac{K_{AC}[C]}{1 + K_{AC}[C]} \mu_{AC} \quad (4.5)$$

Finally Equation 4.6 can be used to relate the change in the electrophoretic mobility of the analyte to the binding constant and ligand concentration.

$$(v\mu_{ep}^A - \mu_{ep,A}) = \frac{(\mu_{ep,AC} - \mu_{ep,A})K_{AC}[C]}{1 + K_{AC}[C]} \quad (4.6)$$

By plotting the change in the electrophoretic mobility ($\mu_{ep}^A - \mu_{ep,A}$) versus the ligand concentration, the binding constant (K_{AC}) and the dissociation constant (K_d), which is $1/K_{AC}$, may be determined.

As mentioned earlier, the goal of this work was to characterize the binding affinity of a J-base aptamer and a standard base aptamer for ATP. After optimizing the ACE experiment to measure the binding constants for these aptamers, other ligand

affinities were explored. In the original selection of the ATP aptamer, the binding affinity was measured only for adenosine due to experimental constraints (Huizenga and Szostak, 1995). However, the authors theorized that similar affinity should be observed for all adenosine analogs with this aptamer. Using ACE, the affinity of the standard based aptamer for adenine, adenosine, AMP, ADP, and ATP was investigated.

Materials and Methods

Chemicals

Tris(hydroxymethyl)aminomethane, sodium chloride, and sodium phosphate monobasic were purchased from Fisher chemical (Pittsburgh, PA). Adenosine, adenine, adenosine 5'-monophosphate (AMP), adenosine 5'-diphosphate (ADP), adenosine 5'-triphosphate (ATP), and guanosine 5'-triphosphate (GTP) were purchased from Sigma Chemical (St. Louis, MO). Magnesium chloride and 5(6)-carboxyfluorescein were purchased from Aldrich Chemical (Milwaukee, WI). Standard base aptamers were synthesized, fluorescently labeled, and purified by Integrated DNA Technologies (Coralville, IA). A fluorescein label was attached to the 3' end of the standard base adenosine aptamer (5'-CTACCTGGGGGAGCATTGGGGAGGAAGGTAGCCGTGCGAAAA-3'). The J-base aptamer (5'-GTATGCGGTAGGAACGJCAGJGGGGGAGCAJAJGGJGJGAJA-3') was prepared and fluorescently labeled by the method developed by Battersby *et al.* (1999) and was generously donated by Professor Steven A. Benner. All solutions were prepared with deionized water purified with a Milli-Q Plus system (Millipore Corp., Marlborough, MA).

Aptamer preparation

Before experiments, a 4 μ M stock of aptamer in electrophoresis buffer was prepared and annealed. For the annealing process, the stock solution was heated at

90° C for 2.5 min and cooled to room temperature. Experimental samples consisted of ~1 μ M aptamer, 800 nM 5(6)-carboxyfluorescein (internal standard), and 7 μ M riboflavin (EOF marker) for unmodified capillary experiments or ~ 200 nM aptamer and 800 nM 5(6)-carboxyfluorescein (internal standard) for coated capillary experiments.

Apparatus

All separations were performed with a Beckman P/ACE 2200 capillary electrophoresis system (Beckman Coulter Fullerton, CA). Laser induced fluorescence (LIF) detection employed the 488 nm excitation line of a 3 mW Argon Ion laser (Beckman-Coulter) and emission was collected at 520 nm. Data was recorded and analyzed with P/ACE software (Beckman-Coulter). Nonlinear regression analysis employing Equation 4.6 was used to determine all dissociation constants. The least squares variance-covariance method was used with a macro written in house using Microsoft Excel.

K_d determinations employing unmodified capillaries

Bare, fused silica capillaries (25 μ m i.d., 360 μ m o.d.) from Polymicro Technologies (Phoenix, AZ), 37 cm in total length with a 30 cm effective length were employed for all separations. Capillaries were pretreated by rinsing with 1 M NaOH, deionized water, and buffer for 10 min each. Capillaries were primed by filling with buffer and applying an electric field of 300 V/cm for 1 hour. The capillary was then stored at room temperature for two days with the capillary ends immersed in vials of buffer in order to prevent drying.

For each ligand concentration, the capillary was equilibrated by rinsing with buffer for 10 min. The sample was introduced onto the capillary with a 5 s, 5 kV

injection and 14 kV was employed for all separations. Separations were performed in a 20 mM Tris, 283 mM NaCl, 2 mM NaH₂PO₄, 10 mM MgCl₂ pH 7.6 buffer.

K_d determinations with a coated capillary

A polyacrylamide coated capillary prepared using a method adapted from Cobb *et al.* (1990) and Dolnik *et al.* (1998) (detailed later in Chapter 5) was employed to reduce the EOF and subsequently the separation time of the highly negative aptamer. Capillaries were 50 µm i.d., 360 µm o.d. and 37 cm in total length in which a 30 cm effective length was employed for all separations. This capillary was stored in water at room temperature with the ends immersed in water to prevent drying. For each ligand concentration, the capillary was equilibrated by rinsing with buffer for 3 min. The separation buffer was 50 mM Tris, 50 mM NaCl, 5 mM MgCl₂ pH 7.6. and 5 s hydrodynamic injections were employed for all analyses.

Results and Discussion

Initial binding determinations were performed on a coated capillary with ATP concentrations in the range of 500 µM – 10 mM. At these concentrations of ATP, binding curves for the standard and J base aptamers depicted a sigmoidal shape suggesting a termolecular complex with 1:2 binding stoichiometry of aptamer to ATP (Figure 4-4) (Battersby *et al.*, 1999). Dissociation constants were determined as $9 \pm 2 \times 10^{-6} \text{ M}^2$ for the J base aptamer and $15 \pm 2 \times 10^{-6} \text{ M}^2$ for the standard base aptamer. Huizenga and Szostak (1995) reported a binding constant of $6 \pm 3 \times 10^{-6} \text{ M}$ for the standard base aptamer with adenosine and suggested only a 1:1 aptamer:adenosine complex was formed. However, a termolecular complex was also observed in NMR studies of the standard base aptamer with AMP (Lin and Patel, 1997). Since no

observable bimolecular complex was detected and NMR studies also observed a 1:2 binding stoichiometry, initial conclusions were drawn suggesting the original binding determinations of a 1:1 aptamer:adenosine complex did not describe aptamer binding with ATP.

A control experiment was performed with another ligand GTP, and because of the selectivity of the aptamer for ATP, no appreciable affinity between the aptamer and GTP should be observed. With the polyacrylamide coated capillary employed for these experiments, the EOF is greatly reduced and the separation is based on the electrophoretic mobilities of the analytes. The buffer used for these experiments (50 mM Tris, 50 mM NaCl, 5 mM MgCl_2 pH 7.6) contained a large concentration of Mg^{2+} ions that interact with the negative phosphate backbone of the DNA aptamer reducing the negative charge and electrophoretic mobility of the aptamer (DNA*) (Figure 4-5A). Upon binding with the negatively charged ATP, the electrophoretic mobility of the aptamer is more negative and a decrease in the migration time of the aptamer is observed (Figure 4-5B). If the shift in the DNA* peak was due solely to binding of ATP, no shift in migration time was expected when incorporating GTP into the electrophoresis buffer. However, when 5 mM GTP was present (Figure 4-5C) a similar shift in the DNA* peak occurred as compared to 5 mM ATP being present in the separation buffer (Figure 4-5B). The shift in the DNA* peaks was not a result of EOF changes, as the polyacrylamide coating suppressed the bulk flow in the capillary and no shift in the internal standard (IS) peak was observed upon adding ATP or GTP to the separation buffer. ATP and GTP can bind with the Mg^{2+} present in the buffer reducing the amount of Mg^{2+} interacting with the aptamer. With less Mg^{2+} bound to the aptamer (as is the case with 5 mM ATP or GTP

present), the mobility of DNA* is increased subsequently decreasing the aptamer migration time.

A Mg free buffer (50 mM Tris, 50 mM NaCl pH 7.6) was employed to further investigate the effects of Mg^{2+} on the shift of the DNA* peak. With no Mg^{2+} present in the buffer, the aptamer electrophoretic mobility is highly negative so the zone migrates rapidly through the capillary (Figure 4-6A). When 5 mM ATP was added to the Mg^{2+} free buffer (Figure 4-6B), only a slight change in the migration time of DNA* was observed which may be indicative of ATP binding to the aptamer. Upon the addition of 5 mM Mg (in the electrophoresis buffer), the electrophoretic mobility of the aptamer is decreased due to binding of Mg^{2+} ions (Figure 4-6C) and with the subsequent addition of 5 mM ATP to a Mg^{2+} containing buffer, a large shift in the DNA* peak is observed (Figure 4-6B). ATP concentrations ranged from 500 μ M-10 mM in the initial ACE experiments. At these concentrations of ATP, the ATP and Mg^{2+} (5 mM) were binding with each other; therefore, changing the concentration of Mg^{2+} interacting with the aptamer and producing the observed shifts in the migration time of DNA*. Other separation conditions accounting for the fluctuations in Mg^{2+} concentration were necessary in order for the binding constants to be determined.

Modifications to the first method were explored, and a new method was developed for determining the binding constants for both aptamers. This method utilized an unmodified capillary, which was equilibrated in the electrophoresis buffer for two days prior to experiments. This long equilibration period was used to help reduce fluctuations in the EOF once ligand was added to the separation buffer. To reflect the initial aptamer selection conditions used by Huizenga and Szostak (1995), a 25 mM Tris,

283 mM NaCl, 2 mM NaH_2PO_4 , 10 mM MgCl_2 pH 7.6 separation buffer was used. With this high salt buffer, 25 μm i.d. capillaries were employed to reduce Joule heating. To minimize the effects of the $\text{ATP}:\text{Mg}^{2+}$ binding on changing the mobility of the aptamer, the ATP concentration range was lowered to 0-200 μM and the Mg^{2+} concentration in the buffer was increased to 10 mM to insure saturation of the aptamer with Mg^{2+} . The aptamer was saturated with Mg^{2+} ions in order to achieve the maximum shift in the aptamer migration time prior to adding ATP.

Binding curves for the standard base aptamer and the J base aptamer (Figure 4-6) showed the two aptamers displayed similar affinity for ATP; however, a larger error was seen in the J base measurement. This large error was produced from experimental limitations. The width of the J base peak was very large, but the change in mobility of the aptamer upon binding with ATP was relatively small (20% change in mobility with binding of ATP). Therefore, errors arose from marking the change in the zone relative to the width of the peak. The dissociation constants were determined as $133 \pm 9 \mu\text{M}$ for the standard base aptamer and $120 \pm 63 \mu\text{M}$ for the J base aptamer (Figure 4-8), and no enhancement in binding affinity for ATP was observed with the J base aptamer. With these separation conditions (10 mM Mg^{2+} in the separation buffer and low ATP concentrations), the affinity of the standard base aptamer was investigated with GTP. No appreciable affinity was measured for the aptamer and GTP (Figure 4-9) demonstrating the specificity of the aptamer. Also with no observable affinity measured for the aptamer and GTP, these improved separation conditions allowed determination of the binding affinity of both aptamers with ATP.

Affinity determinations for adenosine analogs

The initial publication detailing the ATP aptamer was only able to characterize the binding with adenosine due to experimental limitations of the filter assay employed (Huizenga and Szostak, 1995). With our ACE method described above (unmodified capillaries with a 10 mM Mg^{2+} separation buffer), affinity measurements were performed and complex dissociation constants were determined for adenine, adenosine, AMP, ADP, and ATP. ACE electropherograms used to determine the aptamer:ligand dissociation constants displayed characteristic shifts in the aptamer (DNA*) migration time with increasing concentration of the ligand (Figure 4-10). The experimental binding curves (Figure 4-11) showed the weakest affinity complex was the adenine:aptamer complex and interestingly the strongest complex was the ADP:aptamer complex. The dissociation constants were determined as 216 ± 40 , 55 ± 11 , 168 ± 20 , 29 ± 8 , and 133 ± 9 μ M for adenine, adenosine, AMP, ADP, and ATP respectively and are summarized in Figure 4-12. A binding pattern was observed in which the aptamer affinity was dependent on the charge of the analyte. Figure 4-10 shows the ligand structures at pH 7.6, which was used for analysis. The structures of ADP and ATP are drawn to indicate the binding of Mg^{2+} present in the buffer. Most notably is the low affinity determined for the aptamer:adenine complex (K_d 216 ± 40 μ M), suggesting the ribose sugar was key in binding with the aptamer. The low affinity for adenine can be expected as selections of the aptamer were done with immobilized analytes containing the sugar moiety (because of the position on the molecules used for attachment to the column, the sugar was directed into the binding area accessible for aptamers during selection). ADP, which has a net -1 charge, and adenosine, which is neutral, displayed the greatest affinity with the aptamer (K_d 's of 29

± 8 and 55 ± 11 μM respectively). However, AMP and ATP both containing a net -2 charge show similar affinity for the aptamer (K_d 's of 168 ± 20 and 133 ± 9 μM). The lower affinity of the -2 charged ligands with the aptamer suggests the binding affinity of the aptamer is weakened due to the larger negative charges of AMP and ATP.

Binding stoichiometry

To determine the binding stoichiometry of the aptamer complexes, a Scatchard analysis was performed for all ligands. Scatchard analysis is an x-reciprocal plot of the change in electrophoretic mobility relative to the ligand concentration ($\mu_{ep}^A - \mu_{ep,A}/[\text{ligand}]$) with respect to the change in electrophoretic mobility ($\mu_{ep}^A - \mu_{ep,A}$). A Scatchard analysis of the ATP and ADP binding curves with the standard base aptamer (Figure 4-11) displayed no large deviation from linearity suggesting only 1:1 binding of the aptamer:ATP and aptamer:ADP complexes. The other binding curves (adenine, adenosine, and AMP) when analyzed with x-reciprocal plots also showed no evidence for any formation of a termolecular complex as observed with the higher ATP concentrations.

Analytical Applications

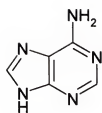
The ATP aptamer was found to have weak affinity for several adenosine analogs. This weak affinity is an ideal interaction for incorporation of the aptamer into an LC stationary phase to selectively retain adenosine analogs and separate them from other compounds. An aptamer stationary phase developed in our lab retained adenosine analogs such as adenosine, AMP, ADP, and ATP and allowed separation of these compounds from a large assortment of other molecules such as GTP, cAMP, and NAD^+ . The most retained compound on the column was adenosine followed by ADP, ATP, and

AMP. The retention of adenosine was affected by the hydrophobicity of the packing particles, but nonetheless retention on the column resembled the dissociation constants determined by ACE measurements.

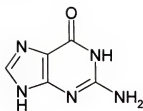
Conclusions

ACE was utilized to measure the affinity of a DNA aptamer with adenine, adenosine, AMP, ADP, and ATP. A binding pattern was observed in which the charge state of the ligand affected binding with the aptamer. The lowest affinities were determined for ADP and adenosine, which have -1 and neutral charges at the pH employed for the separation. Binding was disrupted by the presence of the -2 charges of AMP and ADP as indicative of the lower dissociation constants. The weaker interaction of the aptamer with adenosine analogs was ideal for an aptamer LC stationary phase that has been used to selectively separate analytes.

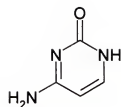
Modified nucleotides are one possibility for increasing the diversity and functionality of aptamers. A scientific achievement was accomplished by incorporating a positively charged functionality into an aptamer even though no enhancement in binding of ATP was measured for the J base aptamer. With continued research and improvements of selection conditions, modified base aptamers could improve aptamer diversity and increase the applicability of aptamers as analytical tools.



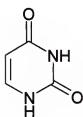
Adenine



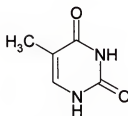
Guanine



Cytosine



Uracil



Thymine

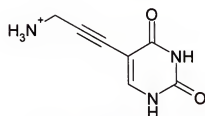
"J" 5-(3'-aminopropynyl)-
2'-deoxyuridine

Figure 4-1 Chemical structures of the five standard bases and the nonstandard J base.

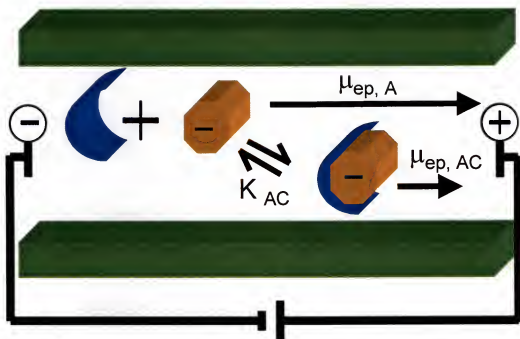


Figure 4-2 Schematic of Affinity Capillary Electrophoresis (ACE). The separation capillary is filled with buffer containing ligand, once the analyte is injected onto the column, the analyte and ligand bind. When the analyte binds to the ligand, its electrophoretic mobility (μ) is changed due to the different charge to mass ratio.

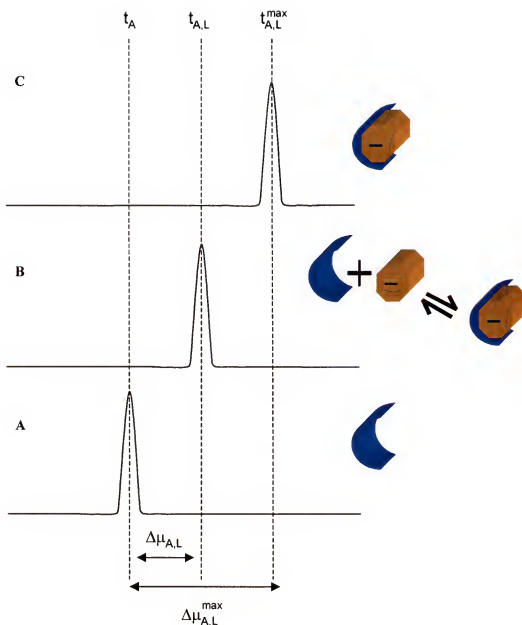


Figure 4-3 The effects of binding on the migration time of the aptamer. With no ligand present (A) the aptamer migrates at t_A . As ATP is added (B), the aptamer migration time is shifted ($t_{A,L}$) due to binding with ATP. The maximum shift in the aptamer migration time ($t_{A,L}^{max}$) is reached once binding sites on the aptamer are saturated with ATP. The electrophoretic mobilities of the aptamer ($\Delta\mu_{A,L}$ and $\Delta\mu_{A,L}^{max}$) are determined by the changing migration time of the aptamer.

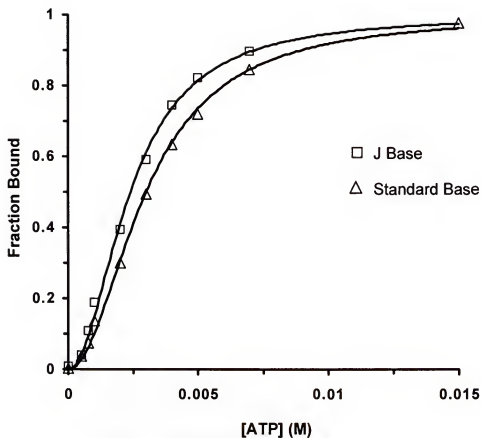


Figure 4-4 Binding curves of the standard base aptamer and J base aptamer in a 50 mM Tris, 50 mM NaCl, 5 mM MgCl_2 pH 7.6 buffer with a polyacrylamide capillary. Dissociation constants were $9 \pm 2 \times 10^{-6} \text{ M}^2$ for the J base aptamer and $15 \pm 2 \times 10^{-6} \text{ M}^2$ for the standard base aptamer.

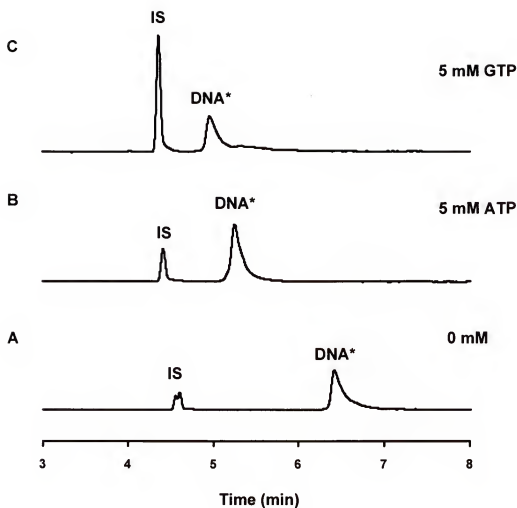


Figure 4-5 Control experiment with the standard base aptamer using a 50 mM Tris, 50 mM NaCl, 5 mM MgCl_2 pH 7.6 buffer with a polyacrylamide coated capillary. (A) 0 mM ligand (B) 5 mM ATP (C) 5 mM GTP.

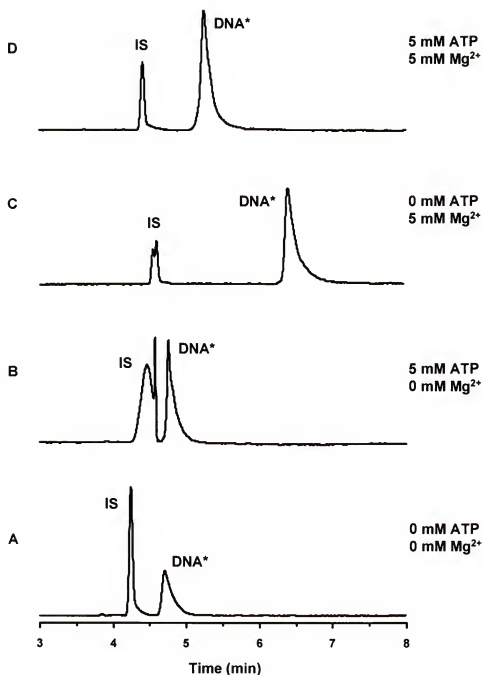


Figure 4-6 Effects of Mg²⁺ in the electrophoresis buffer on the mobility of the standard base aptamer (DNA*). The separation capillary was coated with polyacrylamide and the internal standard (IS) was 5(6)-carboxyfluorescein. In A and B, the separation buffer was 50 mM Tris, 50 mM NaCl pH 7.6. In C and D the separation buffer was 50 mM Tris, 50 mM NaCl, 5 mM MgCl₂ pH 7.6

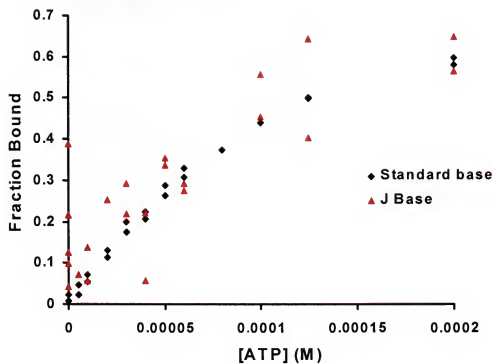


Figure 4-7 Binding curves of the standard base aptamer and J base aptamer with a 25 mM Tris, 283 mM NaCl, 2 mM NaH_2PO_4 , 10 mM MgCl_2 pH 7.6 buffer and a bare capillary. The error in the J base measurement can be seen with the variability of the data points (\blacktriangle).

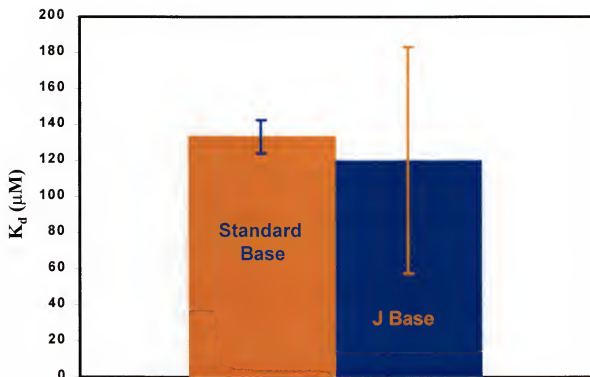


Figure 4-8 Dissociation constants (K_d) of the standard base aptamer and J base aptamer with ATP in a 20 mM Tris, 283 mM NaCl, 2 mM NaH_2PO_4 , 10 mM MgCl_2 pH 7.6 buffer. The K_d of the standard base aptamer was 133 ± 9 μM and 120 ± 63 μM was determined for the J base aptamer.

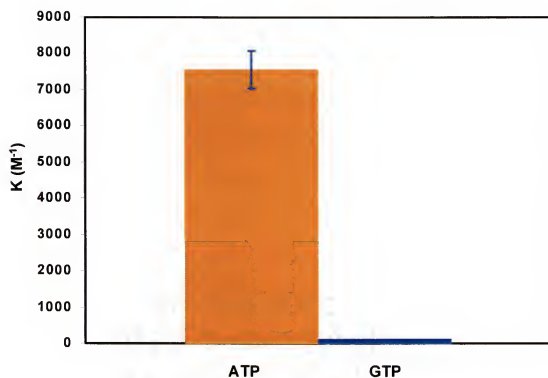


Figure 4-9 Control experiment for the standard base aptamer with ATP and GTP. Binding affinities are expressed as the binding constants (K), and no appreciable affinity was observed between the aptamer and GTP.

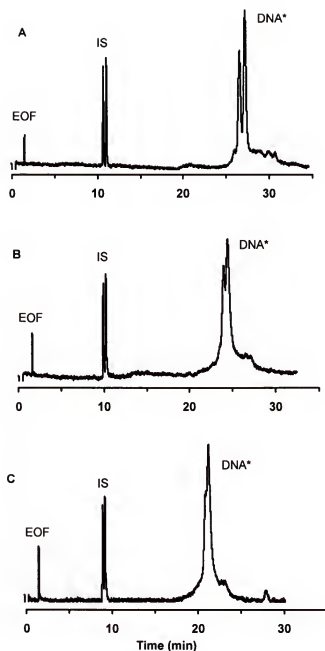


Figure 4-10 ACE electropherograms used for determining the binding constant of the standard base aptamer with ADP. The DNA* (1 μ M) was injected onto the column (5 s at 5 kV) containing varying concentrations of ADP. (A) 0 μ M ADP (B) 30 μ M ADP (C) 80 μ M ADP. Separation capillaries were 25 μ m i.d., and a separation voltage of 14 kV was used for all analyses. The internal standard (IS) was 5(6)-carboxyfluorescein (800 nM) and the EOF marker was riboflavin (7 μ M). The separation buffer was 20 mM Tris, 283 mM NaCl, 2 mM NaH_2PO_4 , 10 mM MgCl_2 pH 7.6.

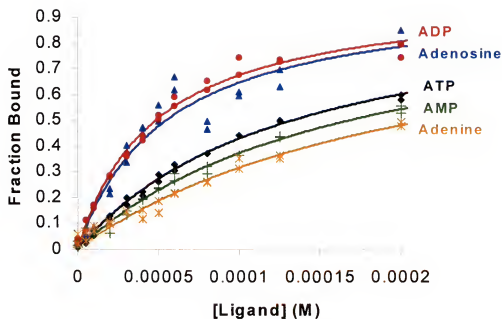


Figure 4-11 Binding curves of the standard base aptamer with adenine, AMP, ATP, adenosine, and ADP. The aptamer makes the strongest complex with ADP and the weakest with adenine.

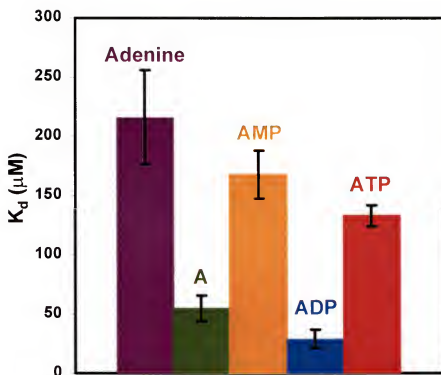


Figure 4-12 Dissociation constants determined for the standard base aptamer with adenine, adenosine, AMP, ADP, and ATP. The measured K_d 's were 216 ± 40 , 55 ± 11 , 168 ± 20 , 29 ± 8 , and 133 ± 9 μM respectively.

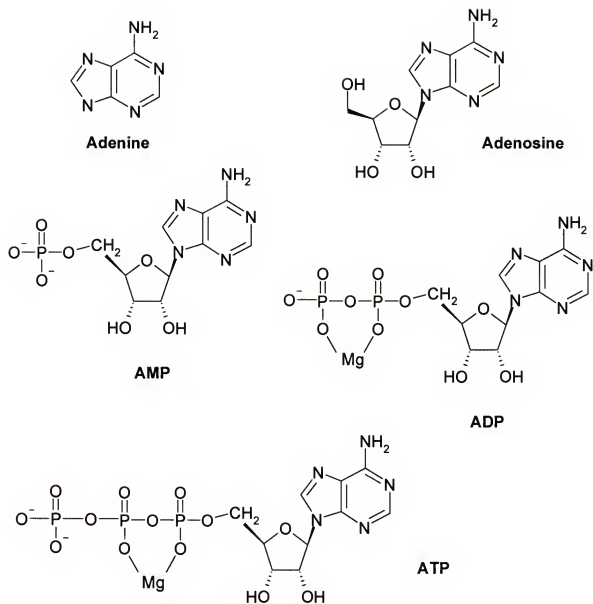


Figure 4-13 Chemical structures of the investigated ligands adenine, adenosine, AMP, ADP, and ATP at pH 7.6 in a Mg^{2+} buffer.

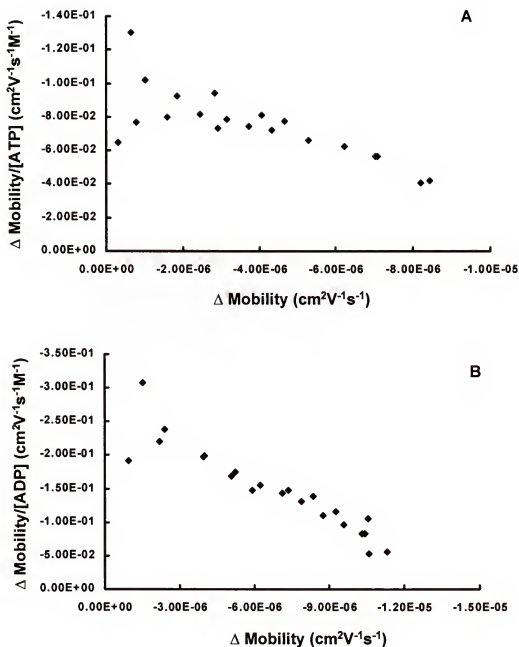


Figure 4-14 Scatchard plot analysis (x-reciprocal plot) of the (A) ATP and (B) ADP binding curves with the standard base aptamer. No large deviation from linearity is apparent, indicative of 1:1 binding stoichiometry.

CHAPTER 5

PREPARATION AND EVALUATION OF POLYMERIC CAPILLARY COATINGS FOR PROTEIN SEPARATIONS

Introduction

Capillary electrophoresis of biopolymeric molecules such as proteins can be problematic due to adsorption to capillary walls. Typically the charge on the surface of a protein is distributed inhomogeneously creating positively charged patches on the protein surface. The buffer pH determines the ionization of the capillary surface, which is comprised of silanol groups (pK_a 's ranging from 5.3-6.3) (Dougherty *et al.*, 1997). With increasing pH the capillary surface becomes negatively charged providing an environment for adsorption due to Coulombic interactions. With adsorption to the capillary walls, peak broadening often occurs resulting in a loss of separation efficiency. Several techniques have been investigated to aid in reducing protein adsorption to capillary walls including: altering the pH and ionic strength of the electrophoresis buffer to promote Coulombic repulsion between the capillary wall and proteins (Bruin *et al.*, 1989; Lauer and McManigill, 1986; McCormick, 1988) incorporating additives into the separation buffer to create a dynamic coating over the capillary wall (Bullock and Yuan, 1991; Bushey and Jorgenson, 1989; Green and Jorgenson, 1989; Swedberg, 1990), and chemically modifying the capillary surface with neutral polymers creating a static coating (Hjertén, 1985; Cobb *et al.*, 1990; Schmalzing *et al.*, 1993; Malik *et al.*, 1993).

When employing low pH separation buffers ($< pH\ 3$), the negatively charged surface of the capillary wall is greatly reduced. Published reports have documented

reduction in protein adsorption when incorporating low pH buffers with unmodified silica capillaries (Grossman *et al.*, 1988; McCormick, 1988). Alternatively, high pH buffers (> pH 11) have also been incorporated into protein CE separations in which the separation buffer is above the isoelectric point (pI) of the protein (Lauer and McManigill, 1986). Above the pI of a protein, a negatively charged protein surface is created, and protein adsorption is reduced because of the repulsion of the protein from the negatively charged capillary surface. However, at extreme pHs hydrolysis and denaturation of proteins can occur (Karger *et al.*, 1989; Swedberg, 1990). This phenomenon is detrimental during detection of aptamer-protein complexes as complex formation might be disrupted due to irreversible damage to the protein.

Dynamic coatings are another possibility to reduce protein adsorption. Typically additives such as neutral polymers, salts, or cationic surfactants are incorporated into the separation buffer. Polymers present in the buffer coat the walls of the capillary, preventing proteins from interacting with the negatively charged silanols present on the capillary surface. Several polymers have been employed as dynamic coatings for CE separations including polyvinylalcohol, poly(ethyleneoxide), and several cellulose derivatives (Cifuentes *et al.*, 1996; Iki and Yeung, 1996; Bullock and Yuan 1991; Stover *et al.*, 1989; Rohlicek and Deyel, 1989). Alternatively, cationic surfactants and salts can interact with the negative charge of the capillary walls and alter the electrokinetic potential and electroosmotic flow (EOF). The EOF can be decreased, neutralized, and possibly reversed when employing cationic surfactants as dynamic coatings. Compounds such as polyarginine, polybrene, polyethyleneimine, diaminoethane, and chitosan have been employed as dynamic coatings (Chiu *et al.*, 1995; Cifuentes *et al.*, 1996; Song *et al.*,

1993; Yao and Li, 1994). Separation efficiencies on the order of 2×10^6 theoretical plates have been reported when incorporating polycations into CE separations (Chiu *et al.*, 1995). However, additives can cause changes in the separation buffer such as increasing the electrical conductivity resulting in Joule heating and decreases in the separation efficiency (Malik *et al.*, 1993).

Static coatings are created when the capillary surface is chemically modified with neutral hydrophilic polymers. An ideal polymer coating would be stable in aqueous buffers over a wide pH range, suppress solute-wall interactions, and be chemically stable for hundreds of injections. Two key processes are necessary to prepare a static wall coating, silanization and polymerization. The silanization step establishes the linkage between the surface of the capillary and the polymer. By covalently linking a neutral, hydrophilic polymer to the capillary surface, the silanol groups on the capillary walls are shielded removing charged sites for protein adsorption. Typically the EOF is also suppressed or even eliminated with a static coating.

Organosilanes such as γ -methacryloxypropyltrimethoxysilane (also denoted the silanization reagent) are used to prepare the capillary surface for interaction with the polymer coating. The silanization reagent reacts with the silanol groups on the capillary surface creating siloxane moieties (Si-O-Si). The siloxanes on the surface then react with a monomer or polymer to establish the static coating. At high pHs, siloxanes are prone to nucleophilic cleavage, limiting the applicability of static coatings employing this type of surface linkage. Other surface modifications have been explored to increase the applicable pH range for static coated capillaries. For example, a Grignard reagent (vinylmagnesium bromide) was employed to establish a Si-C linkage between the

polymer and the capillary surface (Cobb *et al.*, 1990; Dolník *et al.*, 1998). These two types of capillary surface chemistry are depicted in Figures 5-1 and 5-2 in which acrylamide is used as the monomer to create the polymer coating. Polyacrylamide coated capillaries are the most frequently used static coatings; however, the instability of acrylamide coated capillaries at basic pHs has prompted the use of more stable polymers including polyethers, hydroxymethylcellulose and dextran (Malik *et al.*, 1993; Dolník, 1997; Hjerten and Kubo, 1993).

Most coating procedures involve multiple steps in which silanization, chemical bonding of the polymer, and *in situ* polymerization are accomplished separately, ultimately increasing the length of time necessary to prepare a capillary. Malik *et al.* (1993) developed a coating procedure incorporating all three chemical steps into one and reduced the preparation time necessary for coating a capillary. With this method a variety of capillaries with varying diversity were prepared by incorporating polymers such as UCON 75-H-90,000, Superox 4 and Carbowax 20M into the coating procedure. All of these polymers are polyethers with terminal hydroxyl groups. These capillaries were used to analyze an array of analytes including proteins, nucleotides, and histones (Zhao *et al.*, 1992; Malik *et al.*, 1993; O'Neill *et al.*, 1994; Shao *et al.*, 1994).

This work investigated several coating procedures for utility with CE protein separations. The first coating procedure is indicative of a classical acrylamide capillary coating in which γ -methacryloxypropyltrimethoxysilane was used as the silanization reagent (Hjerten, 1985; Clark *et al.*, 1994). Next another acrylamide coating procedure, adapted from that previously reported by Cobb *et al.* (1990) and Dolník *et al.* (1998), was investigated. A Grignard reagent was used to create a Si-C bond on the surface of the

capillary and provide a more stable linkage between the polymer and the capillary wall. The final coating procedure adapted from Malik *et al.* (1993), utilized a single reaction step for silanization, polymer coating, and *in situ* polymerization. Two polymers UCON and Superox at several concentrations were investigated. To compare the capillary coatings, the electroosmotic flow and separation efficiency of several proteins were measured for the various capillaries.

Materials and Methods

Apparatus

All separations were performed with a Beckman P/ACE 2200 capillary electrophoresis system (Beckman Coulter Fullerton, CA) equipped with a UV detector. Unmodified, fused silica capillaries (25 and 50 μm i.d., 360 μm o.d.) were purchased from Polymicro Technologies (Phoenix, AZ). Data was recorded and analyzed with P/ACE software (Beckman-Coulter).

Chemicals

Cytochrome C, lysozyme, ribonuclease A, α -chymotrypsinogen, N,N,N',N'-tetramethylethylenediamine (TEMED), γ -methacryloxypropyltrimethoxysilane, and ammonium persulfate were purchased from Sigma Chemical (St. Louis, MO). Methylene chloride, n-pentane, and light mineral oil were purchased from Fisher chemical (Pittsburgh, PA). Anhydrous tetrahydrofuran (THF), vinylmagnesium bromide in THF, 1,1,1,3,3,3-hexamethyldisilazane, and dicumyl peroxide were bought from Aldrich Chemical (Milwaukee, WI). The polymers UCON 50-HB-5100 and Superox 4 10 G were purchased from Alltech (Deerfield, IL). Acrylamide was obtained from Pharmacia Biotech (Uppsala, Sweden) and thionyl chloride was purchased from Acros Organics

(Morris Plains , NJ). All solutions were prepared with deionized water purified with a Milli-Q Plus system (Millipore Corp., Marlborough, MA).

Classical Acrylamide Coating via Silanol Linkage

Any length of capillary and most inner diameters can be coated with this procedure. Before beginning the coating procedure, an optical window is created by removing a small section of the polyimide from the capillary. Once the window has been created, the capillary is prepared for silanization. Using a pressure bomb, the capillary is rinsed with 1 M NaOH for 30 min, then with deionized water for 5 min, followed by a 1M HCl rinse for 30 min, and finally with a dilute acetic acid rinse for 30 min. The dilute acetic acid solution is prepared by adding dropwise, concentrated acetic acid to deionized water until a pH between 3 and 3.5 is achieved. The silanization reagent, which is prepared fresh, consists of a 4% γ -methacryloxypropyltrimethoxysilane solution in 50% v/v ethanol/dilute acetic acid (prepared in the same manner as describe above). The capillary is rinsed for 10-15 min with the silanization reagent and then the flow stopped. After 30 min the capillary is rinsed again with a fresh solution of the silanization reagent for a few minutes and again the flow is stopped to allow time (approximately another 30 min) for the surface to react. While waiting for the capillary walls to be silanized, the acrylamide solution consisting of 4% w/v acrylamide and 0.2% ammonium persulfate dissolved in deionized water is prepared. This solution should be stirred and degassed for 10-15 minutes. A few minutes before use, 0.1 vol % of TEMED should be added to the acrylamide solution and the entire mixture stirred. The capillary is then rinsed with this solution for 10 min and the flow stopped. After 30 min, the capillary is flushed with fresh acrylamide for a few minutes and the flow is stopped

again. After a reaction time of 1 hour, the capillary should be flushed with water to remove any residual acrylamide. The capillary is filled with water for storage and the ends of the capillary are immersed in water to prevent drying of the coating.

Acrylamide Capillary Coating via Grignard reagent

With this coating procedure, 1m or more of capillary (≥ 25 mm i.d.) is generally prepared. A pressure bomb is used to flush the capillary with all solutions. Before beginning experiments, the bomb is flushed with argon gas, which is dried over Drierite (calcium sulfate) using a drying tube. The first reagent thionyl chloride is used to substitute a chlorine moiety on the capillary surface and prepare the column for further reaction. The silanols (Si-OH) on the capillary surface are chemically modified to Si-Cl as shown in Figure 5-1B. A concentrated solution of thionyl chloride is placed in a pressure bomb while maintaining a flowing stream of argon over the bomb. With one end of the capillary immersed into the thionyl chloride solution, the bomb is sealed. The capillary is flushed with thionyl chloride at a low flow rate (approximately 20 psi). The opposite end of the capillary is inserted into a septum and placed loosely into a vial of acetone. The septum insures the outlet of the capillary remains in the vial so excess thionyl chloride is collected and diluted with the acetone. After rinsing for 2 hours, the flow rate should be reduced by lowering the pressure on the argon tank regulator (10 psi or lower). At this flow rate the capillary is flushed for another 10 hours.

Next the capillary surface is reacted with the Grignard reagent vinylmagnesium bromide to form alkene groups (see Figure 5-1B). The concentrated solution of Grignard reagent is diluted 1:1 with dry THF. A vial sealed with a septum is purged with dry argon, then using a gas tight syringe THF is added. Next, with another gas tight syringe, the Grignard reagent is added. If salts precipitate while adding the Grignard, a new

solution should be prepared before continuing. Grignard reagents are very reactive and care must be taken to reduce exposure to air as magnesium salts will precipitate from the solution. The pressure bomb is not a viable option to use with the Grignard; therefore, to reduce exposure to air, a vacuum apparatus or syringe pump should be employed to pull the reagent through the capillary. When using vacuum, one end of the capillary is laced through the septum and immersed into the Grignard/THF solution while the other end is attached to a vacuum pump with a trap to collect any excess reagent. The vacuum is applied for 6 hours to insure complete reaction on the surface of the capillary. After removal of the vacuum, the end of the capillary in the Grignard solution is placed in a vial of anhydrous THF. The vacuum is reapplied and the capillary should be rinsed with THF for 30-60 min to remove all excess vinylmagnesium bromide. Once the Grignard is flushed from the capillary, the capillary is rinsed with solutions of THF for 20 min, deionized water for 20 min, and finally flushed with argon for 10 min.

For polymerization, acrylamide is used in conjunction with ammonium persulfate (APS) and TEMED. During the THF, H₂O, and argon rinses, the acrylamide solution is prepared. Solutions (10% w/v) of acrylamide and APS are prepared with deionized water. The acrylamide coating solution consists of 1.5 mL of 10% acrylamide, 50 μ L of 10% APS, and 3.5 mL deionized water. This solution is stirred and degassed for 30 min before use. Five minutes before use, 5 μ L of TEMED is added to the acrylamide solution. The final solution should be stirred for 5 min and then placed in the pressure bomb to flush the capillary. The capillary is rinsed with the acrylamide solution for 10 min and then the pressure removed stopping the flow of the solution. The capillary is allowed to react for 30 min and then the capillary is flushed with the acrylamide solution

again for 5 min. The flow is removed and the capillary should be left for another 30 min to allow time for polymerization. Finally the capillary is flushed with deionized water to remove all unreacted polyacrylamide. The capillary should be filled with water and stored with the ends of the capillary immersed in water to prevent any drying of the capillary bed. To create an optical window, fuming sulfuric is dropped slowly over the coated capillary until the polyimide coating is removed.

Polyether capillary coatings

Generally 1m or more of capillary with inner diameters ranging from 10-50 μm can be coated with this procedure. First the capillary is rinsed with methylene chloride for 30 min and then flushed with nitrogen, argon, or air for 10 min. While the capillary is being rinsed, the polymer solution should be prepared. All solutions are prepared in a 50% v/v solution of methylene chloride:pentane. Final solution concentrations of the polymer should be 5-15 mg/mL. To the polymer solution, HMDS and dicumyl peroxide should be added so the final concentrations are 1 mg/mL and 0.1 mg/mL respectively. To aid in dissolving the polymer, a Vortex can be applied for several minutes. Once the solution is ready, flush the capillary for several minutes in order to fill the capillary. Next one end of the capillary is pushed through a septum and the other connected to a vacuum. The entire capillary is immersed into a thermostated bath at a constant temperature of 40°C. Once the vacuum is applied the solvent is evaporated, by observing the lightening in color of the capillary, the progress of solvent evaporation can be monitored. Typically this process takes 10-30 min depending on the length of the capillary and thickness of the polymer coating. Once the solvent is evaporated, the vacuum is removed and the other end of the capillary is removed from the septum. The capillary is then flushed for 30 min

with air. The ends of the capillary are then sealed with a propane/oxygen torch and the capillary is baked at 170°C for 30 min. After cutting the capillary and before use, the capillary is rinsed with methanol, methylene chloride, and methanol again for 30 min each. After the methanol rinse the optical window is prepared by removing a small portion of the polyimide coating (a match may be used to burn away the polyimide). Finally the capillary is rinsed with deionized water for 30 min and electrophoresis buffer before being employed in any separations.

Results and Discussion

Electroosmotic Flow Measurements

Electroosmotic flow (EOF) suppression is one characteristic of a capillary coating. To measure the EOF, a neutral analyte, mesityl oxide, was electrophoresed with each capillary and detected via UV absorption at 214 nm. For unmodified, fused silica capillaries, the EOF is equivalent to the time required for a neutral analyte to travel the length of the capillary. The electrophoretic mobility (μ) of a neutral analyte is zero; therefore, the EOF propels neutrals through the capillary in order to be detected. Typically EOF is greatly reduced in coated capillaries and neutral migration can be very slow. A method developed by Sandoval and Chen (1996) was employed to calculate the electroosmotic flow in the polymer coated capillaries.

To measure the EOF, a plug of analyte (mesityl oxide) is injected onto the column and the separation voltage is applied for a specific period of time. During this time, the neutral analyte migrates through the capillary based on the EOF present; therefore, the smaller the EOF within the capillary, the longer the separation voltage needed to be applied in order to move the neutral marker to the detector. The electric field is removed and the separation is stopped. Another plug of analyte is then injected onto the capillary.

Finally the capillary is rinsed at a low flow rate in which the applied pressure was 0.5 psi. Two peaks should be detected, in which the difference between the two zones is representative of the electroosmotic flow. The EOF is calculated with the following relationship:

$$\mu_{EOF} = \frac{Ll}{Vt_v} \left(1 - \frac{t_1}{t_2} \right) \quad (5.1)$$

in which L is the total length of the capillary (cm), l is the effective separation distance (cm), V is the separation voltage (Volts), t_v is the total time (s) the electric field was applied, t_1 is the migration time (s) of the first peak, and t_2 is the migration time (s) of the second peak.

For determining the EOF, 25 μm i.d. coated capillaries were each 27 cm in total length with an effective separation distance of 20 cm. The investigated columns included an unmodified capillary, a polyacrylamide capillary created with a siloxane linkage, two UCON capillaries (10 mg/mL and 15 mg/mL), and a Superox capillary (4 mg/mL). First a 10 s pressure injection was used to inject a plug of mesityl oxide onto the capillary and the electric field (12 kV) was applied for 10 min. After turning off the electric field, another plug of mesityl oxide was introduced onto the capillary with a 10 s pressure injection. A low pressure rinse (0.5 psi) was applied to the capillary to push the zones past the detector. The EOF in each capillary was calculated by using Equation 5.1.

With a low pH buffer, 40 mM Tris-HCl pH 4.8, the unmodified capillary was found to have an EOF of $12.1 \times 10^{-5} \text{ cm}^2\text{V}^{-1}\text{s}^{-1}$. EOF suppression was observed with both UCON capillaries in which the 10 mg/mL UCON coating was determined to have an EOF of $6.34 \times 10^{-5} \text{ cm}^2\text{V}^{-1}\text{s}^{-1}$ and $1.09 \times 10^{-5} \text{ cm}^2\text{V}^{-1}\text{s}^{-1}$ was measured for the 15 mg/mL UCON capillary, demonstrating the greater suppression of EOF with thicker polymer

coatings. The polyacrylamide coating was found to have an EOF of $0.184 \times 10^{-5} \text{ cm}^2 \text{ V}^{-1} \text{ s}^{-1}$ nearly two orders of magnitude lower than that of the unmodified capillary ($12.1 \times 10^{-5} \text{ cm}^2 \text{ V}^{-1} \text{ s}^{-1}$). The EOF determined for the Superox capillary ($0.517 \times 10^{-5} \text{ cm}^2 \text{ V}^{-1} \text{ s}^{-1}$) was 3 times greater than the polyacrylamide coating ($0.184 \times 10^{-5} \text{ cm}^2 \text{ V}^{-1} \text{ s}^{-1}$); however, both the Superox and polyacrylamide coatings suppressed the EOF by nearly an order of magnitude greater than the UCON coated capillaries. The EOF's determined for the five capillaries are summarized in the following table.

Table 5-1 Electroosmotic flow (μ_{eof}) calculated for each capillary in a 40 mM Tris-HCl buffer pH 4.8.

| Coating | EOF ($\text{cm}^2 \text{ V}^{-1} \text{ s}^{-1}$) |
|-------------------|--------------------------------------------------------|
| Unmodified | 12.1×10^{-5} |
| Polyacrylamide | 0.184×10^{-5} |
| 10 mg/mL UCON | 6.34×10^{-5} |
| 15 mg/mL UCON | 1.09×10^{-5} |
| 4.4 mg/mL Superox | 0.517×10^{-5} |

To investigate the effects of pH on the electroosmotic flow, the same method was employed with a higher pH buffer, 50 mM Tris, 50 mM NaCl, 5 mM MgCl_2 pH 7.6. An increase in EOF was measured for the unmodified, polyacrylamide, and UCON capillaries. The EOF of the Superox capillary with this buffer was unable to be determined as the two neutral zones could not be resolved from each other. The measured electroosmotic flows were $22.7 \times 10^{-5} \text{ cm}^2 \text{ V}^{-1} \text{ s}^{-1}$, $1.94 \times 10^{-5} \text{ cm}^2 \text{ V}^{-1} \text{ s}^{-1}$, $19.8 \times$

$10^{-5} \text{ cm}^2 \text{ V}^{-1} \text{ s}^{-1}$, and $3.38 \times 10^{-5} \text{ cm}^2 \text{ V}^{-1} \text{ s}^{-1}$ for the unmodified, polyacrylamide, 10 mg/mL UCON, and 15 mg/mL UCON capillaries respectively. The EOF in the unmodified capillary ($22.7 \times 10^{-5} \text{ cm}^2 \text{ V}^{-1} \text{ s}^{-1}$) almost doubled at the higher pH when compared to the EOF measured at pH 4.8 ($12.1 \times 10^{-5} \text{ cm}^2 \text{ V}^{-1} \text{ s}^{-1}$). At the higher pH, the EOF in the two UCON capillaries increased by a factor of 3; however, the largest increase in the EOF at the higher pH occurred with the polyacrylamide capillary. At a pH of 7.6 the EOF was measured to be $1.94 \times 10^{-5} \text{ cm}^2 \text{ V}^{-1} \text{ s}^{-1}$ and at the lower pH (4.8) the EOF was determined to be $0.184 \times 10^{-5} \text{ cm}^2 \text{ V}^{-1} \text{ s}^{-1}$. The EOF increased an order of magnitude at the higher pH, demonstrating the instability of this coating at higher pH's. Table 5-2 summarizes the EOF measured for the capillary coatings in the 50 mM Tris, 50 mM NaCl, 5 mM MgCl_2 pH 7.6 buffer as well as the pH effects on the EOF.

Table 5-2 Summary of the electroosmotic flow (μ_{eof}) calculated for each capillary at pH's of 4.8 and 7.6 as well as the increase in EOF with higher pH.

| Coating | EOF (4.8) ($\text{cm}^2 \text{ V}^{-1} \text{ s}^{-1}$) | EOF (7.6) ($\text{cm}^2 \text{ V}^{-1} \text{ s}^{-1}$) | Increase in EOF with pH |
|----------------|--------------------------------------------------------------|--------------------------------------------------------------|----------------------------|
| Unmodified | 12.1×10^{-5} | 22.7×10^{-5} | 2 fold |
| Polyacrylamide | 0.184×10^{-5} | 1.94×10^{-5} | 10 fold |
| 10 mg/mL UCON | 6.34×10^{-5} | 19.8×10^{-5} | 3 fold |
| 15 mg/mL UCON | 1.09×10^{-5} | 3.38×10^{-5} | 3 fold |

In another study, the EOF of a polyacrylamide coated capillary prepared via a Grignard reagent was determined and compared to an unmodified, fused silica capillary. Each capillary was 50 μm i.d., 40 cm effective, and 47 cm total length. A 20 mM

phosphate pH 7.0 buffer was employed and mesityl oxide was used as the neutral marker. The time required for the neutral analyte to travel the length of the capillary was used to measure the EOF in the unmodified capillary. Equation 5.1 in conjunction with the method previously described was used to determine the EOF of the polyacrylamide capillary. At this pH, EOF's of $60.9 \times 10^{-5} \text{ cm}^2 \text{V}^{-1} \text{s}^{-1}$ and $0.961 \times 10^{-5} \text{ cm}^2 \text{V}^{-1} \text{s}^{-1}$ were determined for the unmodified and polyacrylamide capillaries respectively. In comparison to the unmodified capillary, the polyacrylamide capillary suppressed the measurable EOF considerably (by a factor of 63).

To test the stability of this polyacrylamide coating, which employs a Si-C surface linkage between the capillary and the polymer, the EOF was measured at a more basic pH. With a 89 mM Tris, 89 mM borate, 5 mM EDTA, 5 mM KCl pH 8.3 buffer, the EOF was determined as $1.78 \times 10^{-6} \text{ cm}^2 \text{V}^{-1} \text{s}^{-1}$. The EOF determined at a pH of 8.3 was slightly lower than that found previously at pH 7.0 ($0.961 \times 10^{-5} \text{ cm}^2 \text{V}^{-1} \text{s}^{-1}$), which might be indicative of the varying thickness of the coatings present on the capillary surface, since different capillaries were used in the two EOF measurements. Capillary to capillary reproducibility with the Grignard reaction scheme was affected greatly by the reaction of the vinylmagnesium bromide with the capillary surface. On many occasions only small volumes of the Grignard were introduced into the capillary reducing the amount of reagent available for reaction. If the vinylmagnesium bromide did not react with the capillary surface upon addition of an aqueous solvent such as water, the reactive silanols would reform on the capillary surface and the acrylamide would not attach leaving negatively charged sites on the capillary walls increasing the EOF within the capillary.

Protein Resolution and Separation Efficiency

The separation efficiency for proteins is another method to compare the effectiveness of the polymer coatings. For this comparison, the capillaries used previously in EOF investigations were employed to separate a protein mixture containing 1.2 mg/mL cytochrome C, 2.2 mg/mL lysozyme, 2.2 mg/mL ribonuclease A, and 2.2 mg/mL α -chymotrypsinogen. The effective separation distances were 20 cm with total capillary lengths of 27 cm. The separation buffer was 40 mM Tris-HCl pH 4.8, and a 2 s 5.6 kV injection was used to introduce the protein mixture onto the capillary. For the separation an electric field of 207 V/cm (5.6 kV) was employed. The proteins were detected at 214 nm with an absorption detector. The number of theoretical plates is used as a measure of the separation resolution. To calculate the theoretical plates (N), the following relationship was used:

$$N = 5.54 \left(\frac{t_R}{w_{h-h}} \right)^2 \quad (5.2)$$

where t_R is the migration time of the analyte and w_{h-h} is the width of the zone (min) at half height. The separation efficiencies calculated for proteins are summarized in Table 5-3.

The summary shows the low efficiency of the unmodified capillary for the protein separation due to adsorption on the capillary walls. Cytochrome C was not well resolved from the base of the lysozyme peak (Figure 5-3) so the efficiency was not quantitated. All the proteins showed absorption on the unmodified capillary and efficiencies of 4300, 4400, and 3600 plates were calculated for lysozyme, ribonuclease A, and α -chymotrypsinogen respectively. With the polyacrylamide capillary (Figure 5-4) some

improvement was seen in the separation efficiencies. The cytochrome C is now detected but with very low efficiency, 868 plates. The lysozyme peak had considerably lower efficiency on the polaacrylamide coating with only 506 theoretical plates calculated. However, the efficiencies of the ribonuclease A (32000 plates) and α -chymotrypsinogen (20000 plates) were considerably improved with the acrylamide coating relative to the unmodified capillary.

Table 5-3 Separation efficiencies of the protein mixture on each capillary employing a 40 mM Tris-HCl pH 4.8 buffer and 207 V/cm electric field.

| Coating | Cyt C | Lys | Ribo A | α -chymo |
|----------------------|------------|-------|--------|-----------------|
| Unmodified | Unresolved | 4300 | 4400 | 3600 |
| Polyacrylamide | 868 | 506 | 32000 | 20000 |
| 10 mg/mL UCON | 95000 | 50000 | 106000 | 94000 |
| 15 mg/mL UCON | 178000 | 95000 | 95000 | 92000 |
| 4.4 mg/mL Superox | 138000 | 79000 | 59000 | 68000 |

Increased separation efficiency was achieved for all proteins on the polyether (UCON and Superox) coated capillaries. For a 10 mg/mL UCON capillary, separation efficiencies were determined to be 950000 plates for cytochrome C, 50000 plates for lysozyme, 106000 plates for ribonuclease A, and 94000 plates for α -chymotrypsinogen. Figure 5-5 shows the electrophoretic separation of the protein mixture on a 15 mg/mL UCON capillary. Improved separation efficiencies were measured for the cytochrome C (178000 plates) and lysozyme (95000) with the thicker coating; however, similar efficiencies were calculated for ribonuclease A (106000 plates) and α -chymotrypsinogen

(94000 plates) in comparison with the 10 mg/mL UCON capillary. The Superox coating also showed an improvement in efficiency for all peaks in comparison with the unmodified and polyacrylamide capillaries. Efficiencies of 138000, 79000, 59000, and 68000 plates were calculated for cytochrome C, lysozyme, ribonuclease A, and α -chymotrypsinogen respectively on the Superox capillary (Figure 5-6).

In order to compare the polyether coatings with those previously published (Malik *et al.*, 1993), separations with longer effective lengths were investigated. Figure 5-7 is the separation of the protein mixture on a 15 mg/mL UCON capillary with an effective separation distance of 90 cm (97 cm total) and an applied electric field of 258 V/cm. The efficiencies for the four proteins were 882000 plates for cytochrome C, 878000 plates for lysozyme, 175000 plates for ribonuclease A and 412000 plates for α -chymotrypsinogen. Malik *et al.* (1993) reported efficiencies of 1.2 million plates for cytochrome C, 1.1 million plates for lysozyme, 977000 plates for ribonuclease A, and 1.1 million plates for α -chymotrypsinogen. The greater efficiency of the published columns may be due to the thinner films employed for the published capillary separations (UCON concentrations were 0.1 mg/mL – 8 mg/mL compared to ours of 10 and 15 mg/mL UCON). Also a larger molecular weight polymer was used for the published columns (UCON 75-H-90,000). This polymer was not obtainable at the time of this study, so a similar polymer UCON 50-HB-5100 (a lower molecular weight UCON polymer) was used.

With a 4 mg/mL Superox capillary and a 70 cm effective separation distance (77 cm total) the peak efficiencies were 374,000, 92,000, 183,000, and 144,000 plates for cytochrome C, lysozyme, ribonuclease A, and α -chymotrypsinogen respectively (Figure 5-8). Again lower efficiencies were calculated for our columns compared to those

previously published in which efficiencies of 680000, 319000, 426000, and 773000 plates, respectively, were reported for the four proteins (Malik *et al.*, 1993). Again the thickness of the coating may have affected the efficiency of our separation.

In order to demonstrate the effect of coating thickness on the separation efficiency, two 15 mg/mL UCON capillaries were compared. The first, which has been described earlier, was prepared with 15 mg/mL polymer, 1 mg/mL HMDS (silanization reagent), and 0.1 mg/mL dicumyl peroxide (radical initiator). With a 90 cm effective length separation (Figure 5-7), efficiencies of 882000, 878000, 175000, and 412000 plates were calculated for cytochrome C, lysozyme, ribonuclease A, and α -chymotrypsinogen respectively. However, by doubling the concentration of the HMDS and dicumyl peroxide to 2 mg/mL and 0.2 mg/mL while maintaining the polymer concentration at 15 mg/mL, a decrease in efficiency was measured for all peaks. With a 90 cm effective distance (97 cm total length), the separation efficiencies on this column (Figure 5-9) were determined as 418000 for cytochrome C, 47000 for lysozyme, 218000 for ribonuclease A, and 141000 for α -chymotrypsinogen. The EOF was also suppressed more with the increase in the thickness of the UCON coating. The total analysis time was increased from 40 min (Figure 5-7) to 55 min (Figure 5-9) with the increase in the HMDS and dicumyl peroxide concentrations. Table 5-4 summarizes the separation efficiencies calculated for the proteins on the longer effective length UCON and Superox capillaries.

Though relatively high peak efficiencies were achieved on the polyether coated capillaries, peak tailing was observed on all of the investigated capillary columns (Figures 5-5, 5-6, 5-7, and 5-8). The peak asymmetry factor (A_s) was determined for all

peaks with these columns to compare the degree of peak tailing occurring with each coating. A_s was determined at 10% peak height with the following relationship:

$$A_s = \frac{\text{width of B}}{\text{width of A}} \quad (5.3)$$

Each peak was divided in half at the peak maximum in which the right zone of the peak is B whereas the left zone is A. The peak is symmetrical if $A_s = 1$, if $A_s > 1$ the peak is tailing, and if $A_s < 1$ the peak is fronting. All peaks on the polyether coatings were determined to be tailing. Table 5-5 summarizes the asymmetry factors determined on the investigated polyether capillaries.

Table 5-4 Separation efficiencies of the protein mixture on each capillary. For the UCON capillaries a 90 cm effective distance was used for the separation. A 70 cm effective length was used with the Superox capillary. A 40 mM Tris-HCl pH 4.8 buffer was employed for all separations.

| Coating | Cyt C | Lys | Ribo A | α -chymo |
|---------------------------------------------------------|--------|--------|--------|-----------------|
| UCON 15 mg/mL, 1 mg/mL HMDS, 0.1 mg/mL dicumyl peroxide | 882000 | 878000 | 175000 | 412000 |
| UCON 15 mg/mL, 2 mg/mL HMDS, 0.2 mg/mL dicumyl peroxide | 418000 | 47000 | 218000 | 141000 |
| 4.4 mg/mL Superox | 374000 | 92000 | 183000 | 144000 |

Assymetry factors for peaks analyzed on the unmodified and polyacrylamide capillaries were not determined since several peaks were not baseline resolved.

To characterize the efficiency of the acrylamide coating produced with the Grignard reagent, a similar protein mixture was investigated with the 40 mM Tris-HCl pH 4.8 buffer. On this capillary all the peaks were tailing, indicative of adsorption to the surface; therefore, extremely poor efficiencies for the proteins were observed. Since the

Table 5-5 Assymetry factor (A_s) for each protein on the various polyether coatings.

| Coating | Cyt C | Lys | Ribo A | α -chymo |
|----------------------------------------|-------|-----|--------|-----------------|
| 10 mg/mL UCON (20 cm effective) | 3 | 9 | 4 | 3 |
| 15 mg/mL UCON (20 cm effective) | 2 | 4 | 6 | 5 |
| 4.4 mg/mL Superox (20 cm effective) | 2 | 3 | 4 | 4 |
| 15 mg/mL UCON (90 cm effective) | 2 | 2 | 12 | 12 |
| 4.4 mg/mL Superox (70 cm effective) | 3 | 10 | 6 | 5 |

separation efficiency was so poor in this buffer, the theoretical plates of the proteins were not calculated for this coating. In order to compare the utilized coating procedure with that previously published, a set of acidic and basic proteins were analyzed on the polyacrylamide coated capillary. The capillary (50 μ m i.d.) was 47 cm in total length with a 40 cm effective separation distance and a 10 kV separation voltage was employed. Cytochrome C (1.9 mg/mL) and trypsinogen (4.5 mg/mL) were analyzed with a 30 mM citrate pH 2.7 buffer (Figure 5-10). The separation efficiencies were determined as 97000 plates for cytochrome C and 88000 plates for trypsinogen, which coincide with 242000 and 221000 plates/m respectively. Published accounts report 317000 plates/m for cytochrome C and 297000 plates/m for trypsinogen; therefore, a decrease in efficiency was encountered with the experimental procedure described above (Cobb *et al.*, 1990). A solution (0.2 mg/mL each) of bovine serum albumin (BSA) and α -lactalbumin was also investigated with a 50 mM borate pH 9.5 buffer on the

polyacrylamide coated capillary (Figure 5-11) and compared to an unmodified capillary (Figure 5-12). The calculated separation efficiencies are summarized in Table 5-6.

Table 5-6 Separation efficiencies (plates/m) of the protein mixture on an unmodified and polyacrylamide capillaries employing a 50 mM borate pH 9.5 buffer and 213 V/cm electric field.

| Coating | BSA (Plates/m) | α -lactalbumin (Plates/m) |
|------------|-------------------|-------------------------------------|
| Unmodified | 45000 | 180000 |
| Acrylamide | 80000 | 93000 |

As shown in the table, only an improvement in separation efficiency for BSA was found when employing the polyacrylamide coated capillary. Previous accounts utilizing similar fields and effective separation distances reported 69000 plates/m for BSA and 71000 plates/m for α -lactalbumin for the unmodified capillary with an increase in efficiency with the coated capillary to 259000 plates/m for BSA and 293000 plates/m for α -lactalbumin (Cobb *et al.*, 1990). Our results show an improved separation of α -lactalbumin on an unmodified capillary than previously published and an actual decrease in efficiency when employing the coated capillary. The improvement in the BSA efficiency with our polyacrylamide coated capillary is three times less than that found previously. The poorer efficiency of our procedure may be due to the problems previously mentioned that were encountered when working with the Grignard reagent.

Conclusions

Adsorption of analytes to the capillary walls is a major limitation for employing CE separations to analyze biopolymeric molecules such as proteins. Considerable research has been undertaken to reduce adsorption and improve the applicability of CE

for protein separations. This work has investigated several capillary coating procedures and various polymers for effectiveness in preventing protein adsorption. Polyacrylamide coatings are the most commonly employed modified capillaries in which EOF is considerably suppressed compared to that in an unmodified capillary. However, considerable increases in efficiency for an array of proteins were found when employing polyethers such as UCON and Superox for capillary coatings. Also the modified capillary procedure reported here is less time consuming than those generally employed for an acrylamide coating since the surface derivitization, polymer attachment, and *in situ* polymerization are incorporated into one step. Previous reports have used these capillaries over a pH range from 2.5-7, and the capillaries should be stable at slightly more alkaline pH's. At a more basic pH such as 9.5, a chemically stable capillary coating is necessary in which the polyacrylamide coated capillary produced with a Grignard reagent synthesis may be a viable option. The Grignard coating procedure is very laborious and time consuming, which may not be desired for routine analysis; however, these capillaries were found to be very stable (1-2 months) with proper storage.

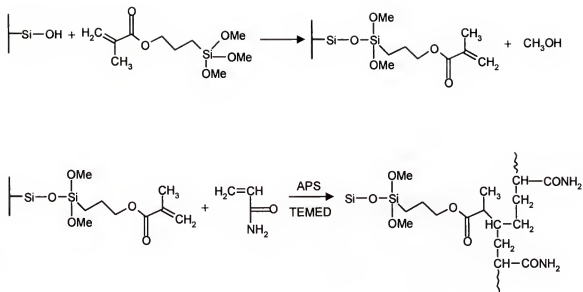


Figure 5-1 Reaction scheme of derivatization on the capillary surface with γ -methacryloxypropyltrimethoxysilane (silanization reagent) in which a Si-O-Si linkage is formed between the capillary surface and the polyacrylamide coating.

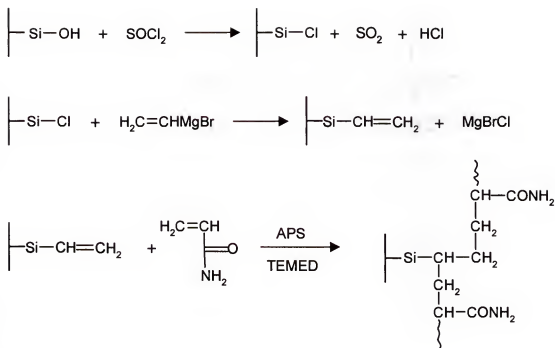


Figure 5-2 Reaction scheme of derivatization on the capillary surface with vinyl magnesium bromide (Grignard reagent) in which a Si-C linkage is formed between the capillary surface and the polyacrylamide coating.

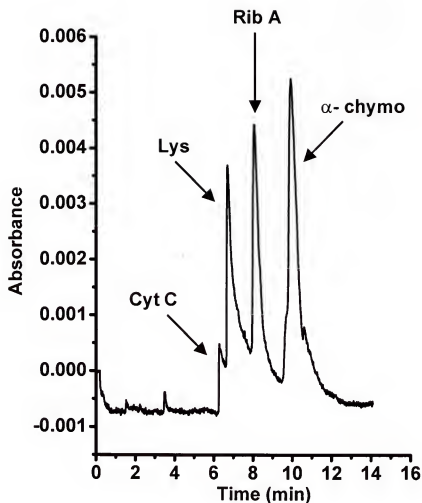


Figure 5-3 Capillary electrophoretic separation of cytochrome C (Cyt C), lysozyme (Lys), ribonuclease A (Rib A), and α -chymotrypsinogen (α -chymo) on a bare capillary with a 40mM Tris-HCl pH 4.8 buffer. The capillary (25 μ m i.d.) was 27 cm total with a 20 cm effective length. A 2s 5.6 kV injection was employed and the separation voltage was 5.6 kV (207 V/cm).

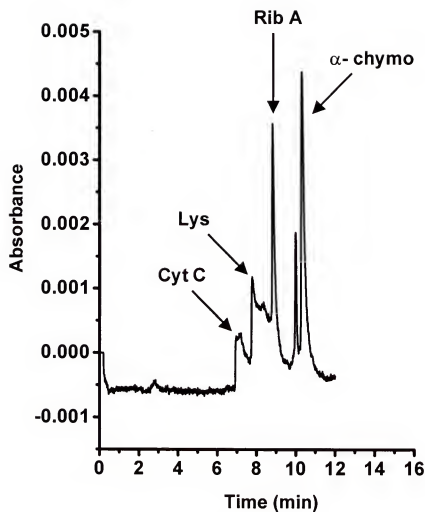


Figure 5-4 Capillary electrophoretic separation of cytochrome C (Cyt C), lysozyme (Lys), ribonuclease A (Rib A), and α -chymotrypsinogen (α -chymo) on a polyacrylamide coated capillary with a 40mM Tris-HCl pH 4.8 buffer. The capillary (25 μ m i.d.) was 27 cm total with a 20 cm effective length. A 2 s 5.6 kV injection was employed and the separation voltage was 5.6 kV (207 V/cm).

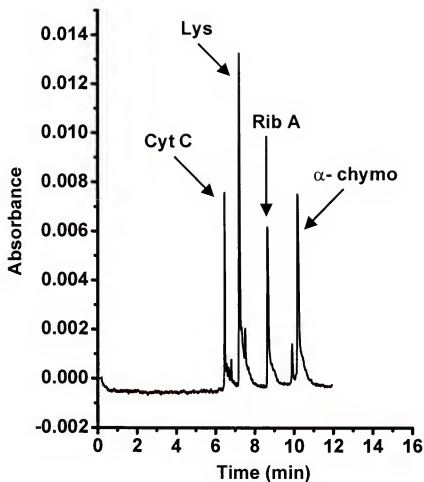


Figure 5-5 Capillary electrophoretic separation of cytochrome C (Cyt C), lysozyme (Lys), ribonuclease A (Rib A), and α -chymotrypsinogen (α -chymo) on a 15 mg/mL UCON coated capillary with a 40mM Tris-HCl pH 4.8 buffer. The capillary (25 μ m i.d.) was 27 cm total with a 20 cm effective length. A 2s 5.6 kV injection was employed and the separation voltage was 5.6 kV (207 V/cm).

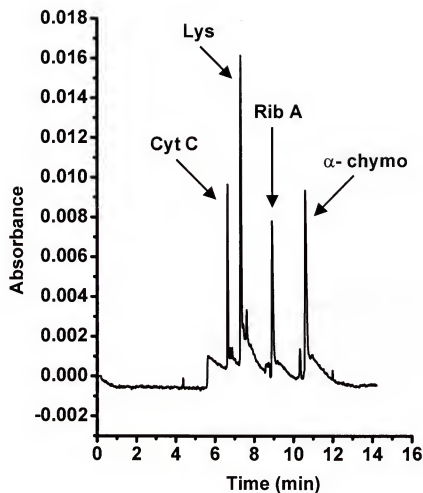


Figure 5-6 Capillary electrophoretic separation of cytochrome C (Cyt C), lysozyme (Lys), ribonuclease A (Rib A), and α -chymotrypsinogen (α -chymo) on a 4 mg/mL Superox coated capillary with a 40mM Tris-HCl pH 4.8 buffer. The capillary (25 μ m i.d.) was 27 cm total with a 20 cm effective length. A 2s 5.6 kV injection was employed and the separation voltage was 5.6 kV (207 V/cm).

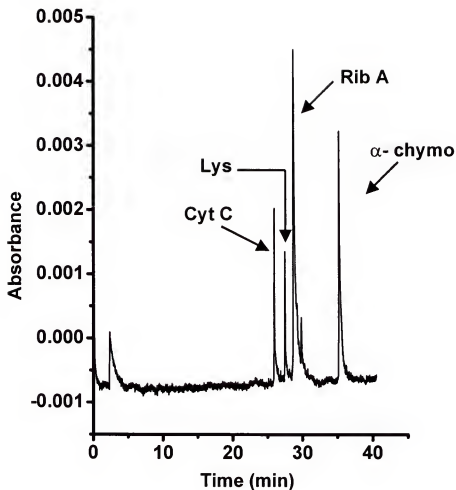


Figure 5-7 Capillary electrophoretic separation of cytochrome C (Cyt C), lysozyme (Lys), ribonuclease A (Rib A), and α -chymotrypsinogen (α -chymo) on a 15 mg/mL UCON coated capillary with a 40mM Tris-HCl pH 4.8 buffer. The capillary (25 μ m i.d.) was 97 cm total with a 90 cm effective length. A 2s 10 kV injection was employed and the separation voltage was 25 kV (258 V/cm).

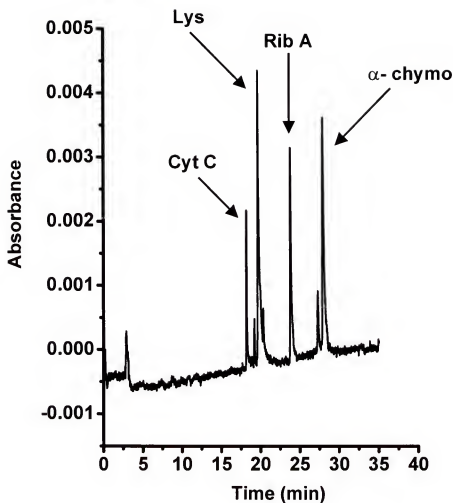


Figure 5-8 Capillary electrophoretic separation of cytochrome C (Cyt C), lysozyme (Lys), ribonuclease A (Rib A), and α -chymotrypsinogen (α -chymo) on a 4 mg/mL Superox coated capillary with a 40mM Tris-HCl pH 4.8 buffer. The capillary (25 μ m i.d.) was 77 cm total with a 70 cm effective length. A 2s 10 kV injection was employed and the separation voltage was 20 kV (260 V/cm).

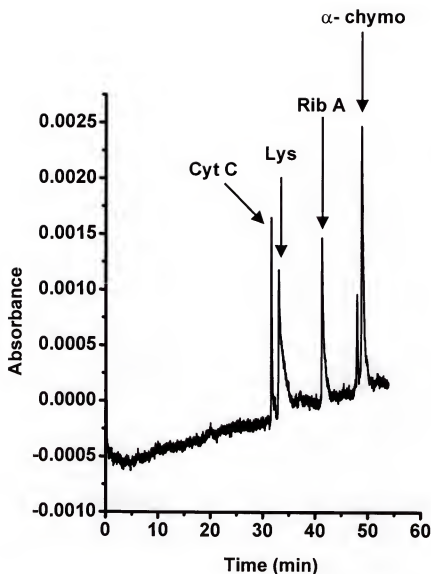


Figure 5-9 Capillary electrophoretic separation of cytochrome C (Cyt C), lysozyme (Lys), ribonuclease A (Rib A), and α -chymotrypsinogen (α -chymo) on a 15 mg/mL UCON coated capillary prepared with 2 mg/mL HMDS and 0.2 mg/mL dicumyl peroxide. The separation buffer was 40mM Tris-HCl pH 4.8. The capillary (25 μ m i.d.) was 97 cm total with a 90 cm effective length. A 5s 10 kV injection was employed and the separation voltage was 20 kV (206 V/cm).

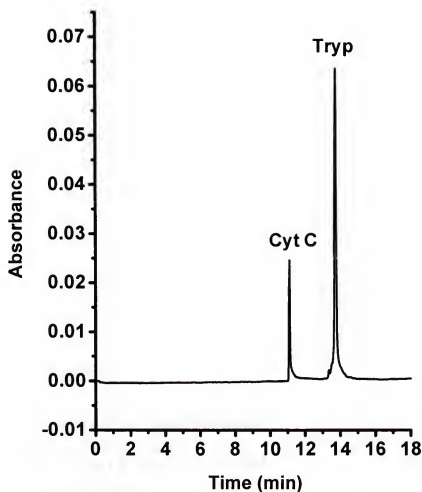


Figure 5-10 Capillary electrophoretic separation of cytochrome C (Cyt C) and trypsinogen (tryp) on a polyacrylamide coated capillary prepared with a Grignard reaction. The separation buffer was 30mM citrate pH 2.7. The capillary (50 μ m i.d.) was 47 cm total with a 40 cm effective length. A 3s pressure injection was employed and the separation voltage was 10 kV (213 V/cm).

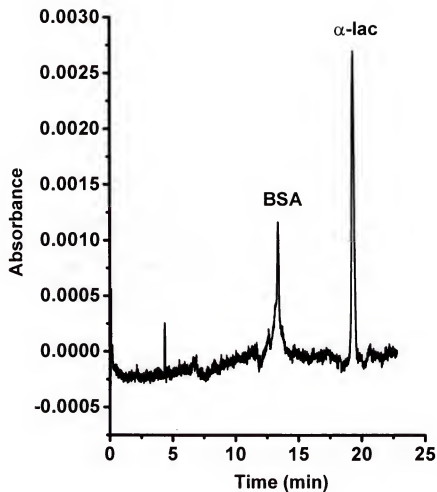


Figure 5-11 Capillary electrophoretic separation of α -lactalbumin (α -lac) and bovine serum albumin (BSA) on a polyacrylamide coated capillary prepared with a Grignard reaction. The separation buffer was 50mM borate pH 9.5. The capillary (50 μ m i.d.) was 47 cm total with a 40 cm effective length. A 5s pressure injection was employed and the separation voltage was 10 kV (213 V/cm).

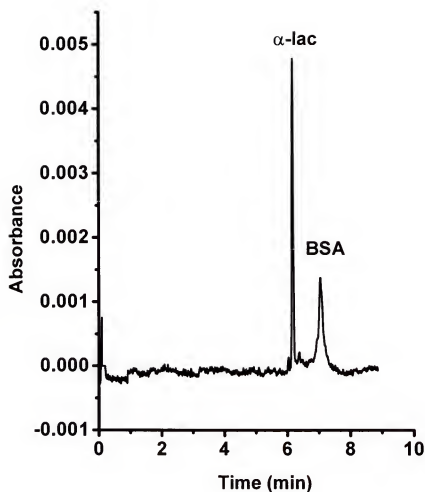


Figure 5-12 Capillary electrophoretic separation of α -lactalbumin (α -lac) and bovine serum albumin (BSA) on an unmodified capillary with a 50mM borate pH 9.5 separation buffer. The capillary (50 μ m i.d.) was 47 cm total with a 40 cm effective length. A 5s pressure injection was employed and the separation voltage was 10 kV (213 V/cm).

CHAPTER 6

SUMMARY AND FUTURE DIRECTIONS

This work has focused on developing noncompetitive aptamer CE assays for use as analytical diagnostic tools. Buffer composition was determined to be crucial in formation and detection of aptamer complexes. Aptamer assays for the proteins thrombin and IgE were developed by employing a TKG pH 8.4 buffer with unmodified capillaries. The weaker affinity thrombin complex was bridged with the free aptamer indicating complex dissociation during the separation. However, when techniques such as coated capillaries and polymer gel networks, which suppress EOF, were implemented to reduce complex dissociation, no complex was detected; therefore, the EOF in the unmodified capillary was pushing the complex through the column enabling detection. Moderate electric fields (200-600 V/cm) were found to have little effect on detection of the IgE aptamer complex; however, the time spent on the column greatly affected the amount of complex detected. The largest concentration of complex was detected with shorter column times (less than 50 s) which were achieved with short separation distances (7 cm). With increased column time, the aptamer complex concentration was observed to decrease due to dissociation.

The TKG pH 8.4 separation conditions were applicable for two aptamers specific for proteins (MW 34 and 200 kD). Future work should investigate other aptamers with these separation conditions, especially aptamers specific for smaller analytes such as drugs and peptides. The electrophoretic separation of the free aptamer from a drug-aptamer complex may be more complicated due to the small change in the electrophoretic

mobility of the aptamer upon binding with a small molecule (similar to noncompetitive assays utilizing antibodies). The TKG pH 8.4 buffer may be inadequate for aptamer assays for small targets and separation modifiers (similar to those developed for noncompetitive CEIA) may be necessary to increase the resolution of the free aptamer and complex. Developing assays for aptamer-small molecule complexes utilizing CE aptamer assays for chemical monitoring may be possible. SELEX experiments would be necessary in order to develop aptamers for neuropeptides and neurotransmitters or other biological molecule of interest. Also, RNA aptamers need to be investigated as they typically have greater affinity and functionality for their target molecules. Experimental conditions and handling procedures would need to be modified to insure the RNA aptamers are not denatured since RNA is very reactive and easily degrades.

Aptamer diversity and functionality needs to be enriched to increase the applicability of aptamers as analytical tools. Modified nucleotides are one possibility for enhancing aptamer diversity and functionality. A J base aptamer specific for ATP was investigated to determine if any enhancement in binding of ATP was achieved by incorporation of the positively charged J nucleotide into the DNA aptamer. Though no enhancement in binding of ATP was measured for the J base aptamer, a novel scientific achievement was accomplished by incorporating a positively charged functionality into an aptamer. Future research needs to explore other functionalized bases as well as improvements in aptamer selection conditions in order to produce more diverse, possibly higher affinity oligonucleotides.

Another aspect of this work utilized affinity capillary electrophoresis to measure the binding affinity of a DNA aptamer with adenine, adenosine, AMP, ADP, and ATP. A

binding pattern was observed in which the charge state of the ligand affected binding with the aptamer. The lowest affinities were determined for ADP and adenosine, which have -1 and neutral charges at the pH employed for separation. Binding was disrupted by the presence of the -2 charges of AMP and ADP as indicative of the lower dissociation constants. Because of the weaker interaction of the aptamer with adenosine analogs an aptamer LC stationary phase has been developed and used to selectively separate adenosine analytes collected from islets.

The final goal of this work was to investigate several capillary coating procedures and various polymers for effectiveness in preventing protein adsorption. Adsorption of analytes to the capillary walls is a major limitation when employing CE separations to analyze biopolymeric molecules such as proteins. Polyacrylamide coatings are the most commonly employed modified capillaries used in CE separations; however, considerable increases in efficiency for an array of proteins was measured for polyether columns. Also the modified capillary procedure used for polyether coatings was less time consuming than that employed for an acrylamide coating since the surface derivitization, polymer attachment, and *in situ* polymerization were incorporated into one step. UCON and Superox columns may be used over a wide pH range (2.5-7), but a more chemically stable coating would be necessary at a higher pH. For alkaline pH's, the polyacrylamide coated capillary produced with a Grignard reagent procedure may be a viable option; however, the coating procedure is very laborious and time consuming which is undesirable for routine analyses.

REFERENCES

- Alazard, R.; Betermier, M.; Chandler, M. *Mol. Microbiol.* **1992**, 6, 1707.
- Battersby, T.R.; Ang, D.N.; Burgstaller, P.; Jurczyk, S.C.; Bowser, M.T.; Buchanan, D.D.; Kennedy, R.T.; Benner, S.A. *J. Am. Chem. Soc.* **1999**, 121, 9781.
- Barron, A.E.; Blanch, H.W. *Electrophoresis* **1994**, 12, 597.
- Barron, A.E.; Soane, D.S.; Blanch, H.W. *J. Chromatogr. A* **1993**, 652, 3.
- Barry, J.P.; Muth, J.; Law, S.J.; Karger, B.L.; Vouros, P. *J. Chromatogr. A* **1996**, 732, 159.
- Bao, J.J. *J. Chromatogr. B* **1997**, 699, 463.
- Benedek, K.; Guttman, A. *J. Chromatogr. A* **1994**, 680, 375.
- Bock, L.C.; Griffin, L.C.; Latham, J.A.; Vermass, E.H.; Toole, J.J. *Nature* **1992**, 355, 564.
- Bowser, M.T.; Chen, D.D.Y. *Electrophoresis* **1998**, 19, 383.
- Bruin, G.J.M.; Chang, J.P.; Kuhlman, R.H.; Zegers, K.; Kraak, J.C.; Poppe, H. *J. Chromatogr.* **1989**, 471, 429.
- Bullock, J.A.; Yuan, L.C. *J. Microcol. Sep.*, **1991**, 3, 241.
- Bushey, M.M.; Jorgenson, J.W. *J. Chromatogr.* **1989**, 480, 301.
- Butler, J.M.; McCord, B.R.; Jung, J.M.; Allen, R.O. *Biotechniques* **1994**, 17, 1062.
- Chen, D.Y.; Aldelhelm, K.; Cheng, X.L.; Dovichi, N.J. *Analyst* **1994**, 119, 349.
- Chen, F.T.; Evangelista, R.A. *Clin. Chem.* **1994**, 4019, 1819.
- Cheng, S.B.; Skinner, C.D.; Taylor, J.; Attiya, S.; Lee, W.E.; Picelli, G.; Harrison, D.J. *Anal. Chem.* **2001**, 73, 1472.

- Chervet, J.P.; van Soest, R.E.J.; Urmses, M. *LC Packings* **1990** technical communication.
- Chiari, M.; Nesi, M.; Fazio, M.; Righetti, P.G. *Electrophoresis* **1992**, 12, 690.
- Chiu, R.W.; Jimenez, J.C.; Monnig, C.A. *Anal. Chim. Acta*, **1995**, 307, 193.
- Chu, Y.; Avila, L.Z.; Gao, J.; Whitesides, G.M. *Acc. Chem. Res.* **1995**, 28, 461.
- Ciesolka, J.; Yarus, M. *RNA* **1996**, 2, 785.
- Cifuentes, A.; Rodriguez, M. A.; Garcia-Montelongo, F.J. *J. Chromatogr. A*, **1996**, 742, 257.
- Clark, B.K.; Nickles, C.L.; Morton, K.C.; Kovac, J.; Sepaniak, M.J. *J. Microcol. Sep.* **1994**, 6, 503.
- Cobb, K.A.; Dolník, V.; Novotny, M. *Anal. Chem.* **1990**, 62, 2478.
- Cohen, A.S.; Najarian, D.R.; Karger, B.L. *J. Chromatogr.* **1990**, 516, 49.
- Davis, K.A.; Abrams, B.; Lin, Y.; Jayasena, S.D. *Nucleic Acids Res.* **1996**, 24, 702.
- DeAuda, J.A.; Coutre, S.E.; Moon, M.R.; Vial, C.M.; Griffin, L.C.; Law, V.S.; Komeda, M.; Leung, L.L.K.; Miller, D.C. *Ann. Thorac. Surg.* **1994**, 58, 344.
- Dermaux, A.; Sandra, P. *Electrophoresis* **1999**, 20, 3027.
- Dolník, V. *Electrophoresis* **1997**, 18, 2353.
- Dolník, V.; Xu, D.; Yadav, A.; Bashkin, J.; Marsh, M.; Tu, O.; Mansfield, E.; Vainer, M.; Madabhushi, R.; Barker, D.; Harris, D. *J. Microcol. Sep.* **1998**, 10, 175.
- Dougherty, A. M.; Cooke, N.; Shieh, P. In *Handbook of Capillary Electrophoresis*, Landers, J.P., Ed. CRC Press: Boca Raton, **1997**, p 675.
- Drolet, D.W.; Moon-McDermott, L.; Romig, T.S. *Nature Biotechnol.* **1996**, 14, 1021.
- Ellington, A.D.; Szostak, J.W. *Nature* **1990**, 346, 818.
- Ellington, A.D.; Szostak, J.W. *Nature* **1992**, 355, 850.
- Evangelista, R.A.; Chen, F.T.A. *J. Chromatogr.* **1994**, 680, 587.
- Famulok, M. *J. Am. Chem. Soc.* **1994**, 116, 1698.

- Famulok, M.; Mayer, G. In *Combinatorial Chemistry in Biology*, Famulok, M.; Winnacker, E.L.; Wong, C.H., Eds. Springer-Verlag: Berlin, **1999**, v 243, p 123.
- Foulds, G.J.; Etzkorn, F.A. *Nucleic Acids Res.* **1998**, 26, 4304.
- Foulds, G.J.; Etzkorn, F.A. *J. Chromatogr. A* **1999**, 862, 231.
- Fried, M.G.; Bromberg, J.L. *Electrophoresis* **1997**, 18, 6.
- Fried, M.G.; Crothers, D.M. *Nucleic Acids Res.* **1981**, 9, 6505.
- Fung, E.N.; Yeung, E.S. *Anal. Chem.* **1995**, 67, 1913.
- Ganzler, K.; Greve, K.S.; Cohen, A.S.; Karger, B.L.; Guttman, A.; Cooke, N.C. *Anal. Chem.* **1992**, 64, 2665.
- Geiger, A.; Burgstaller, P.; Eltz, H.; Roeder, A.; Famulok, M. *Nucleic Acids Res.* **1996**, 24, 1029.
- Gelfi, C.; Perego, M.; Righetti, P.G. *Electrophoresis* **1996**, 17, 1470.
- German, I.; Buchanan, D.D.; Kennedy, R.T. *Anal. Chem.* **1998**, 70, 4540.
- Gomez, F.A.; Avila, L.Z.; Chu, Y.H.; Whitesides, G.M. *Anal. Chem.* **1994**, 66, 1785.
- Green, J.S.; Jorgenson, J.W. *J. Chromatogr.* **1989**, 478, 63.
- Grossman, P.D.; Wilson, K.J.; Petrie, G.; Lauer, H.H. *Anal. Biochem.* **1988**, 173, 265.
- Hafner, F.T.; Kautz, R.A.; Iverson, B.L.; Tim, R.C.; Karger, B.L. *Anal. Chem.* **2000**, 72, 5779.
- Hage, D.S. *Anal. Chem.* **1993**, 65, 420R.
- Heegaard, N.H.H.; Kennedy, R.T. *Electrophoresis* **1999**, 20, 3122.
- Heegaard, N.H.H.; Robey, F.A. *J. Immunol. Meth.* **1993**, 166, 103.
- Hicke, B.J.; Watson, S.R.; Koenig, A.; Lynott, C.K.; Bargatze, R.F.; Chang, Y.; Ringquist, S.; Moon-McDermott, L.; Jennings, S.; Fitzwater, T.; Han, H.; Varki, N.; Albinana, I.; Willis, M.C.; Varki, A.; Parma, D. *J. Clin. Invest.* **1996**, 98, 2688.
- Hjertén, S. *J. Chromatogr.* **1985**, 347, 191.
- Hjertén, S.; Kubo, K. *Electrophoresis* **1993**, 14, 390.
- Honda, S.; Taga, A.; Suzuki, K.; Suzuki, S.; Kakehi, K. *J. Chromatogr.* **1992**, 597, 377.

- Hubert, S.J.; Slater, G.W.; Viovy, J.L. *Macromolecules* **1996**, 29, 1006.
- Huizenga, D.E.; Szostak, J.W. *Biochemistry* **1995**, 34, 656.
- Iki, N.; Yeung, E.S. *J. Chromatogr. A*, **1996**, 731, 273.
- James, W. In *Encyclopedia of Analytical Chemistry: Applications, Theory, and Instrumentation*, Myers, R.A., Ed., John Wiley & Sons: Sussex, United Kingdom, **2000**.
- Janini, G.M.; Fisher, R.J.; Henderson, L.E.; Issaq, H.J. *J. Liq. Chromatogr.* **1995**, 18, 3617.
- Jayasena, S.D. *Clin. Chem.* **1999**, 45, 1628.
- Jenison, R.D.; Gill, S.C.; Pardi, A.; Polisky, B. *Science* **1994**, 263, 1425.
- Jellinek, D.; Green, L.S.; Bell, C.; Janjić, N. *Biochemistry* **1994**, 33, 10450.
- Karger, B.L.; Cohen, A.S.; Guttman, A.J. *J. Chromatogr.* **1989**, 492, 585.
- Kleijnung, F.; Klusmann, S.; Erdmann, V.A.; Scheller, F.W.; Furste, J.P.; Bier, F.F. *Anal. Chem.* **1998**, 70, 328.
- Klepnárík, K.; Fanali, S.; Boek, P. *J. Chromatogr.* **1993**, 638, 283.
- Kubik, M.F.; Stephens, A.W.; Schneider, D.; Marlar, R.A.; Tasset, D. *Nucleic Acids Res.* **1994**, 22, 2619.
- Lam, M.T.; Wan, Q.H.; Boulet, C.A.; Le, X.C. *J. Chromatogr. A* **1999**, 853, 545.
- Lane, D.; Prentki, P.; Chandler, M. *Microbiol. Rev.* **1992**, 56, 509.
- Lauer, H.H.; McManigill, D. *Anal. Chem.* **1986**, 58, 166.
- Lee, Y.H.; Maus, R.G.; Smith, B.W.; Winefordner, J. D. *Anal. Chem.* **1994**, 66, 4142.
- Li, W.X.; Kaplan, A.V.; Grant, G.W.; Toole, J.J.; Leung, L.L.K. *Blood* **1994**, 83, 677.
- Lin, C.H.; Patel, D.J. *Chem. Biol.* **1997**, 4, 817.
- Lin, Y.; Padmapriya, A.; Morden, K.; Jayasena, S.D. *Proc. Natl. Acad. Sci. USA* **1995**, 92, 11044.
- Luckey, J.A.; Drossman, H.; Kostichka, A.J.; Mead, D.A.; D'Cunha, J.; Norris, T.B.; Smith, L.M. *Nucleic Acids Res.* **1990**, 18, 4417.
- Malik, A.; Zhao, Z.; Lee, M.L. *J. Microcol. Sep.* **1993**, 5, 119.

- Mazzeo, J.R. In *Handbook of Capillary Electrophoresis*, Landers, J.P., Ed. CRC Press: Boca Raton, 1997, p 49.
- McCormick, R.M. *Anal. Chem.* **1988**, 60, 2322.
- Morris, K.N.; Jensen, K.B.; Julin, C.M.; Weil, M.; Gold, L. *Proc. Natl. Acad. Sci. USA* **1998**, 95, 2902.
- Nieuwalandt, D.; Wecker, M.; Gold, L. *Biochemistry* **1995**, 34, 5651.
- O'Neill, K.; Shao, X.; Zhao, Z.; Malik, A.; Lee, M.L. *Anal. Biochem.* **1994**, 222, 185.
- Pentoney, S.L. Jr.; Konrad, K.D.; Kaye, W.I. *Electrophoresis* **1992**, 13, 467.
- Potyarailo, R.A.; Conrad, R.C.; Ellington, A.D.; Hieftje, G.M. *Anal. Chem.* **1998**, 70, 3419.
- Rohlicek, V.; Deyel, Z. *J. Chromatogr.* **1989**, 494, 87.
- Rodriguez-Diaz, R.; Wehr, T.; Zhu, M.D. *Electrophoresis* **1997**, 18, 2134.
- Ruiz-Martinez, M.C.; Carrilho, E.; Berka, J.; Kieleczawa, J.; Miller, A.W.; Foret, F.; Carson, S.; Karger, B.L. *BioTechniques* **1996**, 20, 1058.
- Sandoval, J.E.; Chen, S. *Anal. Chem.* **1996**, 68, 2771.
- Sassanfar, M.; Szostak, J. *Nature* **1993**, 364, 550.
- Schmalzing, D.; Nashabeh, W. *Electrophoresis* **1997**, 18, 2184.
- Schmalzing, D.; Nashabeh, W.; Yao, X.W.; Mhatre, R.; Regnier, F.E.; Afeyan, N.B.; Fuchs, M. *Anal. Chem.* **1995**, 67, 606.
- Schmalzing, D.K.; Piggee, C.A.; Foret, F.; Carrilho, E.; Karger, B.L. *J. Chromatogr. A* **1993**, 652, 149.
- Schmerr, M.J.; Jenny, A. *Electrophoresis* **1998**, 19, 409.
- Schultz, N.M.; Kennedy, R.T. *Anal. Chem.* **1993**, 65, 3161.
- Schultz, N.M.; Huang, L.; Kennedy, R.T. *Anal. Chem.* **1995**, 65, 3161.
- Shao, X.; O'Neill, K.; Zhao, Z.; Anderson, S.; Malik, A.; Lee, M. *J. Chromatogr. A* **1994**, 680, 463.
- Shimura, K.; Karger, B.L. *Anal. Chem.* **1994**, 66, 9.

- Song, L.G.; Qu, Q.Y.; Yu, W.L. *J. Chromatogr. A* **1993**, 657, 175.
- Stebbins, M.A.; Hoyt, A.M.; Sepaniak, M.J.; Hurlburt, B.K. *J. Chromatogr. B* **1996**, 683, 77.
- Stover, F.S.; Haymore, B.L.; McBeath, R.J. *J. Chromatogr.* **1989**, 470, 241.
- Sunada, W.M.; Blanch, H.W. *Electrophoresis* **1997**, 18, 2243.
- Swedberg, S.A. *Anal. Biochem.* **1990**, 185, 1.
- Swerdlow, H.; Gesteland, R. *Nucleic Acids Res.* **1990**, 18, 1415.
- Swerdlow, H.; Zhang, J.Z.; Chen, D.Y.; Harke, H.R.; Grey, R.; Wu, S.; Fuller, C.; Dovichi, N.J. *Anal. Chem.* **1991**, 63, 2835.
- Tao, L.; Kennedy, R.T. *Anal. Chem.* **1996**, 68, 3899.
- Tim, R.C.; Kautz, R.A.; Karger, B.L. *Electrophoresis* **2000**, 21, 220.
- Timperman, A.T.; Khatib, K.; Sweedler, J.V. *Anal. Chem.* **1995**, 67, 139.
- Tsuda, T.; Sweedler, J. V.; Zare, R. N. *Anal. Chem.* **1990**, 62, 2149.
- Tuerk, C.; Gold, L. *Science* **1990**, 249, 505.
- Tuerk, C.; MacDougal, S.; Gold, L. *Proc. Natl. Acad. Sci. USA* **1992**, 89, 6988.
- Wang, K.Y.; McCurdy, S.; Shea, R.G.; Swaminathan, S.; Bolton, P.H. *Biochemistry* **1993**, 32, 1899.
- Wang, T.; Aiken, J.H.; Huie, C.W.; Hartwick, R.A. *Anal. Chem.* **1991**, 63, 1372.
- Wiegand, T.W.; Williams, P.B.; Dreskin, S.C.; Jouvin, M.; Kinet, J.; Tasset, D. *J. Immunol.* **1996**, 157, 221.
- Williams, K.P.; Liu, X.; Schumacher, T.N.M.; Lin, H.Y.; Ausiello, D.A.; Kim, P.S.; Bartel, D.P. *Proc. Natl. Acad. Sci. USA* **1997**, 94, 11285.
- Xian, J.; Harrington, M.G.; Davidson, E.H. *Proc. Natl. Acad. Sci. USA* **1996**, 93, 86.
- Xue, Y.; Yeung, E. *Anal. Chem.* **1994**, 66, 3575.
- Yao, Y.J.; Li, S.F.Y. *J. Chromatogr. A* **1994**, 663, 97.
- Yang, Q.; Goldstein, I.J.; Mei, H.; Engelke, D.R. *Proc. Natl. Acad. Sci. USA* **1998**, 95, 5462.

Ye, L.; Le, C.; Xing, J.Z.; Ma, M.; Yatocoff, R. *J. Chromatogr. B* **1998**, 714, 59.

Zagursky, R.J.; McCormick, R.M. *BioTechniques* **1990**, 9, 74.


Zhang, J.; Voss, K.O.; Shaw, D.F.; Roos, P.; Lewis, D.F.; Yan, J.; Jiang, R.; Ren, H.; Hou, J.Y.; Fang, Y.; Puyang, X.; Ahmadzadeh, H.; Dovichi, N.J. *Nucleic Acids Res.* **1999**, 27, e36.

Zhao, Z.; Malik, A.; Lee, M.L. *J. Microcol. Sep.* **1992**, 4, 411.

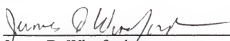
BIOGRAPHICAL SKETCH

Danielle Denise Buchanan was born September 20, 1974, in Nashville, TN, to Lorraine and Charles Buchanan. After graduating in 1992 from Bourbon County High School in Paris, KY, she went on to attend the University of Kentucky in Lexington, KY. In May 1996 she received her Bachelor of Science degree in chemistry as well as a minor in mathematics. While attending college, she was also employed by Mallinckrodt-Baker Specialty Chemicals in Paris, KY, working as a quality control technician. In August 1996 she began her studies at the University of Florida under the direction of Dr. Robert T. Kennedy. Her graduate work focused on developing novel bioanalytical tools incorporating aptamers into noncompetitive capillary electrophoresis affinity assays. In August 2001 she received her Doctor of Philosophy degree.


I certify that I have read this study and that in my opinion it conforms to acceptable standards of scholarly presentation and is fully adequate, in scope and quality, as a dissertation for the degree of Doctor of Philosophy.


Robert T. Kennedy, Chairman
Professor of Chemistry


I certify that I have read this study and that in my opinion it conforms to acceptable standards of scholarly presentation and is fully adequate, in scope and quality, as a dissertation for the degree of Doctor of Philosophy.


James D. Winefordner
Graduate Research Professor of Chemistry

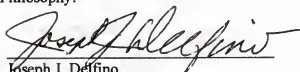
I certify that I have read this study and that in my opinion it conforms to acceptable standards of scholarly presentation and is fully adequate, in scope and quality, as a dissertation for the degree of Doctor of Philosophy.


Weihong Tan
Associate Professor of Chemistry

I certify that I have read this study and that in my opinion it conforms to acceptable standards of scholarly presentation and is fully adequate, in scope and quality, as a dissertation for the degree of Doctor of Philosophy.


Steven A. Benner
Professor of Chemistry

I certify that I have read this study and that in my opinion it conforms to acceptable standards of scholarly presentation and is fully adequate, in scope and quality, as a dissertation for the degree of Doctor of Philosophy.


Joseph J. Deffino
Professor of Environmental Engineering
Sciences

This dissertation was submitted to the Graduate Faculty of the Department of Chemistry in the College of Liberal Arts and Sciences and to the Graduate School and was accepted as partial fulfillment of the requirements for the degree of Doctor of Philosophy.

August 2001

Dean, Graduate School